GEOSCIENCES DIVISION

TEXAS INSTRUMENTS
INCORPORATED
EXCHANGE BANK BUILDING
DALLAS 35, TEXAS
(P. O. BOX 35084)

AFCRL - 802

FINAL REPORT

Contract AF 19(604)-8078

11 July 1961

ANALYSIS AND REDUCTION OF

DATA RECORDED UNDER PROJECT COWBOY

Project Manager: Lawrence Strickland

Author: Robert W. Wylie

TEXAS INSTRUMENTS INCORPORATED

Geosciences Division

Exchange Bank Building

Dallas 35, Texas

Prepared for

GEOPHYSICS RESEARCH DIRECTORATE

Air Force Cambridge Research Laboratories

Office of Aerospace Research

United States Air Force

Bedford, Massachusetts

WORK SPONSORED BY ADVANCED RESEARCH PROJECTS AGENCY

Project VELA UNIFORM

ARPA Order No. 180-61, Amendment 2

Project Code No. 8100, Task 2

"Requests for additional copies by Agencies of the Department of Defense, their contractors, and other Government agencies should be directed to the:

ARMED SERVICES TECHNICAL INFORMATION AGENCY
ARLINGTON HALL STATION
ARLINGTON 12, VIRGINIA

Department of Defense contractors must be established for ASTIA services or have their 'need-to-know' certified by the cognizant military agency of their project or contract." All other persons and organizations should apply to the:

U. S. DEPARTMENT OF COMMERCE
OFFICE OF TECHNICAL SERVICES
WASHINGTON 25, D. C.

TABLE OF CONTENTS

LIST OF ILLUSTRATIONS

LIST OF ILLUSTRATIONS (Contd.)

LIST OF TABLES

SUMMARY

The analyses conducted under Project Cowboy by Texas Instruments, was performed on eight chemical detonations. These shots consisted of 200-, 500-, and 1000-pound decoupled shots in a 30-ft. spherical cavity. An additional decoupled 1000-pound shot was detonated in a 12-ft. spherical cavity. Tamped shots had yields of 200, 500, and two 1000 pounds. Analyses from the data recorded indicated the following results.

1. The predominant energy of the decoupled signals is concentrated in the first few arrivals whereas the tamped signals are characterized by many arrivals of rather constant amplitude.

2. The 500- and 1000-pound tamped and decoupled shots revealed that the tamped shots transmitted a greater quantity of low frequency energy than the decoupled shots.

3. The total seismic energy is partitioned differently between the various modes of propagation for tamped and decoupled shots and is a function of the size of the explosive and cavity.

4. The effect of decoupling can be thought of as a linear filtering of the tamped signal response.

5. Amplitude density ratios computed from spectral response characteristics indicated that the decoupling is a function of frequency, shot size, and distance from the source.

Seismic attenuations are usually frequency dependent; therefore, the decoupling analysis presented in this report is based on defining decoupling as the amplitude density ratio as a function of frequency. Depending on the time length and area of the seismogram from which the samples are selected, the ratios of the average amplitude response can describe the decoupling as determined for the first arriving refractions, body wave segment of the record, or the total seismic signal return. These ratios are only dependent upon the seismic signal and noise variations. The analysis included energy density spectra of signals and power density spectra of the noise samples for the 500- and 1000-pound decoupled and tamped events. Time samples were analyzed, e.g., .256-second samples of the first arrivals and 2.048-second samples of noise and signal. Surface wave energy is not included in the analysis.

Seventeen shots were detonated by the A. E. C., under Project Cowboy, in an effort to establish the decoupling capabilities of cavity source environments for nuclear detonations. Texas Instruments participation in Project Cowboy was to determine the characteristics, and analyze the data obtained, of decoupled shots, seismometer coupling, environment, and travel paths relative to chemical explosions in spherical cavities.

The test shots were conducted in early 1960. Special research equipment built with company funds for use in seismic research was used in the analysis and reduction of data gathered. S-41 seismometers having a frequency of 4 cps were used to monitor the eight shots.

SECTION I

INTRODUCTION

The degree to which the seismic waves from an underground nuclear explosion can be attenuated by detonation in a cavity is of vital importance in evaluating the capabilities of a world wide nuclear surveillance program. In this regard a test series of chemical explosions was undertaken by the A. E. C. called Project Cowboy. In this test series, chemical explosions of similar sizes were detonated in spherical cavities washed out in the salt formation and in grouted bore holes. Seventeen shots were detonated in an effort to establish, by extrapolation from these scaled experiments, the decoupling capabilities of cavity source environments for nuclear detonations.

Many reports have been written by the participants in Project Cowboy concerning various aspects of the tests covering logistics, geologic studies, near source effects, and seismic effects as recorded at the surface at distances from several hundred feet to 60 miles. This report attempts to avoid duplication, having drawn on the information of the previous reports, and due to the nature of the analysis, presents information which is unique and will further the knowledge of the decoupling capabilities of cavity environments as recorded in a practical field situation. The data and analysis presented was recorded and analyzed with special research equipment built with company funds for use in seismic research.

SECTION II

DATA COLLECTION

Texas Instruments recorded shots 6 through 13 (four tests, two shots each) held one week apart with special research equipment previously designed for recording seismic information. These tests began on 30 January 1960 and terminated on 20 February 1960 corresponding to tests, 6, 7, 8, 9, 10, 11, 12 and 13 as indicated in the reports of Adams and Allen[1] and others. The seismometers were laid along a line as shown on the map in Figure 1 with the source to seismometer separations given in Table I. The seismometer locations were fixed throughout the tests with Station 5A corresponding to Station 5 of the earlier reports (Adams and Allen[1]). The differences in separations are due only to shot location changes. The time laps from decoupled to tamped shots was one hour and the seismometers were left in place during the interim; therefore, the transfer characteristics of the seismometer and seismometer environments can be assumed equivalent for any of the recorded shot pairs.

The data and analysis presented was carried out on the response from the six S-41 velocity sensitive seismometers at stations 5A, 5B, 5C, 5D, 5E and 5F. These seismometers have a 4-cps natural frequency and response characteristics similar to that shown in Figure 2. The recording system passed a frequency band from DC to 250 cps and preserved a 66-db dynamic range on magnetic tape recordings used in the analysis of the data. The field records are shown in Figures 3, 4, 5, and 6 for the S-41 seismometer responses for the eight shots monitored. These figures show the 200-pound tamped and decoupled shots, the 500-pound tamped and decoupled shots, the 1000-pound tamped and decoupled (30 ft. sphere) shots, and the 1000-pound tamped and decoupled (12 ft. sphere) shots, respectively.

A general analysis of this data is presented in Appendix B.

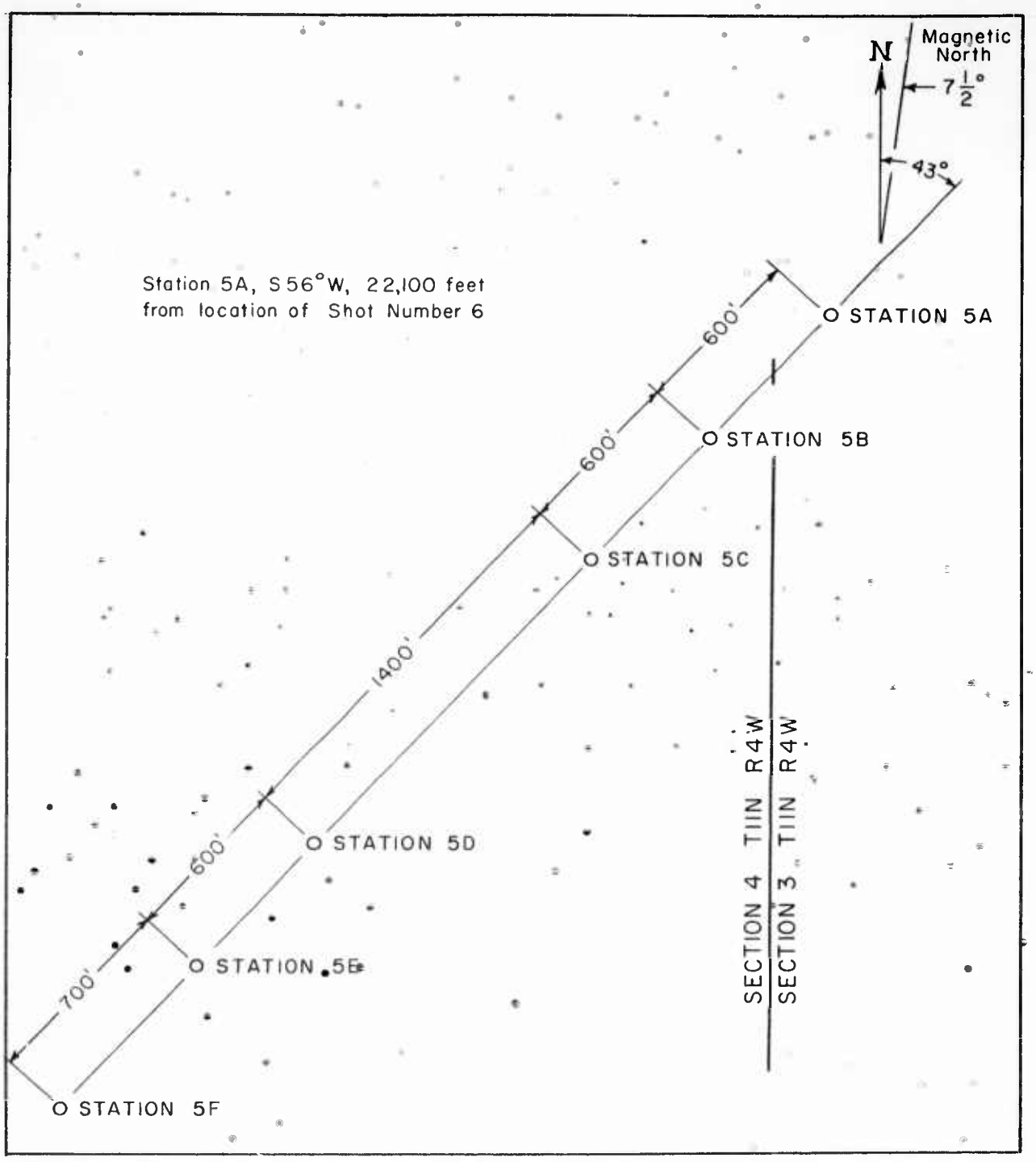

Fig. 1

Seismometer Spread

TABLE I

SOURCE TO SEISMOMETER SEPARATION

Shot Number	Shot Size *	Type of Shot	Source to Seismometer Separation Stat. 5A **	Stat. 5B	Stat. 5C	Stat. 5D	Stat. 5E	Stat. 5F
6	200	Decoupled 30 ft. sphere	22,100	22,696	23,292	24,683	25,279	25,975
7	200	Tamped	21,600	22,195	22,790	24,179	24,774	25,470
8	500	Decoupled 30 ft. sphere	22,100	22,696	23,292	24,683	25,279	25,975
9	500	Tamped	21,690	22,285	22,880	24,270	24,865	25,561
10	1000	Decoupled 30 ft. sphere	22,100	22,696	23,292	24,683	25,279	25,975
11	1000	Tamped	21,752	22,346	22,941	24,329	24,924	25,619
12	1000	Decoupled 12 ft. sphere	21,858	22,453	23,047	24,436	25,031	25,747
13	1000	Tamped	21,574	22,168	22,762	24,151	24,745	25,440

* Shot size in pounds

** Distances in feet

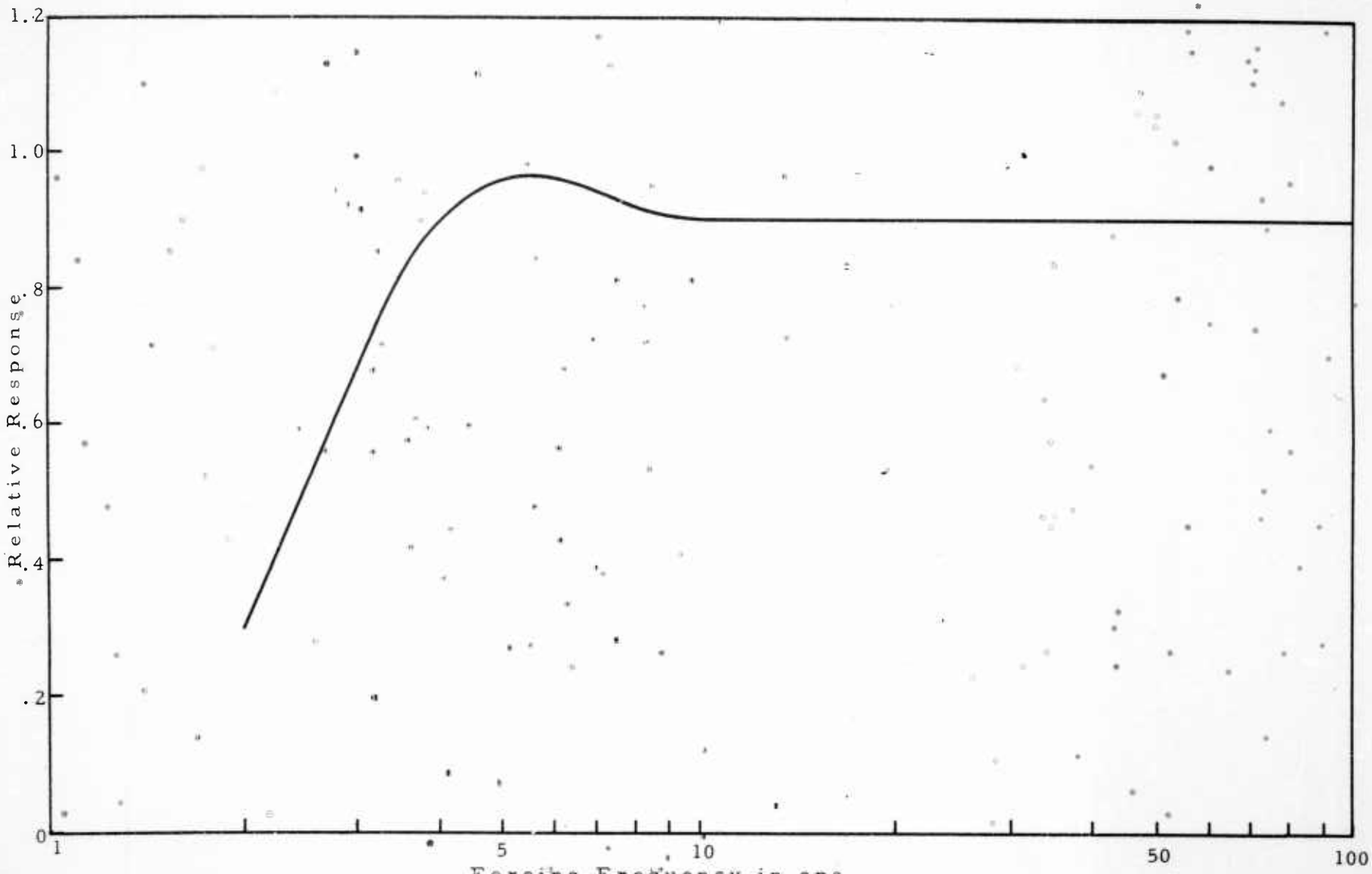

Fig. 2

S-41 Seismometer Characteristics

200 POUND DECOUPLED

30 FT. SPHERE

SHOT #6

S-41 SEISMOMETER

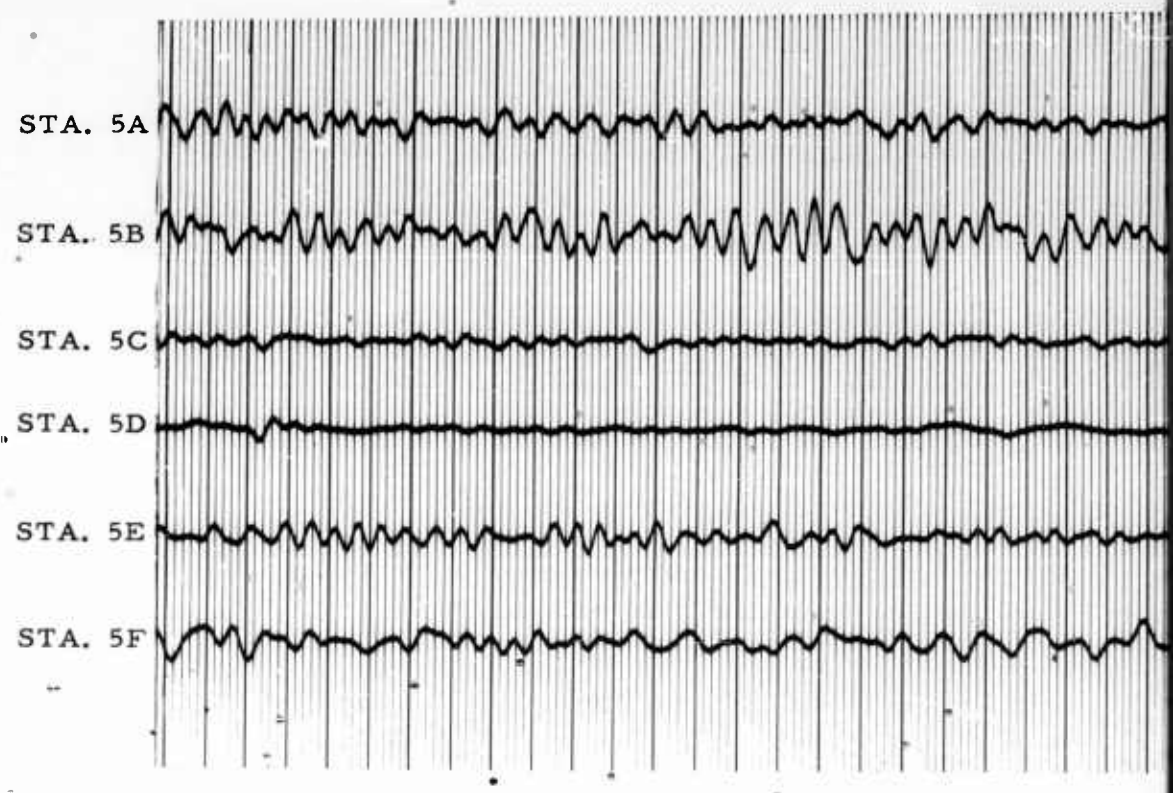

200 POUND TAMPED

SHOT #7

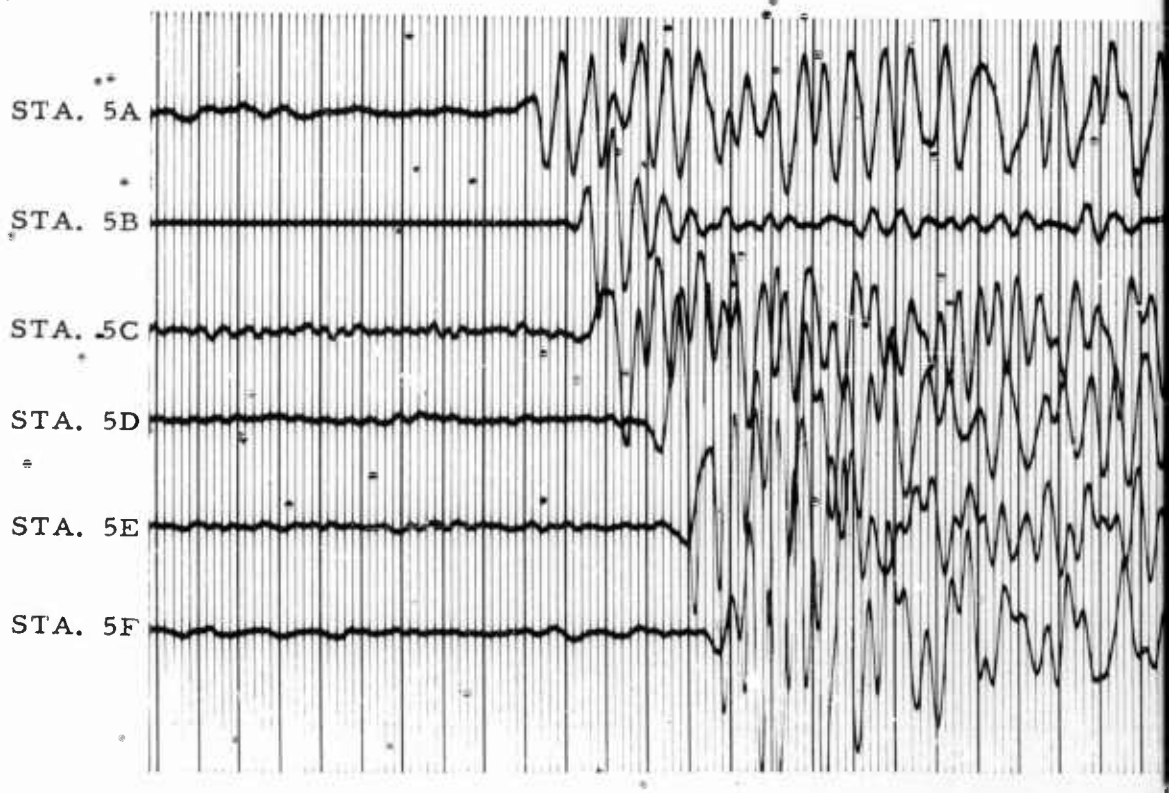

1

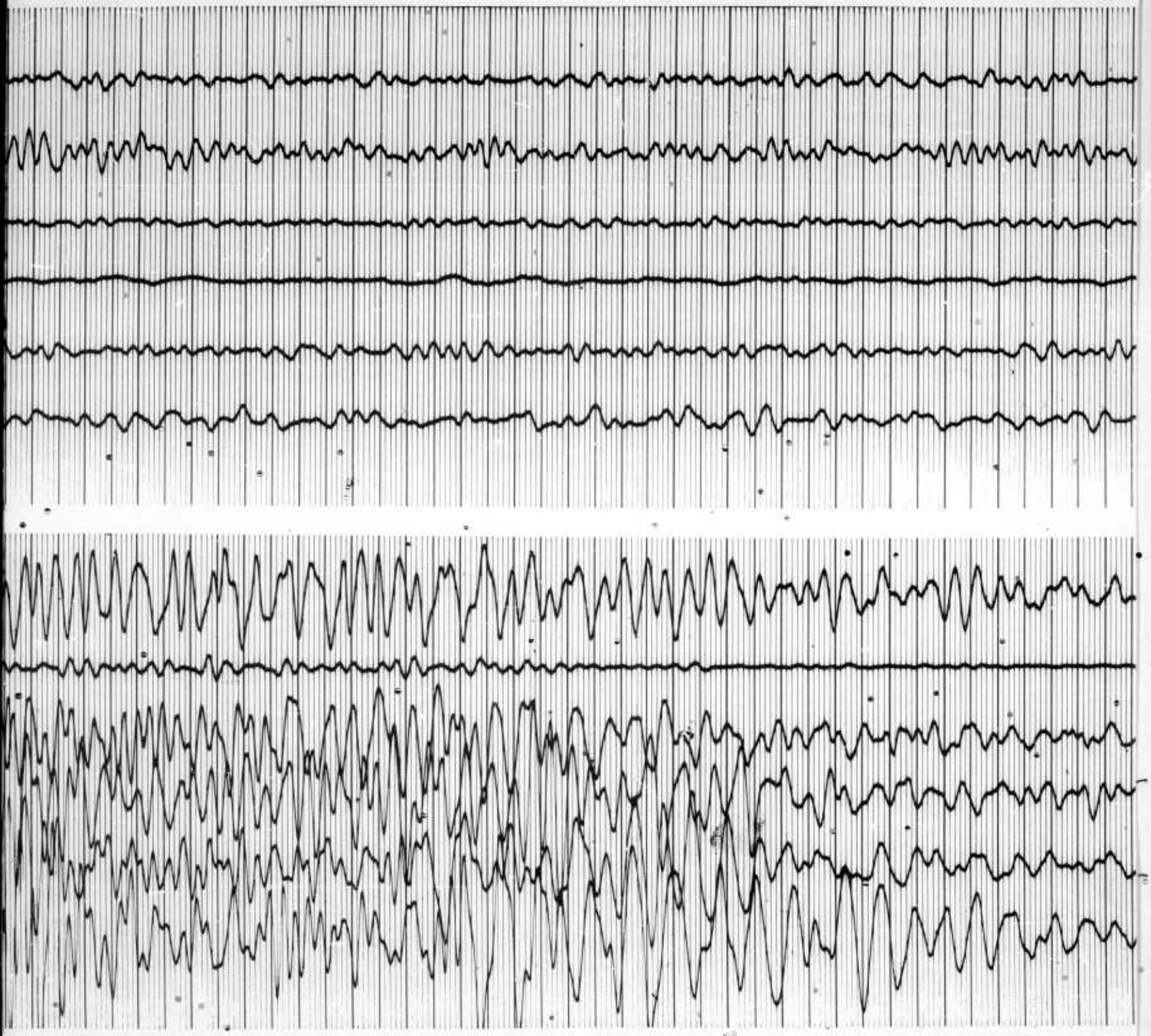

Fig. 3

S-41 Seismometer Responses for 200 pound Tamped and Decoupled Shots

2

500 POUND DECOUPLED

30 FT. SPHERE

SHOT #8

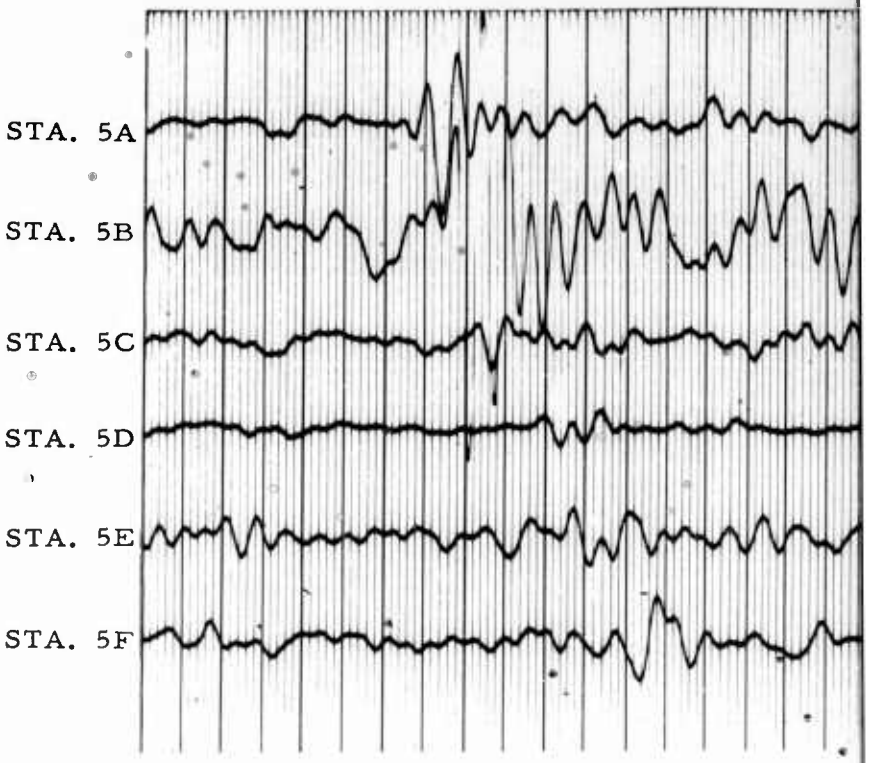

S-41 SEISMOMETER

500 POUND TAMPED

SHOT #9

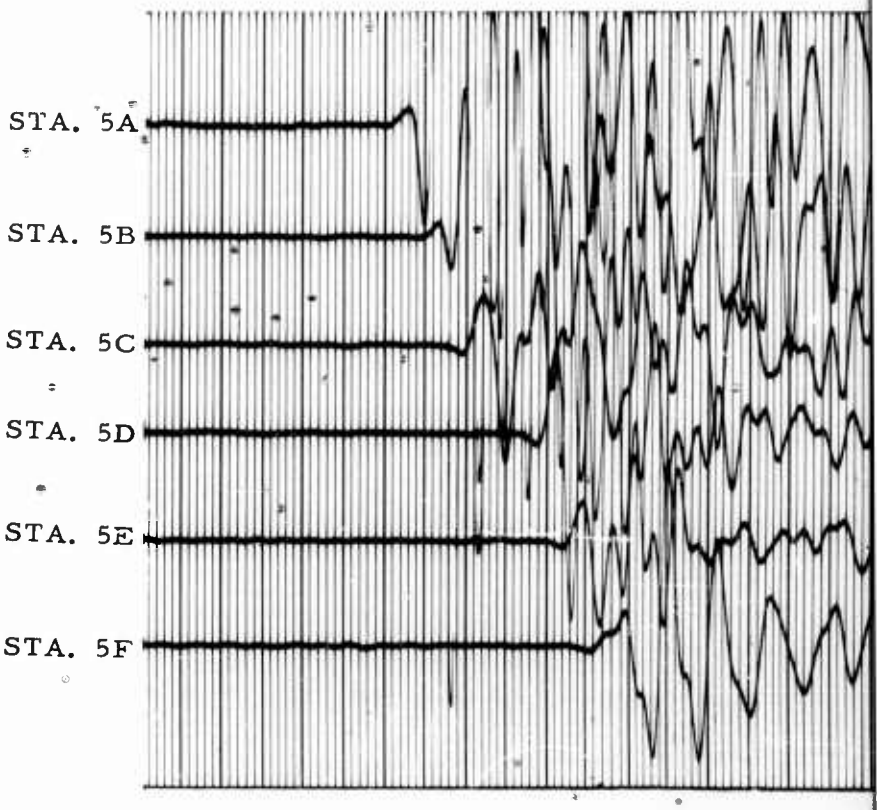

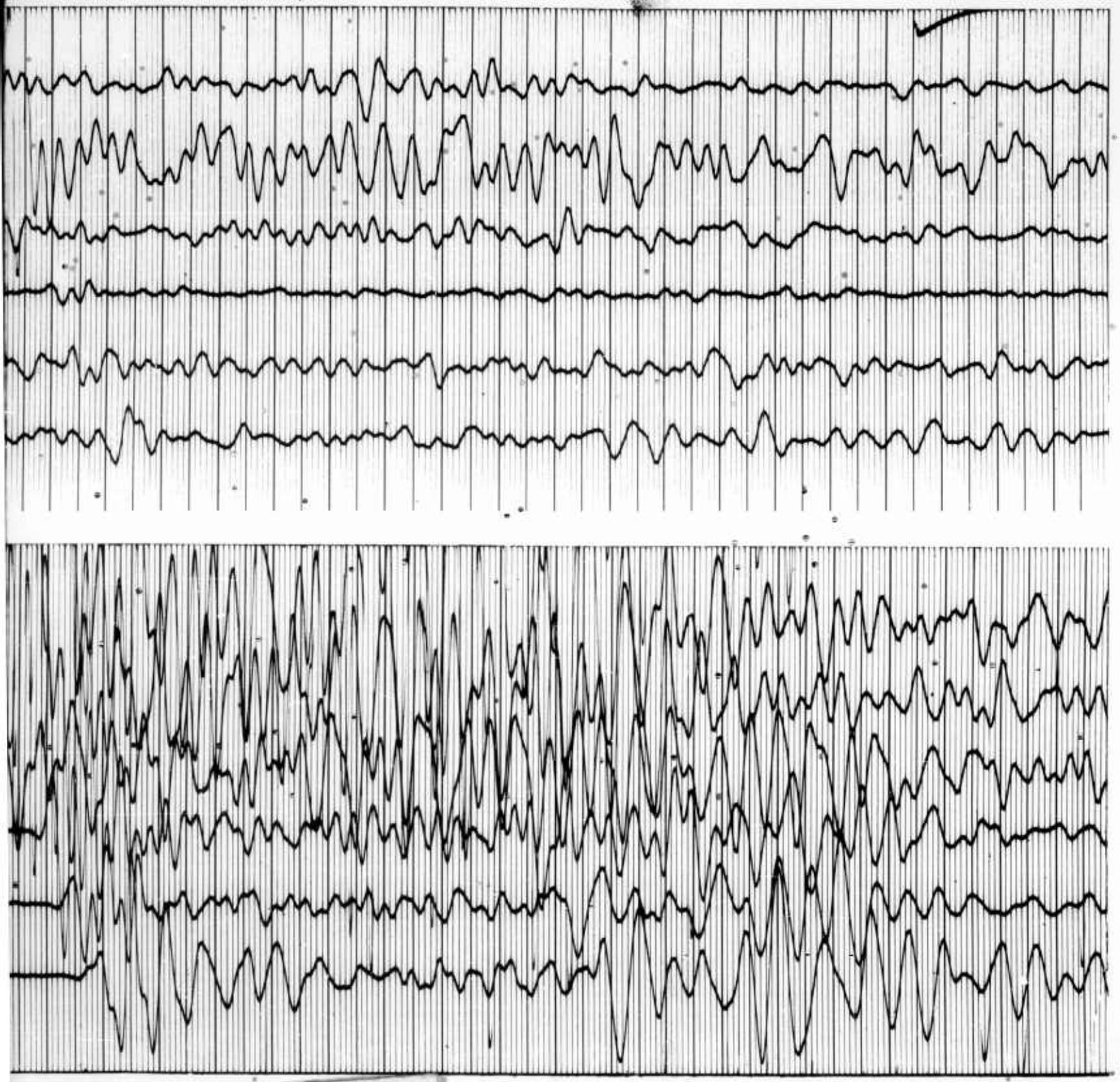

Fig. 4.
S-41 Seismometer Responses for 500 pound
Tamped and Decoupled Shots

1000 POUND DECOUPLED

30 FT. SPHERE

SHOT #10

S-41 SEISMOMETER

1000 POUND TAMPED

SHOT #11

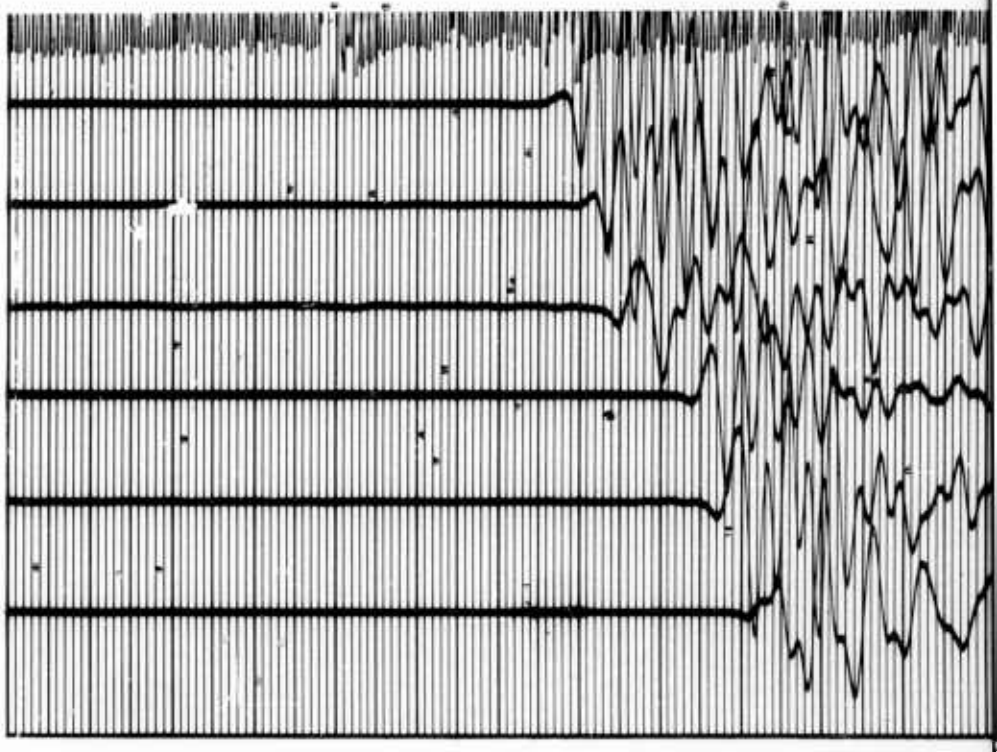

1

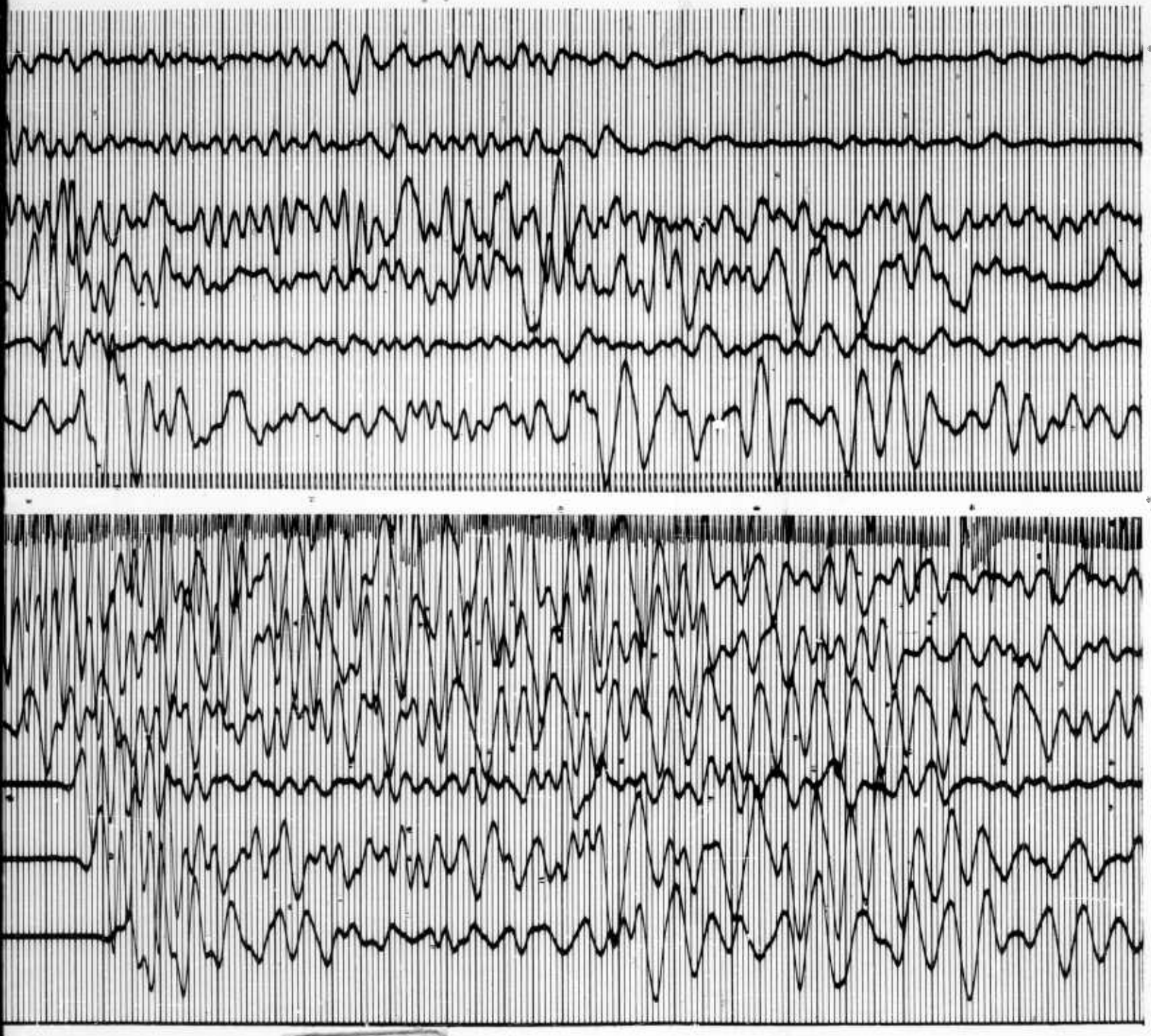

2

Fig. 5

S-41 Seismometer Responses for 1000 pound Tamped and Decoupled Shots (30 ft. sphere)

1000 POUND DECOUPLED

12 FT. SPHERE

SHOT #12

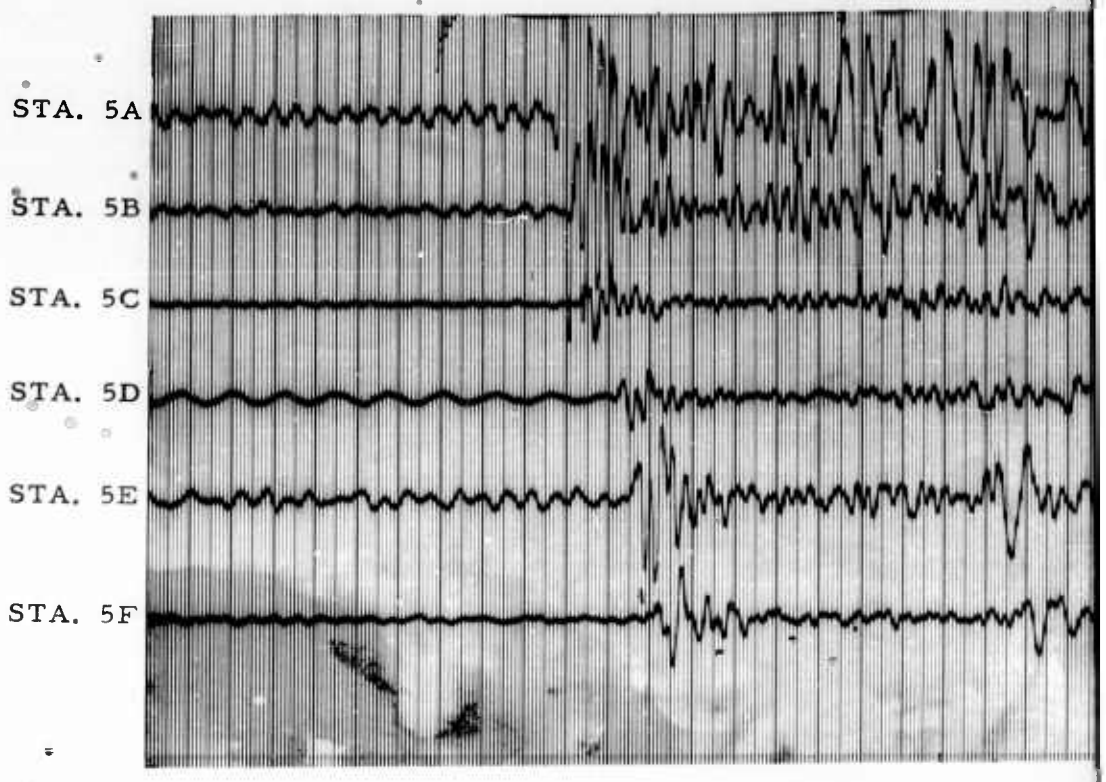

S-41 SEISMOMETER

1000 POUND TAMPED

SHOT #13

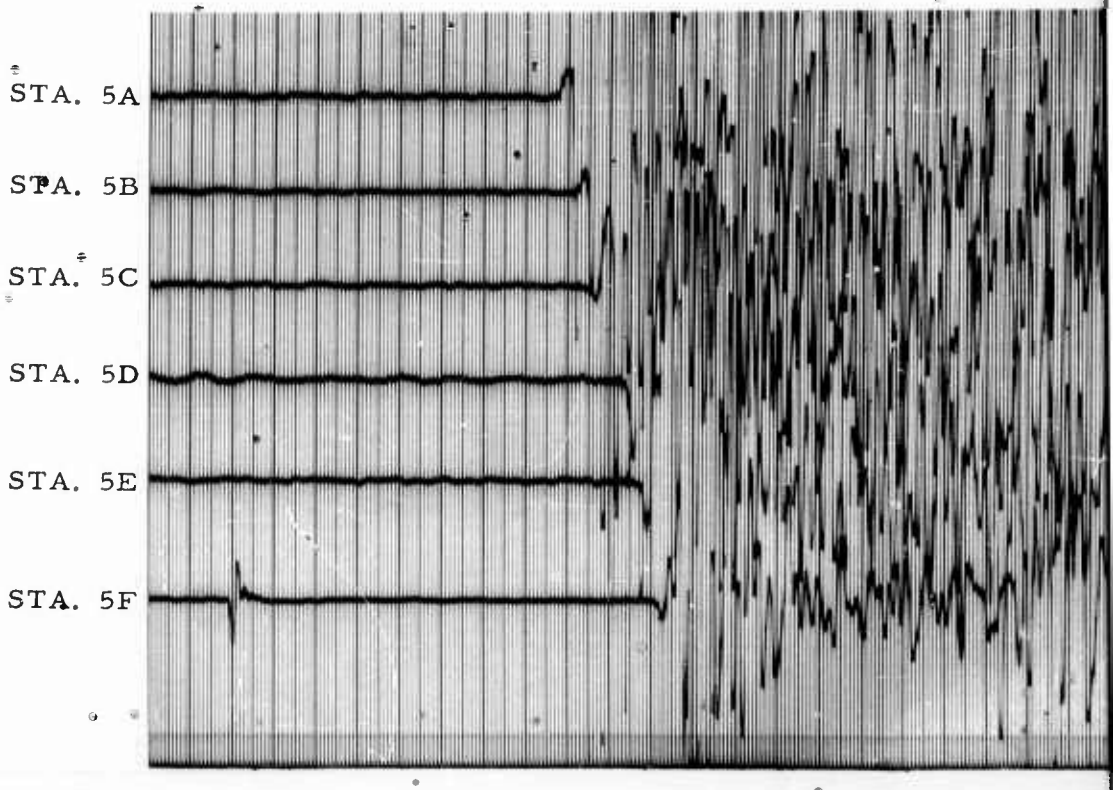

1

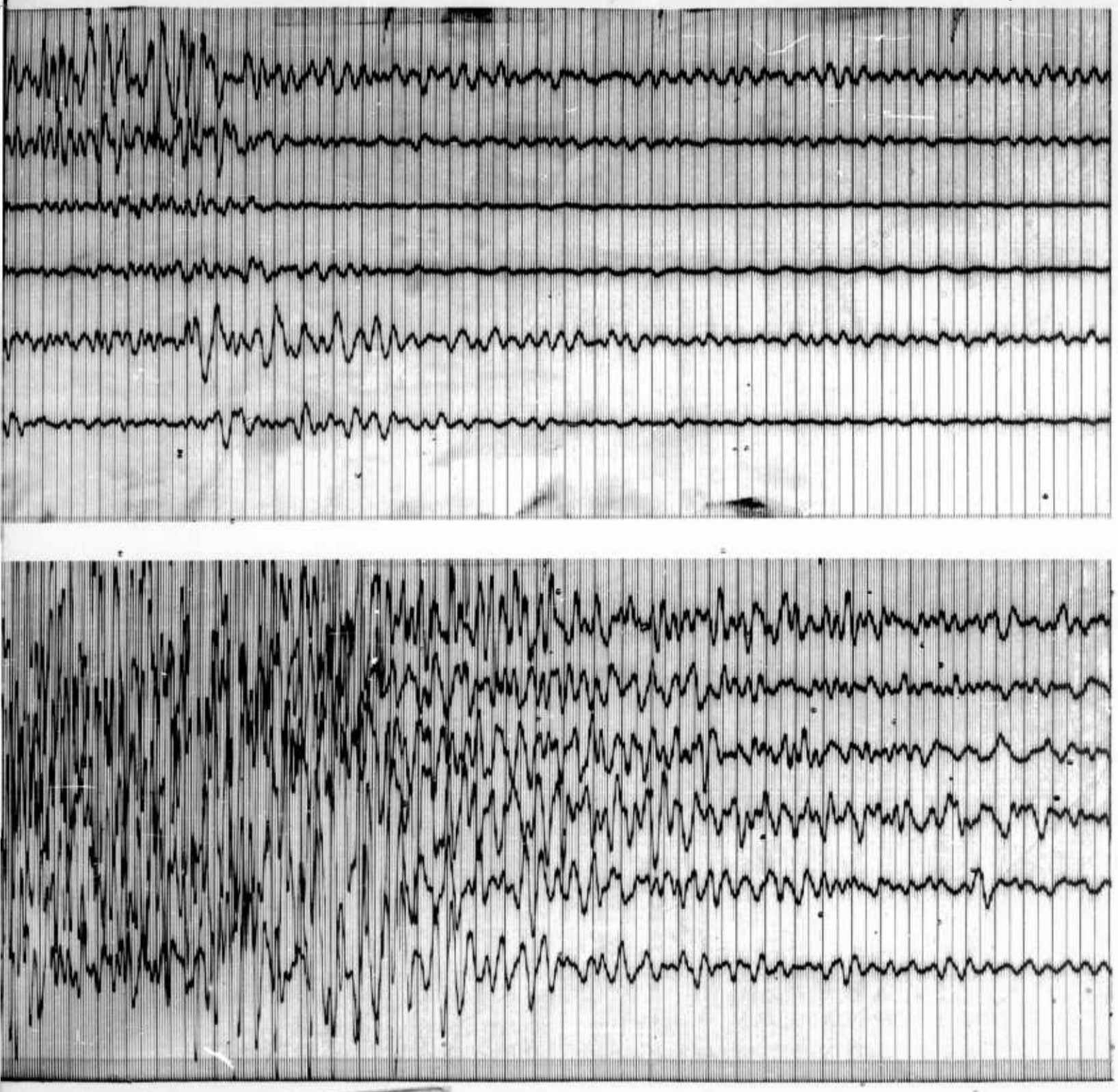

Fig. 6
S-41 Seismometer Responses for 1000 pound Tamped and Decoupled Shots (12 ft. sphere)

SECTION III

DATA ANALYSIS

A. DECOUPLING

The main purpose of Project Cowboy was to determine the attenuating capabilities of a cavity source environment for chemical explosives in an effort to obtain data which could be scaled to underground nuclear tests. The theory upon which the experiment was based has been presented by Latter, et al[3]. Briefly, the theory states that the energy from an explosion which is propagated as seismic energy depends on the volume contained within the surface marking the transition from non-elastic to elastic wave propagation. In the case of a tamped shot in a homogeneous medium this boundary depends only on the type and size of the charge, the characteristics of the medium, and the depth of the shot. For a cavity source environment this volume will be greatly reduced and hence there will be less energy radiated as seismic waves. If the sphere is large enough for the critical pressure to have been obtained within the cavity the theory also predicts the amount of attenuation expected.

Definition of the decoupling as it is seen by surface seismometers in a typical field situation depends on the type of data available and for what use the information is being evaluated. First, the earth is not a homogeneous half space, nor does the earth function as a simple filter in a noiseless situation. Secondly, a ratio of peak amplitudes may be sufficient in some instances, while in others the knowledge that decoupling in one frequency band for a particular portion of the record is quite low will supersede the knowledge that the ratio of total energy response is quite high. Thus, there is a need for several well defined ratios to adequately represent decoupling as determined from surface seismic recordings.

To describe the differences in signal response from a tamped and decoupled shot of similar charge size, a ratio of amplitudes is required, preferably as a function of frequency. Since amplitudes are what is seen on a seismic record it is more natural for a decoupling factor to be described as a ratio of amplitudes rather than a ratio of energies.

The most simple ratio is that of peak particle velocities as recorded by seismometers for a given shot pair. As this factor will not depend on frequency, nor on energy present over a time period of one or several cycles, nor on any other changes in character except amplitude, it can be related only to the detectability by amplitude comparison when signal-to-noise ratios are greater than one. The accuracy is quite dependent on the noise level; i.e., it might be a comparison of different phases and is at best the ratio of signals plus or minus noise. Nevertheless, when

signal-to-noise ratios are large, as was the case with Murphy's measurements near the source,[4] this ratio of amplitudes is quite meaningful.

The desire to add frequency as a parameter follows from the fact that seismic attenuations are usually frequency dependent. The majority of the decoupling analysis will therefore depend on defining decoupling as the amplitude density ratio as a function of frequency. The analysis represents the ratios of the average amplitude response over a specified length of seismic record in a given frequency band. Depending on the time length and area of the seismogram from which the samples are selected these ratios can describe the decoupling as determined for the first arriving refractions, the body wave segment of the record, or the total seismic signal return. These ratios are only dependent upon the seismic signal and noise variations. The transfer characteristics of the seismometer, the seismometer environment, the recording system, and the earth travel path can be assumed constant between tamped and decoupled shots. Hence, the ratio of the amplitude density responses is only dependent on the differences in amplitude density characteristics of the source signals and the ambient seismic noise. In this case we need not limit the analysis to recordings with high signal-to-noise ratios for it is often possible to compensate for the noise.

B. COMPUTATION OF SIGNAL AND NOISE SPECTRA FOR DECOUPLING CALCULATIONS

Signal and noise are statistically different and in an operation calling for the subtraction of frequency responses much care must be taken in order to maintain valid results. The signals as recorded on a seismogram can be thought of as aperiodic functions having a finite duration and energy. Seismic noise, however, is best modeled by a random function as it has infinite time duration and energy. The spectral analysis of the signals and noise follows the interpretation of Y. W. Lee[2]:

1. The appropriate signal or noise section of the data is defined as

$$f_1(t) \text{ from } \underline{-T \text{ to } +T}.$$

2. An autocorrelation approximating the integral is

$$\phi_{11}(\tau) = \lim_{T \to \infty} \frac{1}{2T} \int_{-T}^{T} f_1(t)\, f_1(t+\tau)\, dt$$

for the finite sample time -T to +T.

3. The cosine transform of the autocorrelation is

$$\Phi_{11}(\omega) = \frac{1}{2\pi} \int_{-\infty}^{\infty} \phi_{11}(\tau)\, e^{-i\omega t}\, dt$$

The Fourier transform of the autocorrelation of an aperiodic function is an energy density spectrum of the time function $f_1(t)$. The Fourier transform of the autocorrelation of a random function is a power density spectrum per 2T unit time of the function $f_1(t)$. Since power is defined as energy expended over a unit time, it is seen that if the noise and signal samples are of the same length or the values normalized to the same length the two spectra are directly comparable. As a result of this normalization these power density and energy density estimates can be directly related to amplitude density estimates used in calculations of decoupling by taking the square root of each value. These energy density spectra are also directly related to ground particle velocities as shown in Appendix A.

Figures 7 through 14 present smoothed energy density spectra of signals and power density spectra of the noise samples for the 500 and 1000-pound decoupled and tamped events 8, 9, 10, and 11 as recorded by the S-41 seismometers at stations 5B, 5D, 5E and 5F. In the case of the 500-pound shots, .256-second samples of the first arrivals have been analyzed in addition to the 2.048-second noise and signal samples. On some of the graphs the noise spectra have been subtracted from the signal plus noise values for the decoupled events in order to present an estimate of noiseless decoupled signal spectra.

The analysis herein did not include the spectra of samples longer than the 2.048-seconds presented and hence no surface wave energy is included in the analysis. The tamped shot signal return appears to continue for many seconds after the initial refraction arrivals whereas the decoupled shots do not appear to have generated the same ratio of surface wave to body wave energy and the surface wave modes are not apparent on the field records. An analysis of the first two seconds of energy return will therefore not be a true total energy spectrum, especially for the tamped shots. As the surface waves appear to be predominantly of low frequency content, this truncation of the signal should only affect the energy density spectra for frequencies less than 10 cps.

C. DECOUPLING CALCULATIONS

1. Peak Amplitude Comparison

The ratio of the peak particle velocities was computed for the 500-pound tamped and decoupled shots as recorded at stations 5A through

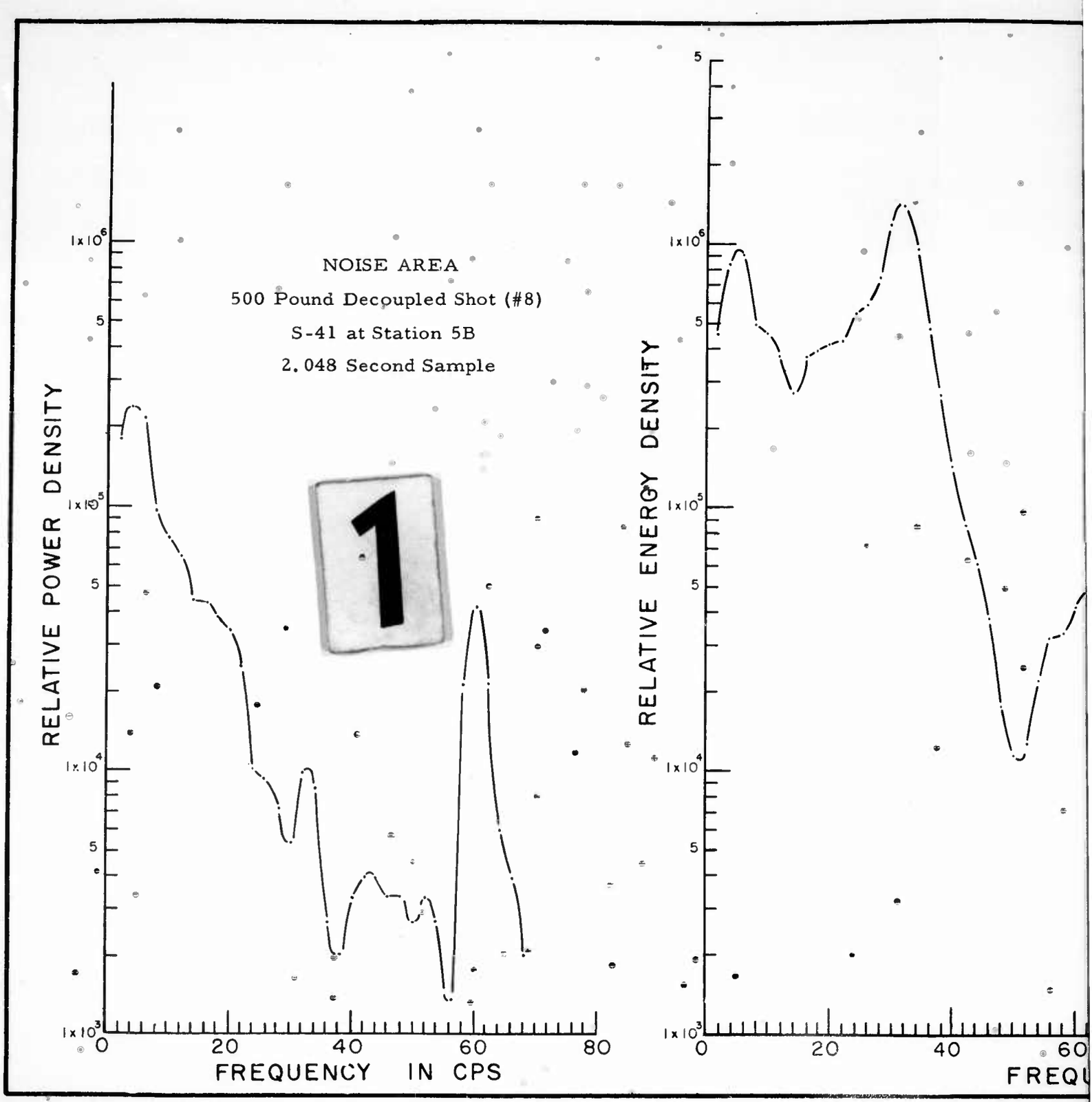
NOISE AREA
500 Pound Decoupled Shot (#8)
S-41 at Station 5B
2.048 Second Sample
1
RELATIVE POWER DENSITY
1x10^6
5
1x10^5
5
1x10^4
5
1x10^3
0
20
40
60
80
FREQUENCY IN CPS
RELATIVE ENERGY DENSITY
1x10^6
5
1x10^5
5
1x10^4
5
1x10^3
0
20
40
60
FREQU

SIGNAL AREA

500 Pound Decoupled Shot (#8)

S-41 at Station 5B

2.048 Second Sample

2

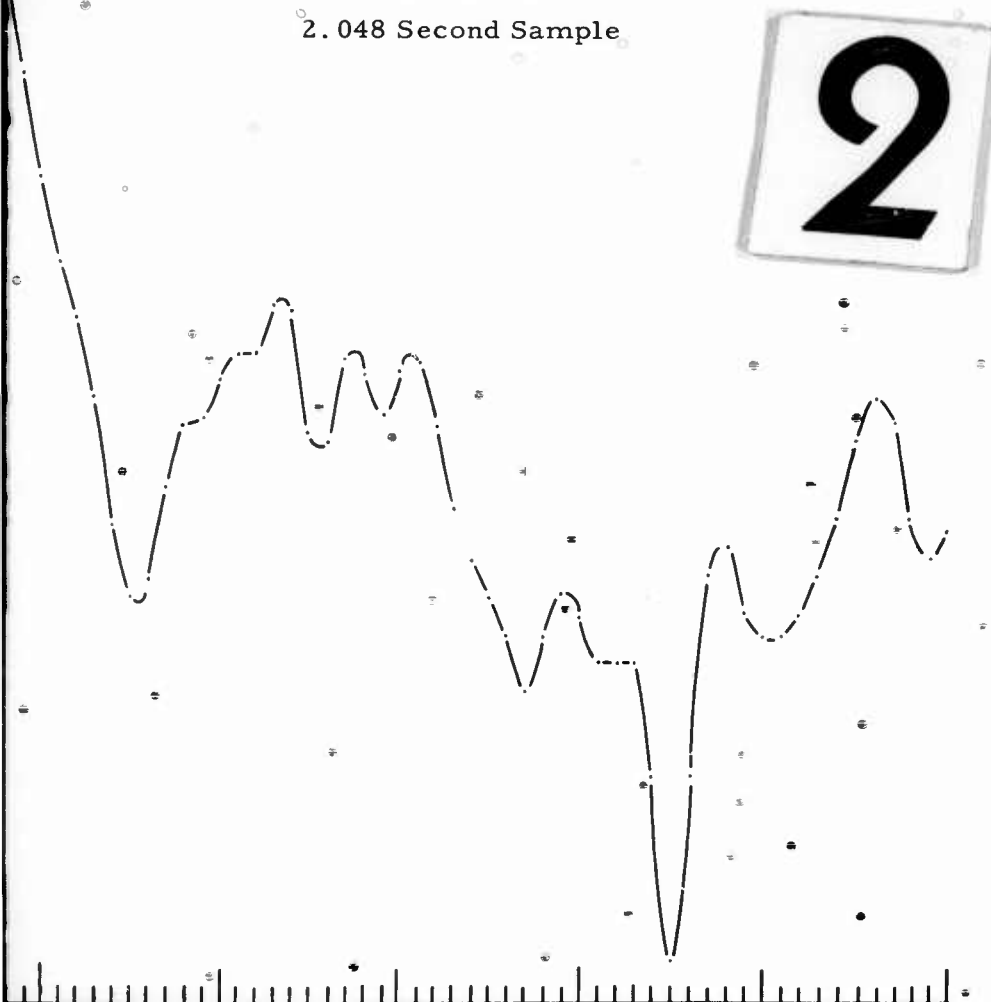

SIGNAL MINUS

500 Pound De

S-41 at

2.048 Sec

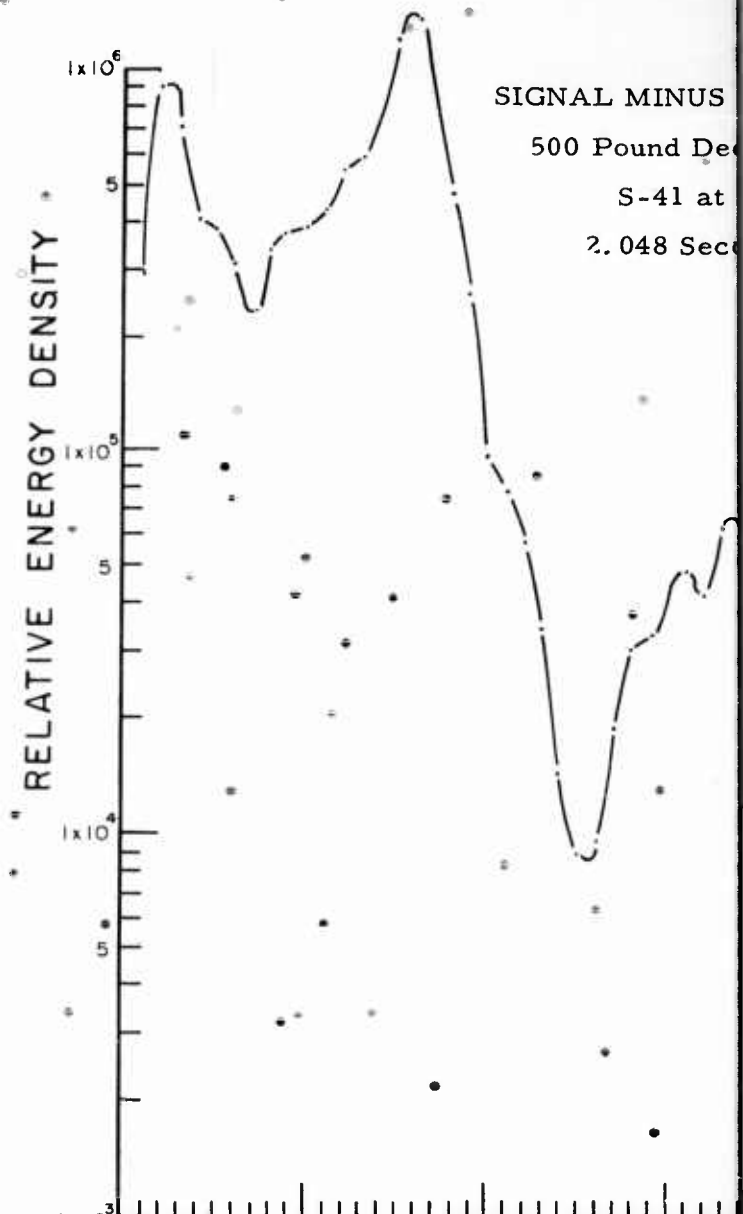

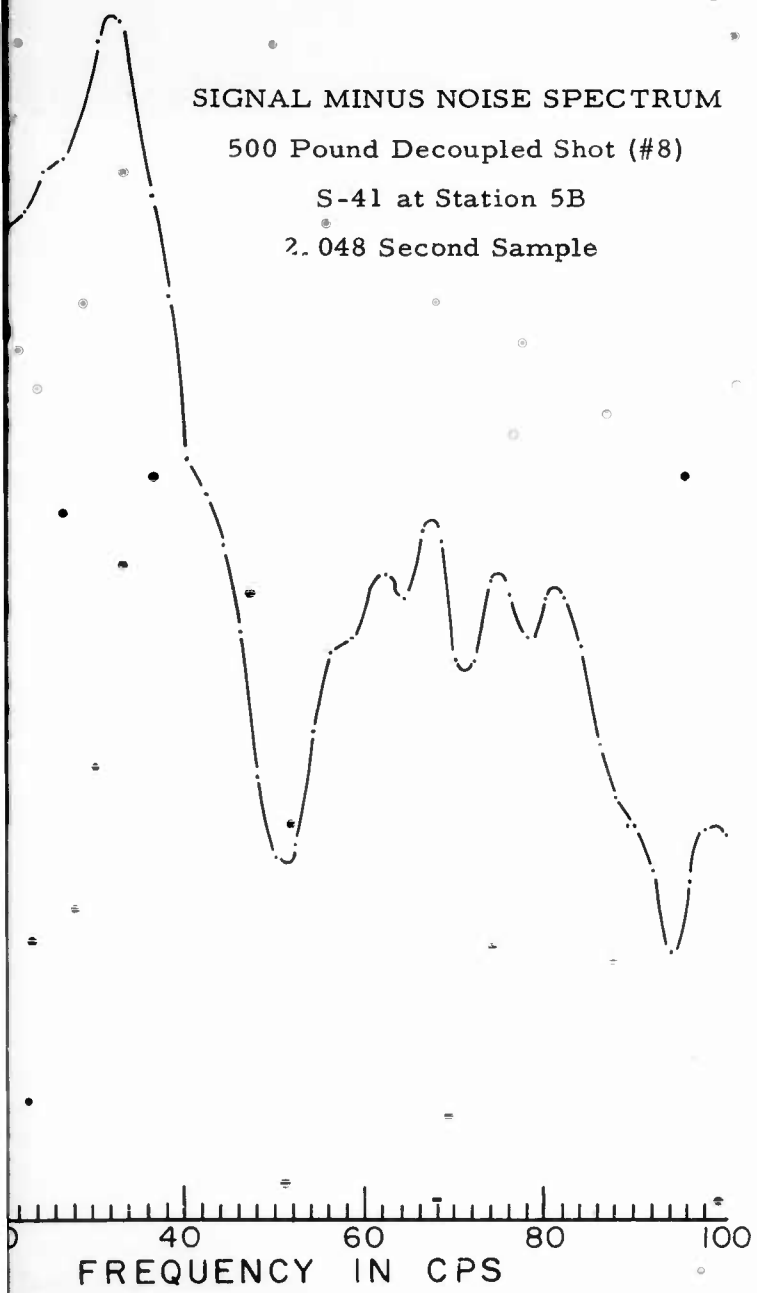
SIGNAL MINUS NOISE SPECTRUM
500 Pound Decoupled Shot (#8)
S-41 at Station 5B
2.048 Second Sample
40
60
80
100
FREQUENCY IN CPS

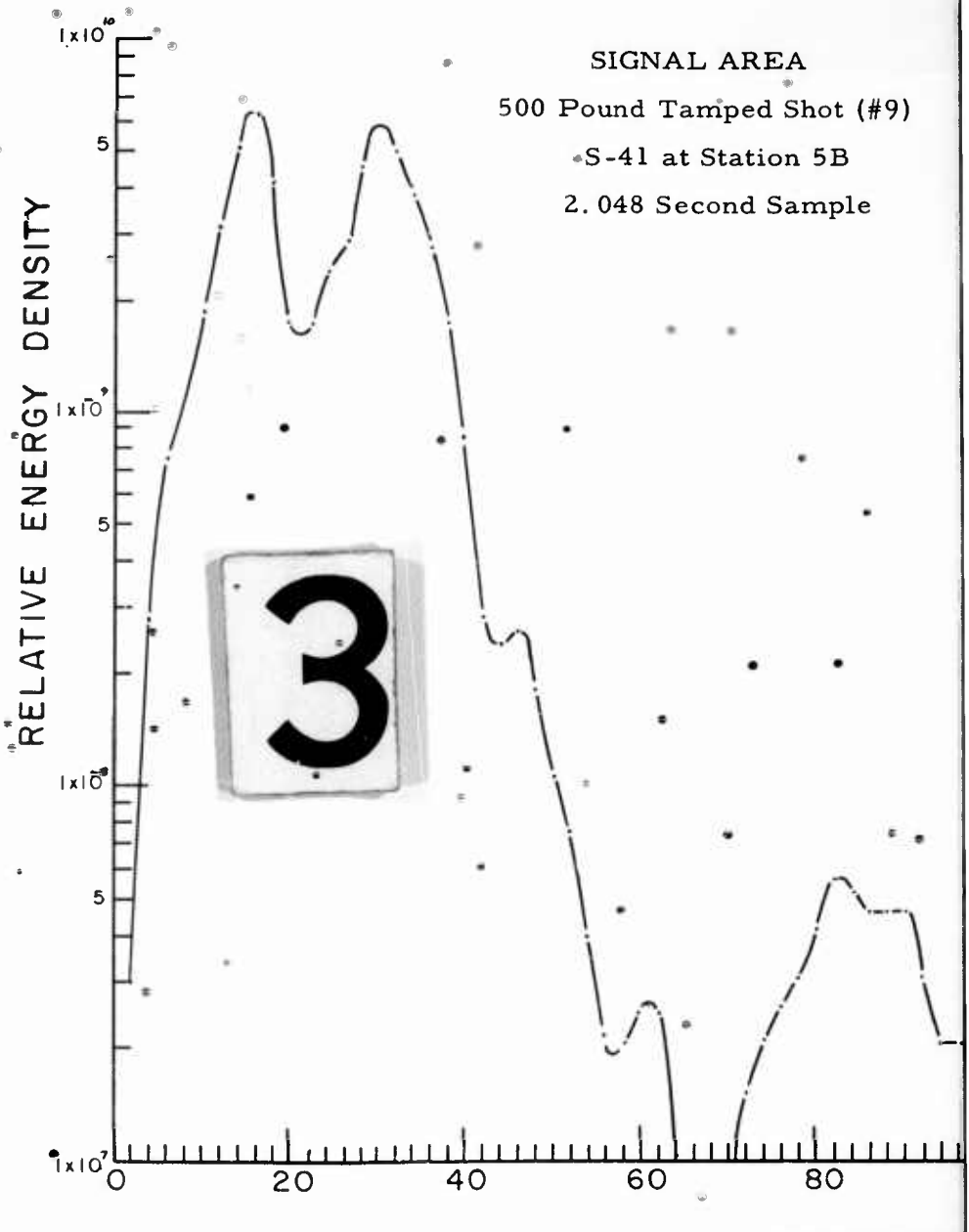
SIGNAL AREA
500 Pound Tamped Shot (#9)
S-41 at Station 5B
2.048 Second Sample
RELATIVE ENERGY DENSITY
1x10
5
1x10
5
1x10
5
1x10
0
20
40
60
80

4

SIGNAL AREA

500 Pound Tamped Shot (#9)

S-41 at Station 5B

2.048 Second Sample

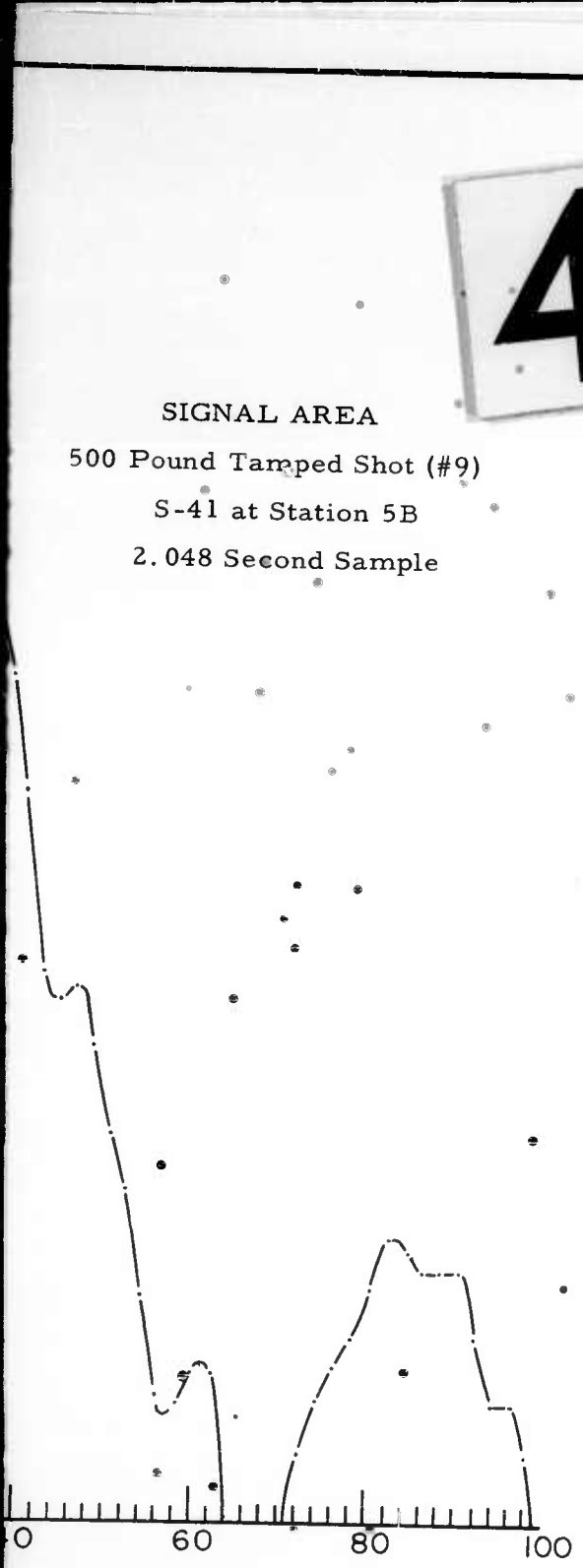

SIGNAL AREA

500 Pound Decoupled Shot

Station 5B

.256 Second Sample

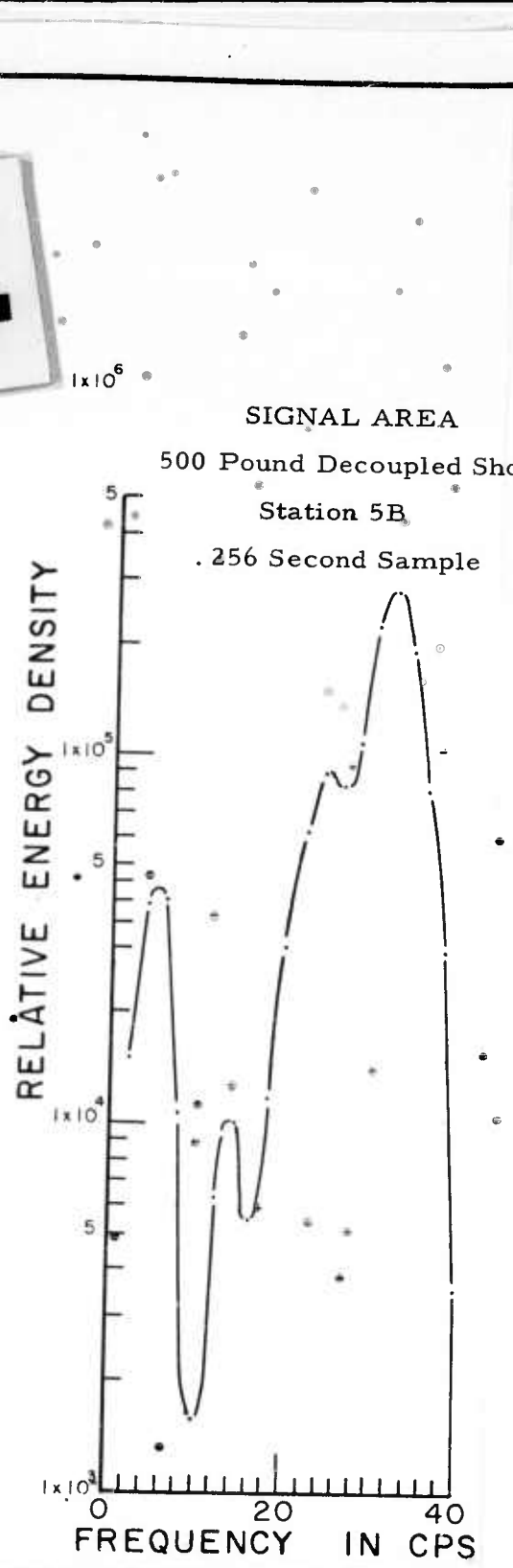

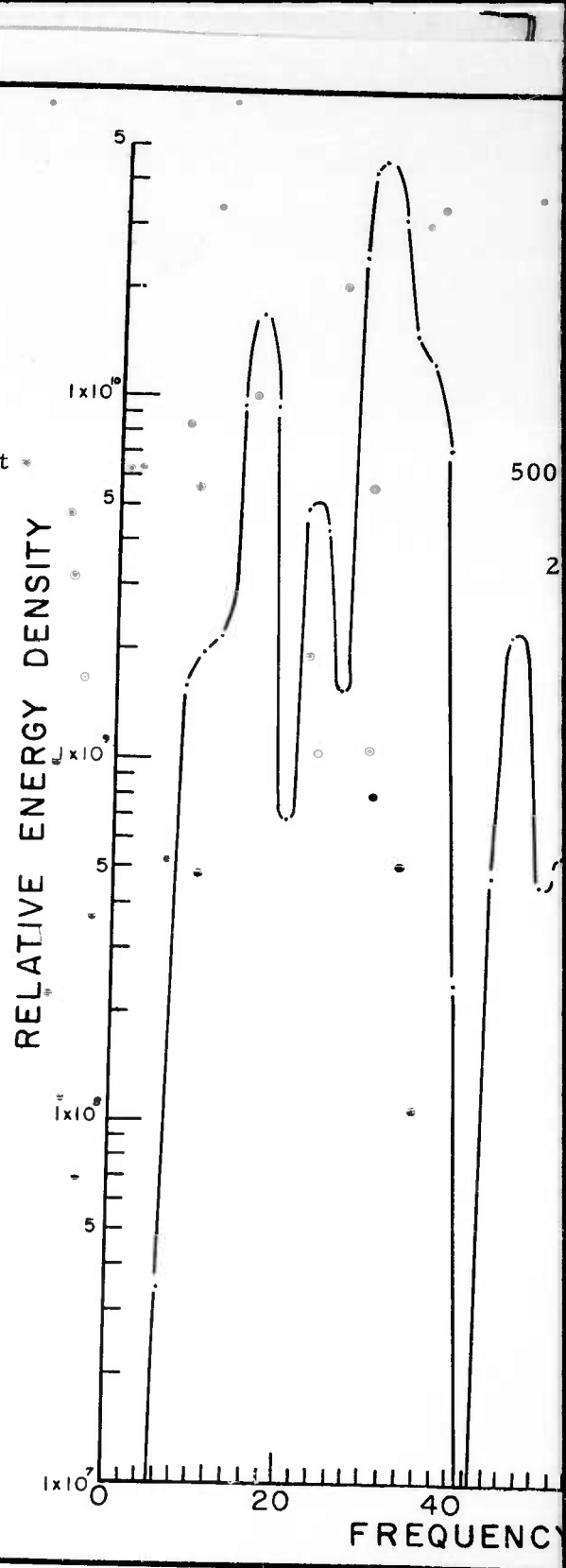

Smoothed Energy De
Power Density Spec
for the 500 p
and Tamp

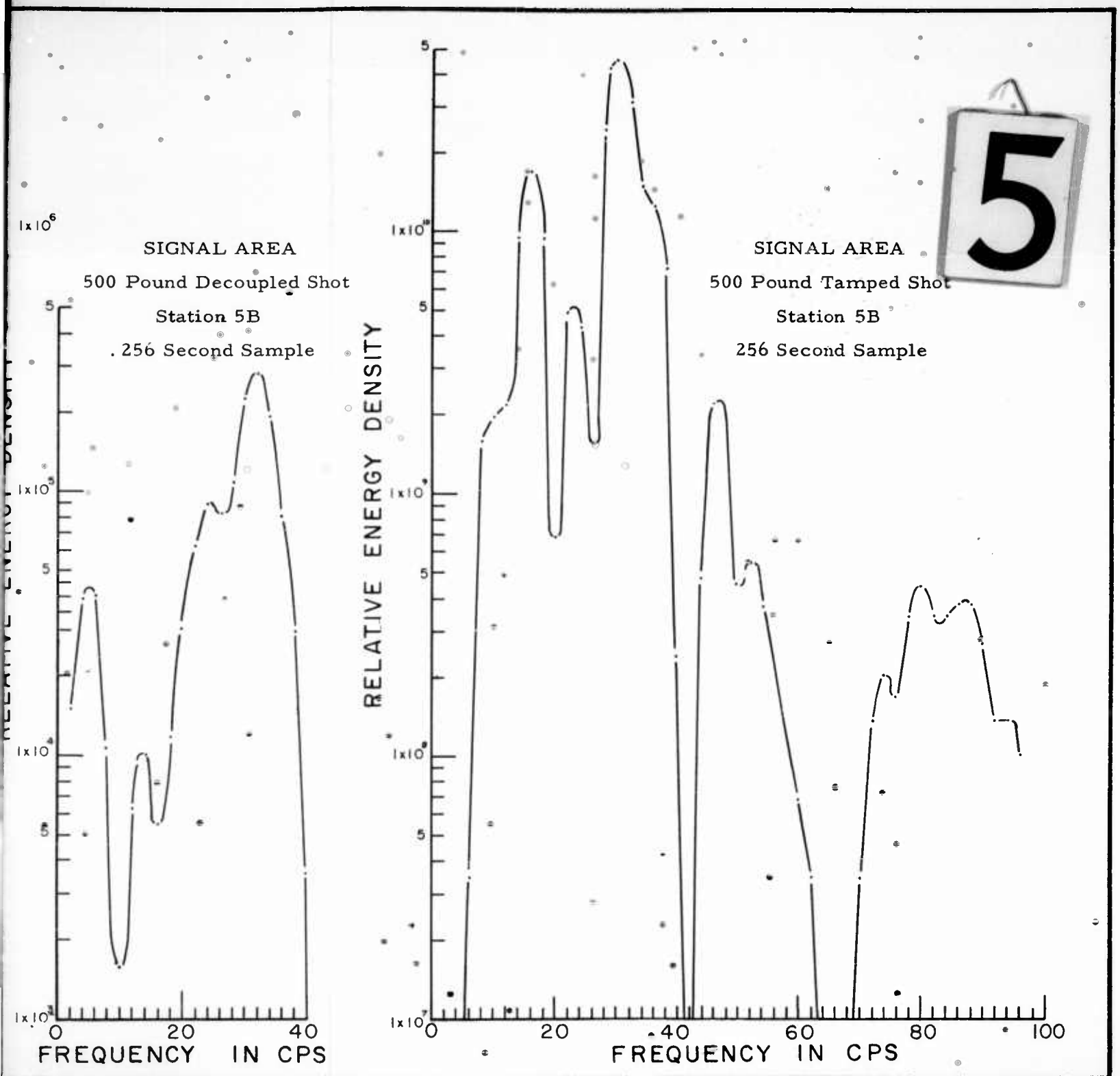

Fig. 7

Smoothed Energy Density Spectra of Signals and Power Density Spectra of the Noise Samples for the 500 pound Decoupled and Tamped Events

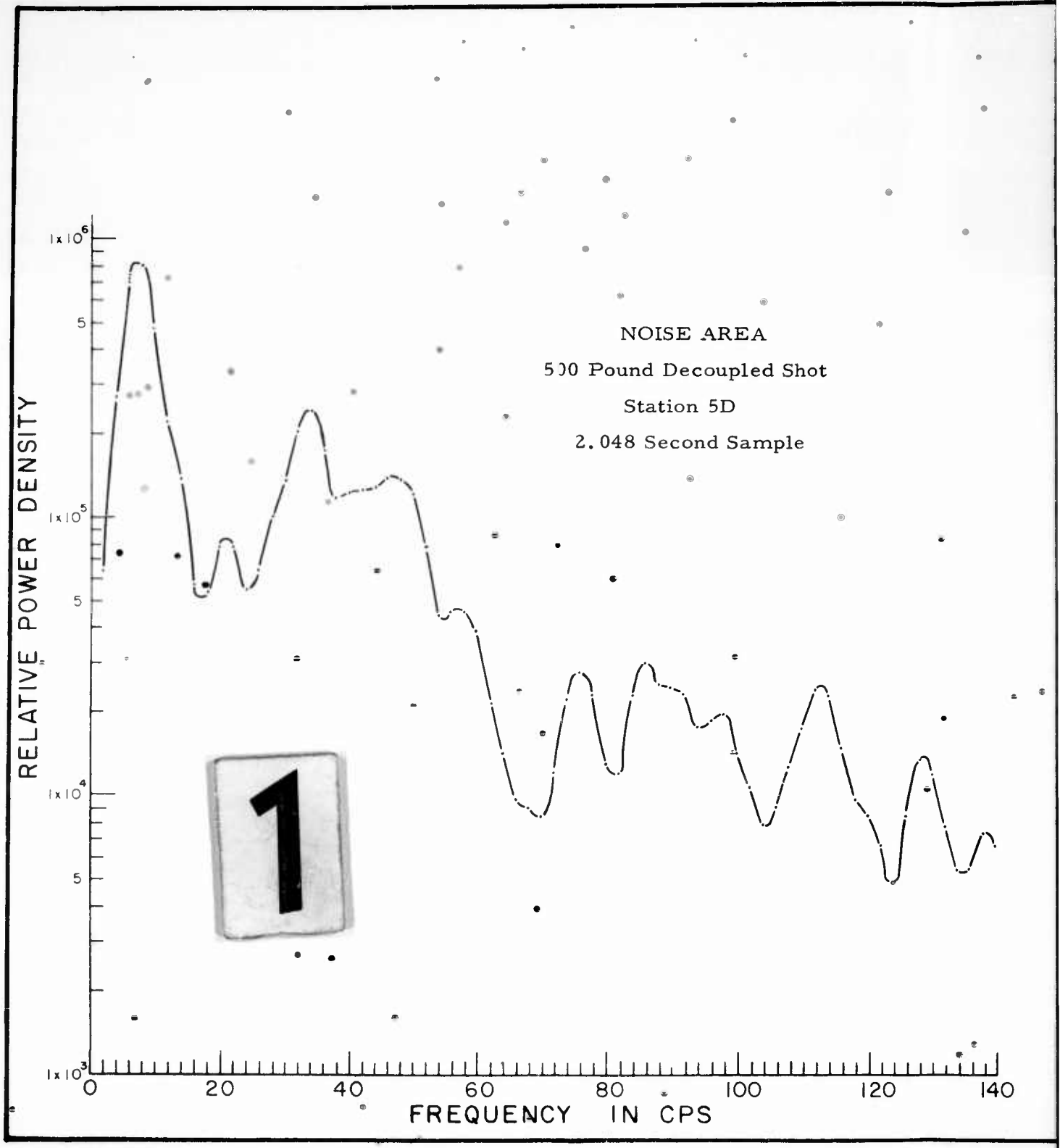
NOISE AREA
500 Pound Decoupled Shot
Station 5D
2.048 Second Sample
RELATIVE POWER DENSITY
1x10^6
5
1x10^5
5
1x10^4
5
1x10^3
0
20
40
60
80
100
120
140
FREQUENCY IN CPS

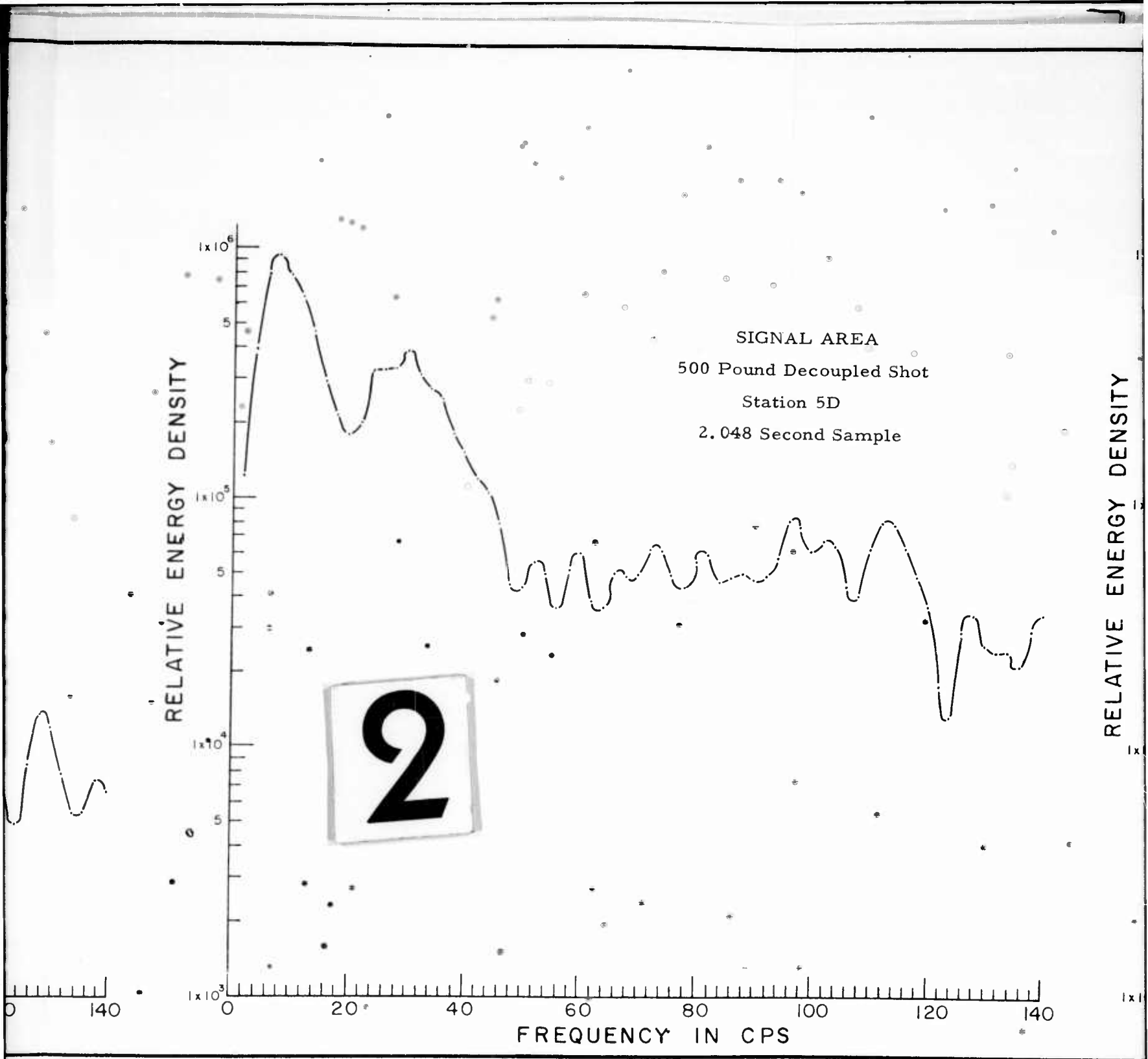
SIGNAL AREA
500 Pound Decoupled Shot
Station 5D
2.048 Second Sample
RELATIVE ENERGY DENSITY
1x10^6
5
1x10^5
5
1x10^4
5
1x10^3
0
20
40
60
80
100
120
140
FREQUENCY IN CPS
2

SIGNAL AREA

500 Pound Tamped Shot

Station 5D

2.048 Second Sample

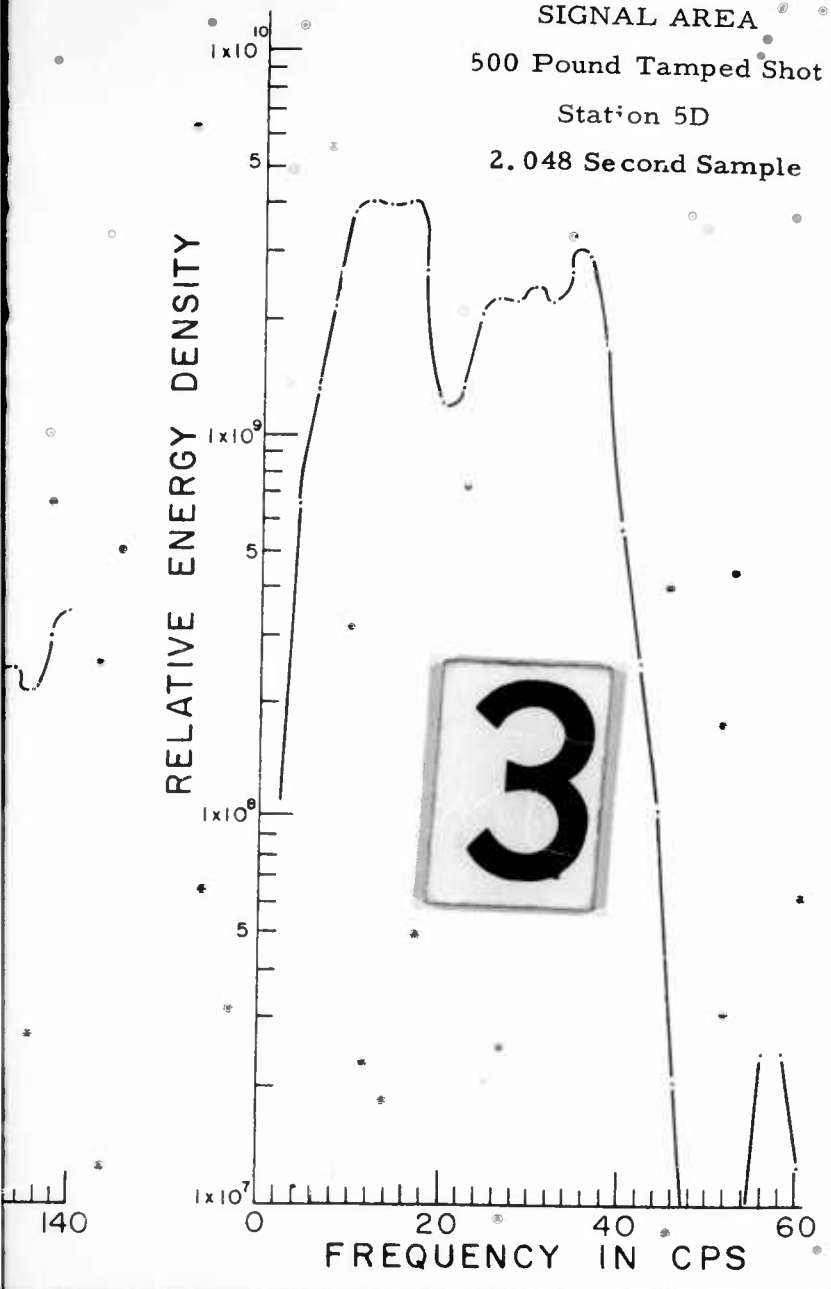

3

SIGNA

500 Pound D

Statio

.256 Seco

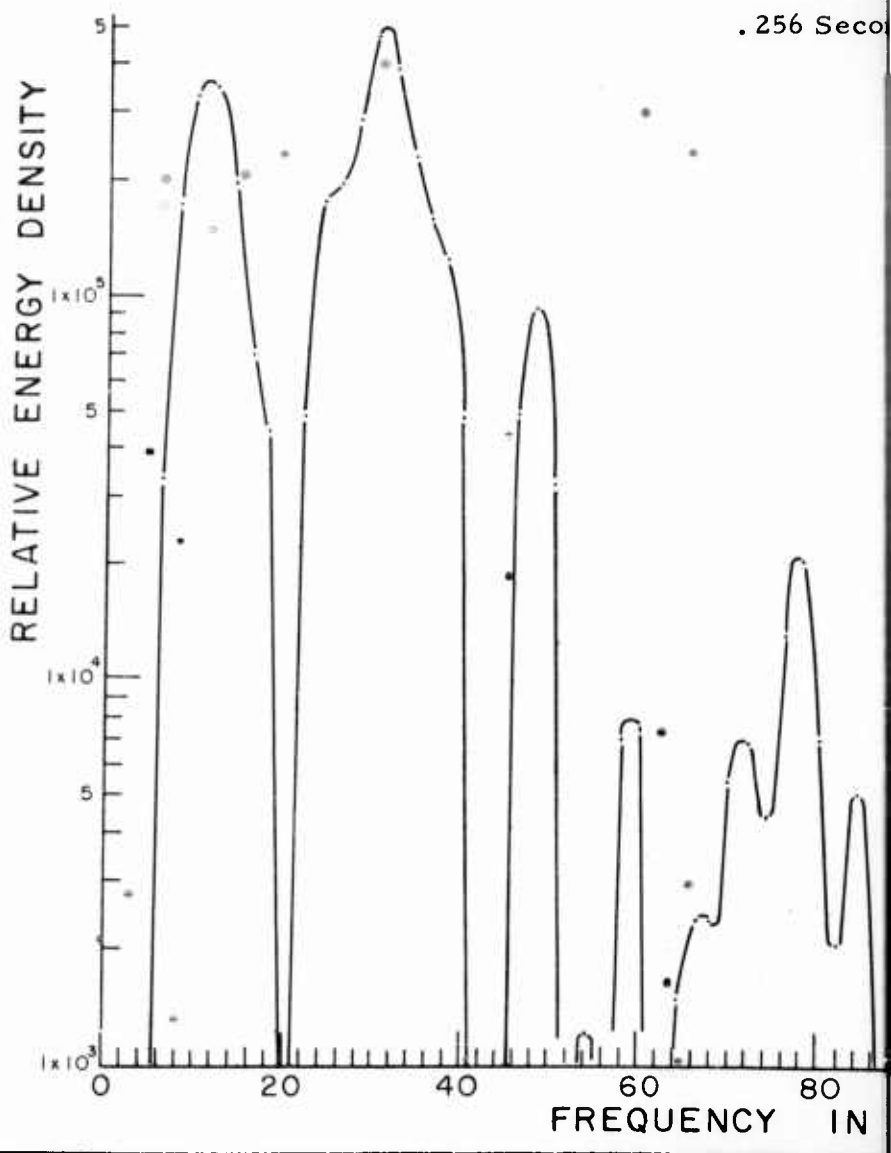

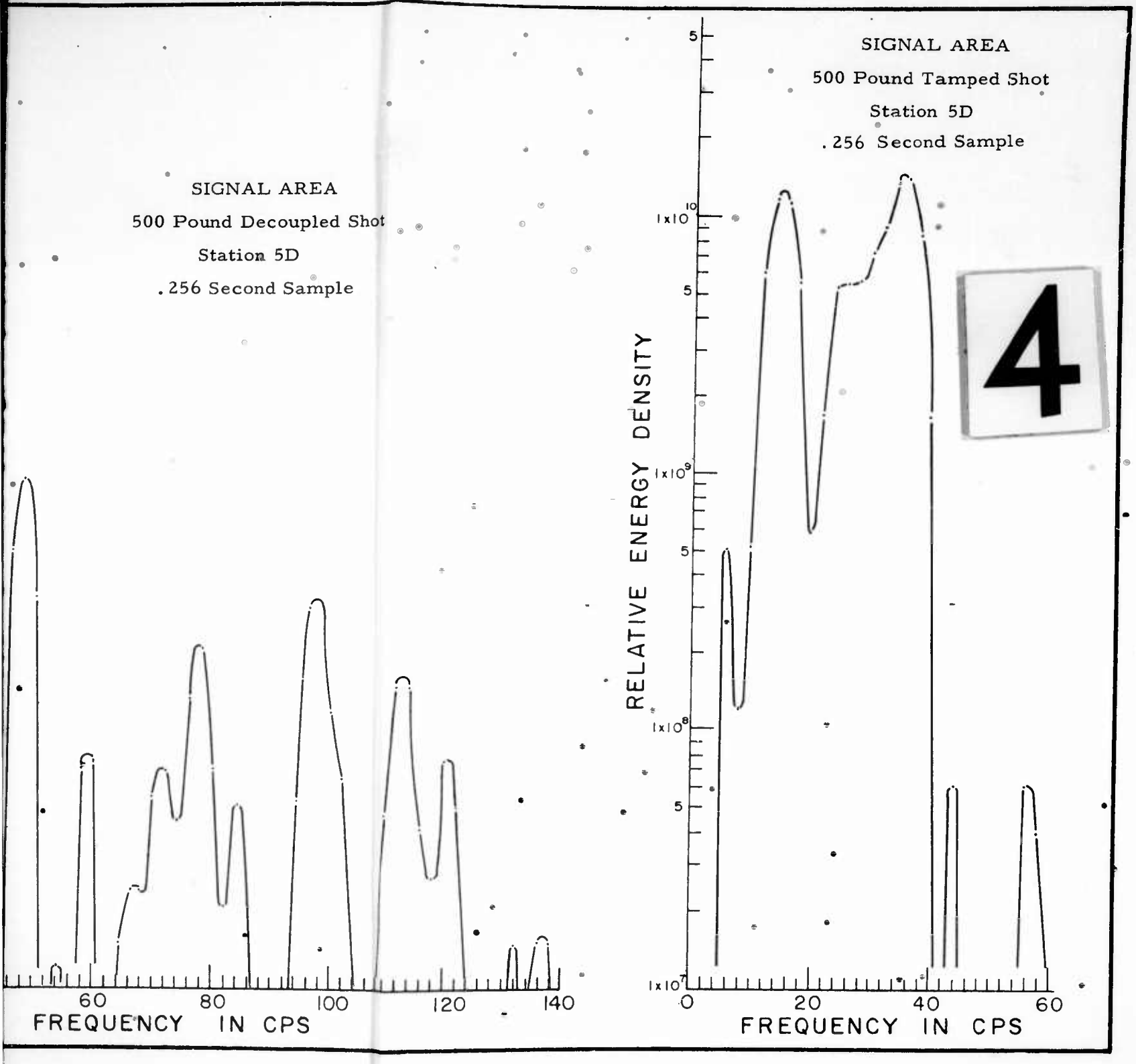

Fig. 8

Smoothed Energy Density Spectra of Signals and Power Density Spectra of the Noise Samples for the 500 pound Decoupled and Tamped Events

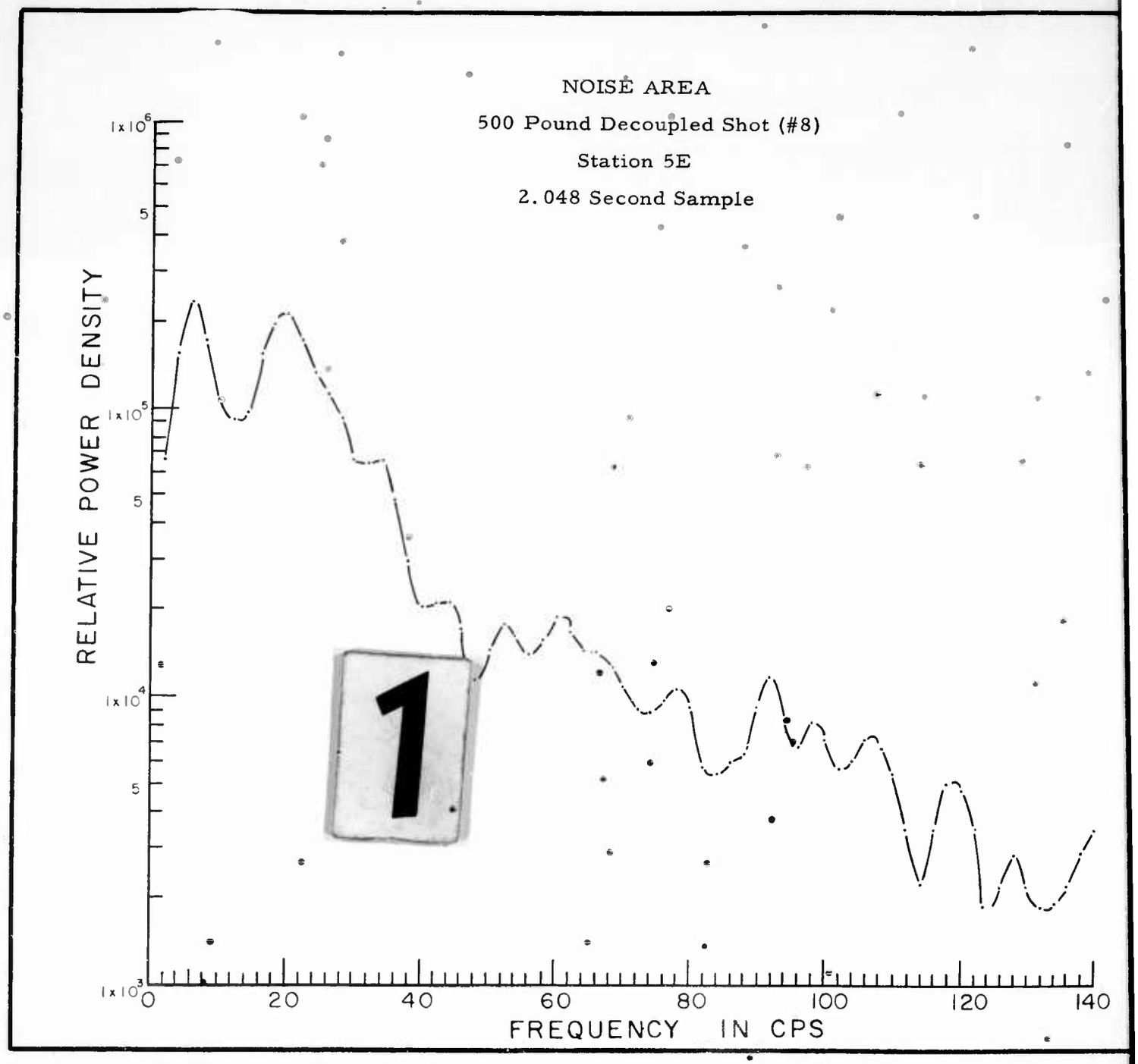
NOISE AREA
500 Pound Decoupled Shot (#8)
Station 5E
2.048 Second Sample
RELATIVE POWER DENSITY
1x10^6
5
1x10^5
5
1x10^4
5
1x10^3
0
20
40
60
80
100
120
140
FREQUENCY IN CPS

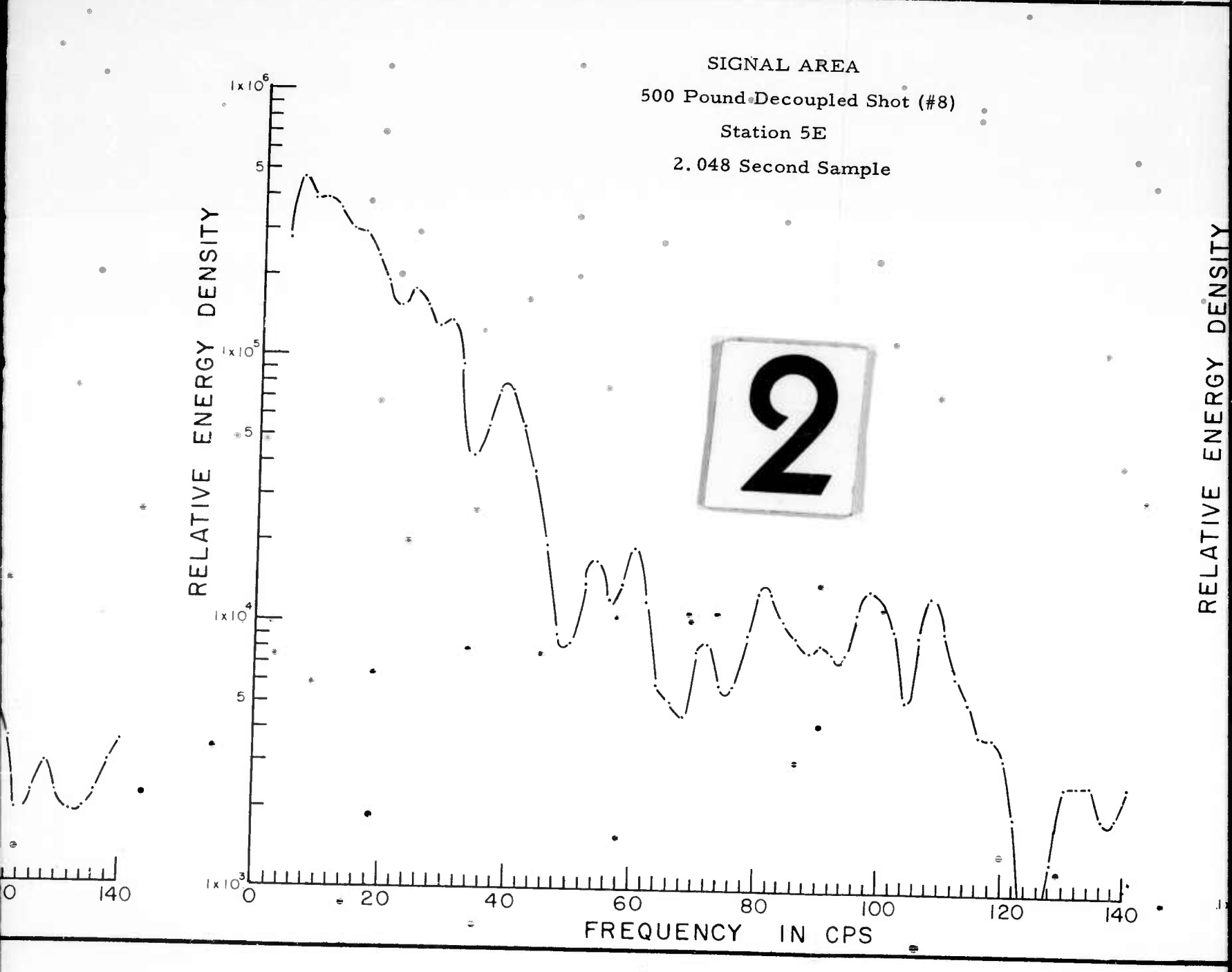
SIGNAL AREA
500 Pound Decoupled Shot (#8)
Station 5E
2.048 Second Sample
2
RELATIVE ENERGY DENSITY
1x10^6
5
1x10^5
5
1x10^4
5
1x10^3
0
20
40
60
80
100
120
140
FREQUENCY IN CPS
RELATIVE ENERGY DENSITY

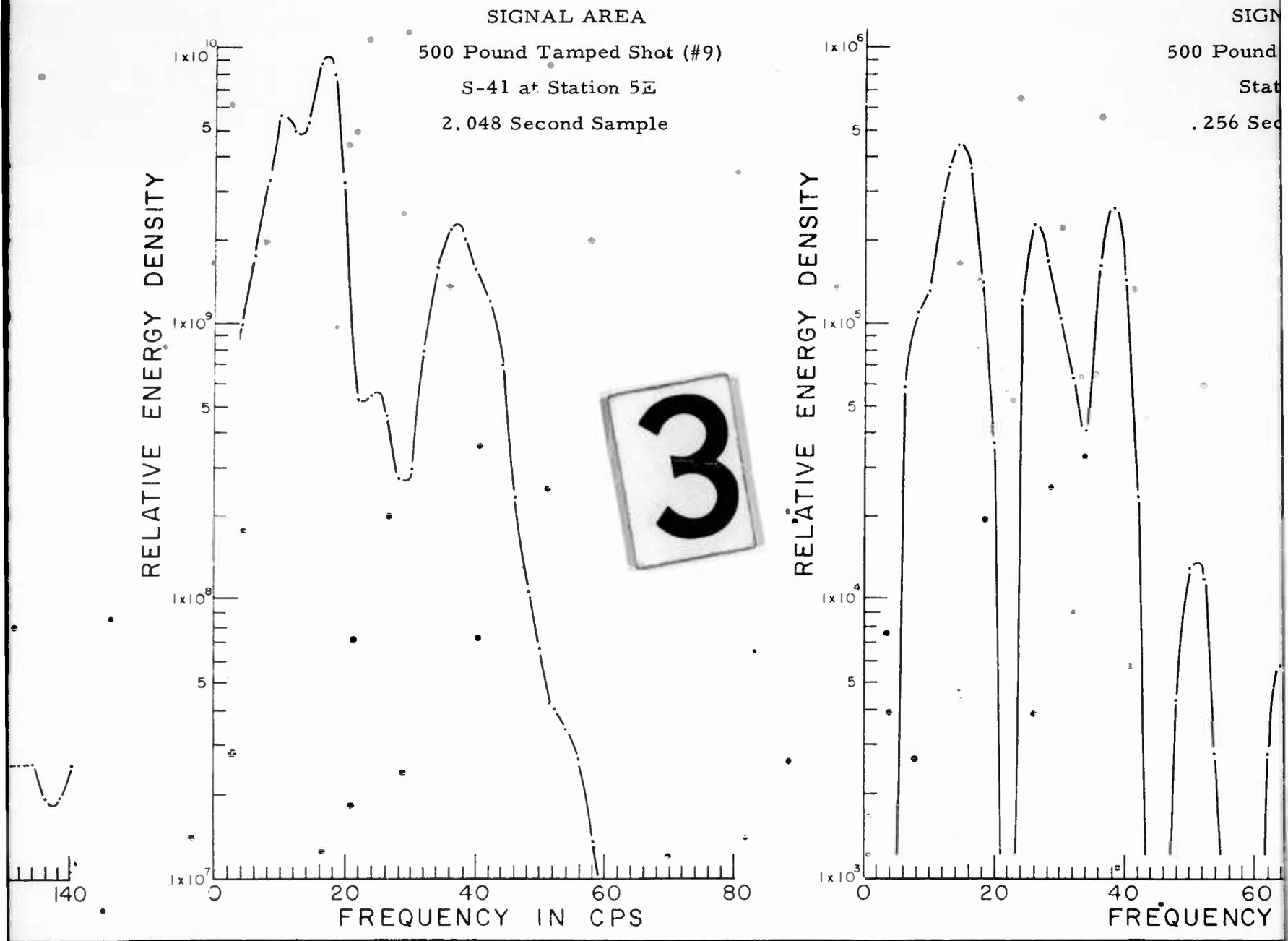
SIGNAL AREA
500 Pound Tamped Shot (#9)
S-41 at Station 5E
2.048 Second Sample
RELATIVE ENERGY DENSITY
1x10^10
5
1x10^9
5
1x10^8
5
1x10^7
0
20
40
60
80
140
FREQUENCY IN CPS
3
SIGN
500 Pound
Stat
.256 Sec
RELATIVE ENERGY DENSITY
1x10^6
5
1x10^5
5
1x10^4
5
1x10^3
0
20
40
60
FREQUENCY

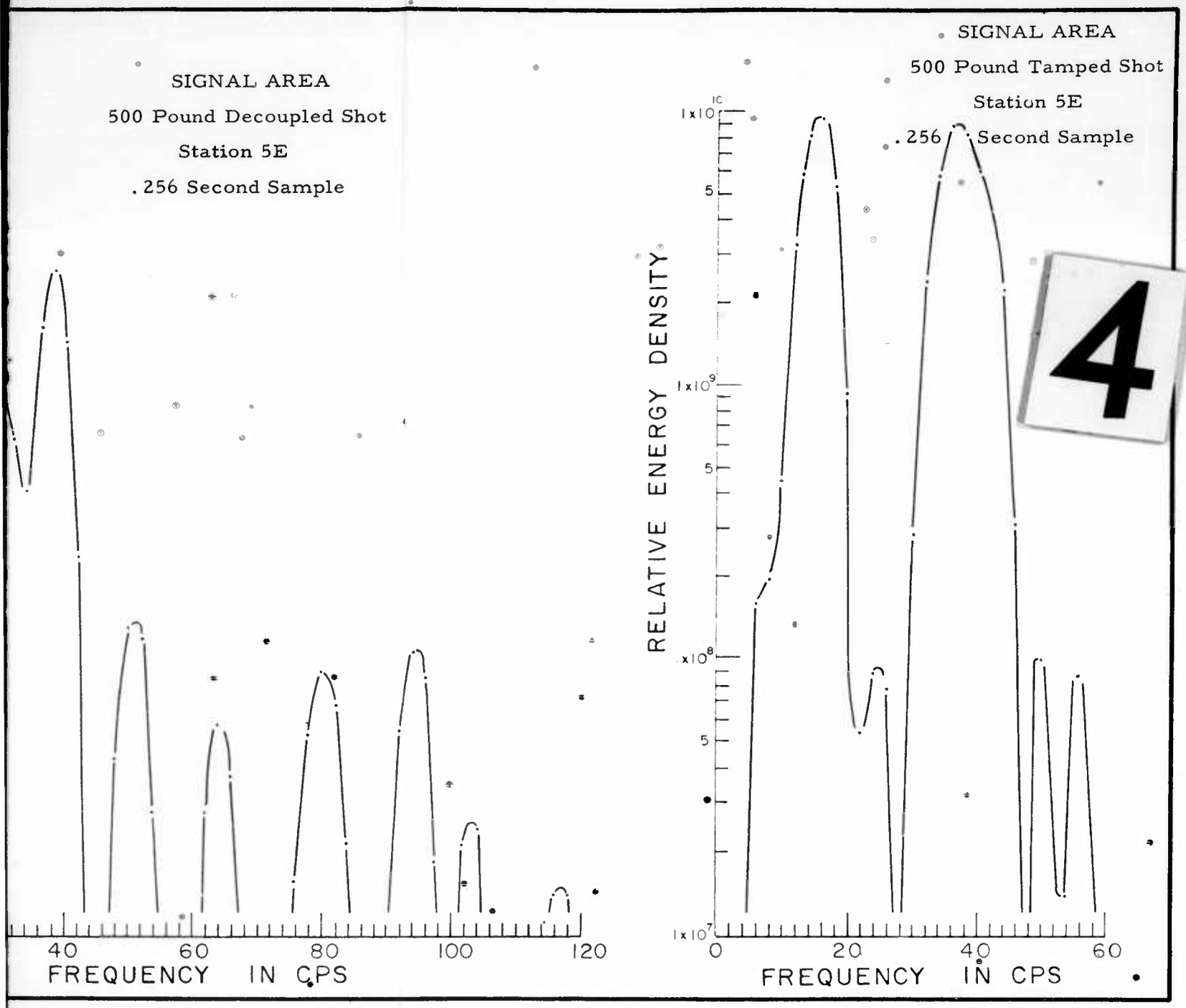

Fig. 9
Smoothed Energy Density Spectra of Signals and
Power Density Spectra of the Noise Samples
for the 500 pound Decoupled
and Tamped Events

NOISE AREA

500 Pound Decoupled Shot

Station 5F

2.048 Second Sample

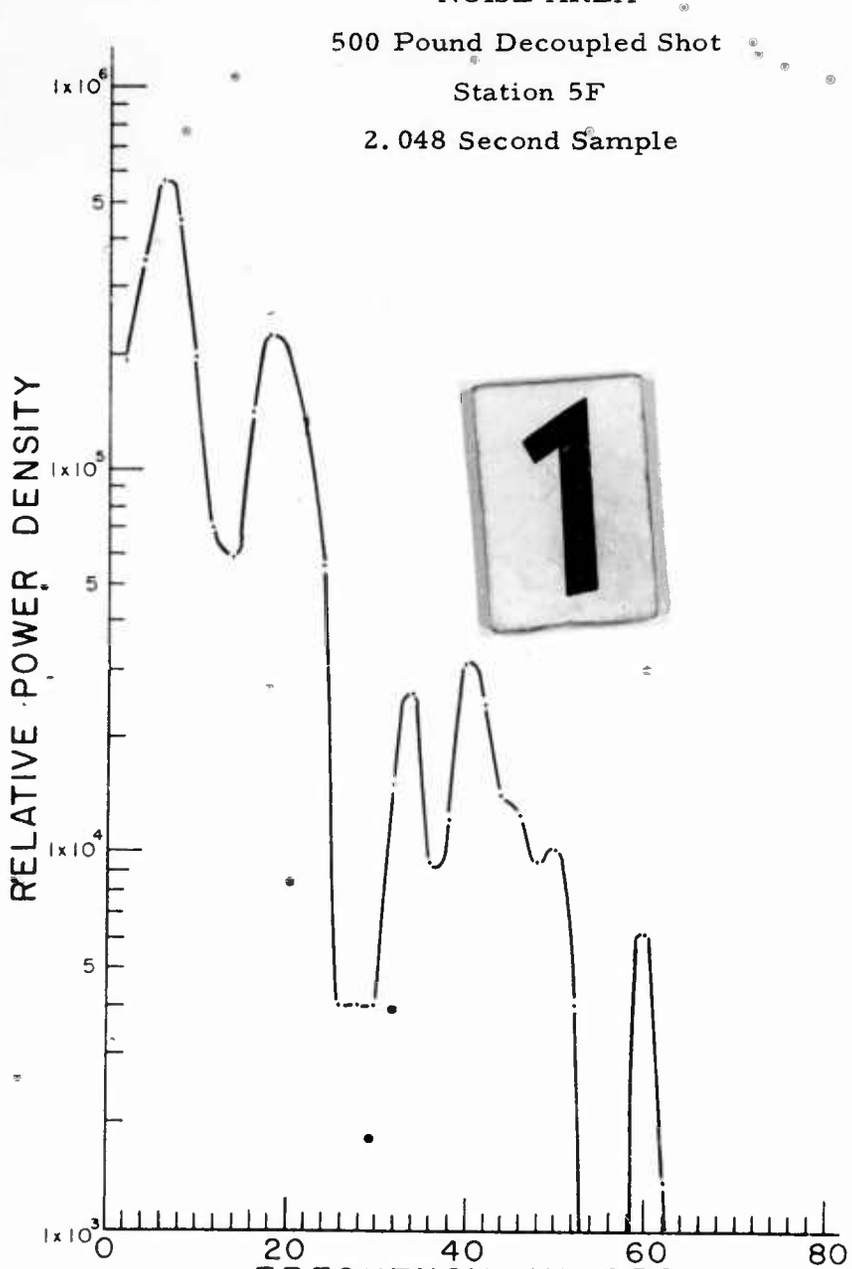

SIGN

500 Pound

Sta

2.048 Sec

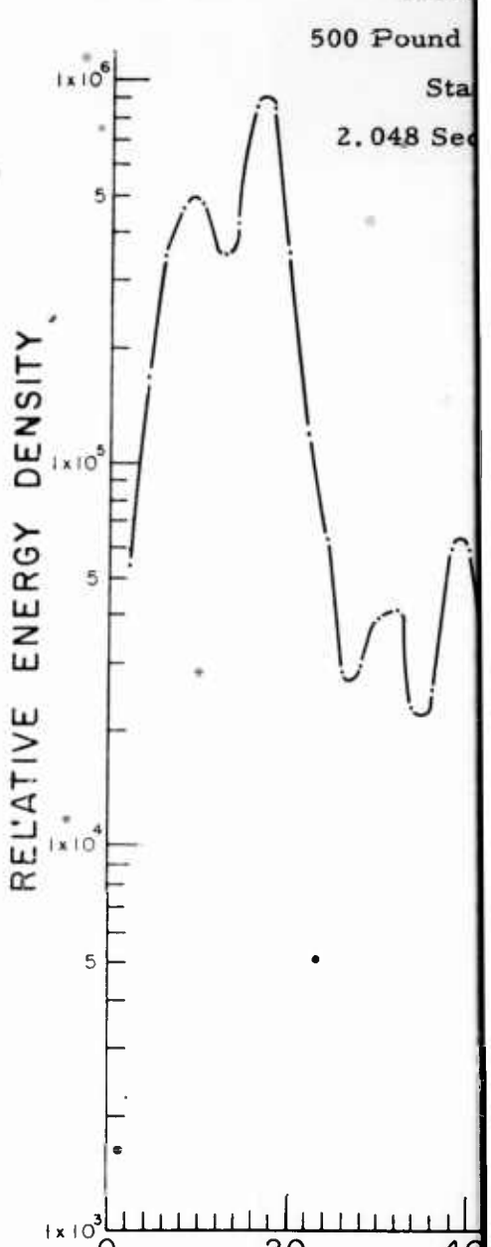

SIGNAL AREA
500 Pound Decoupled Shot
Station 5F
2.048 Second Sample

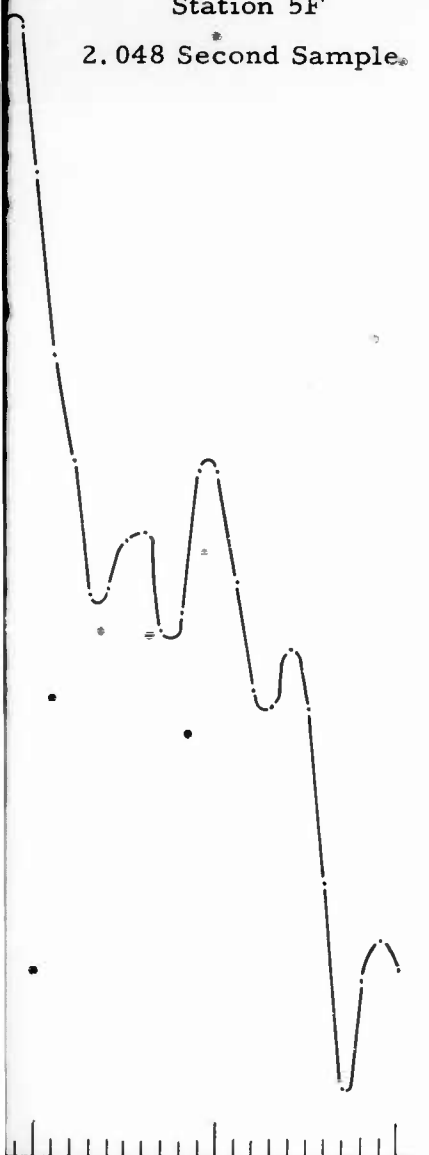

SIGNAL AREA
500 Pound Tamped Shot
Station 5F
2.048 Second Sample

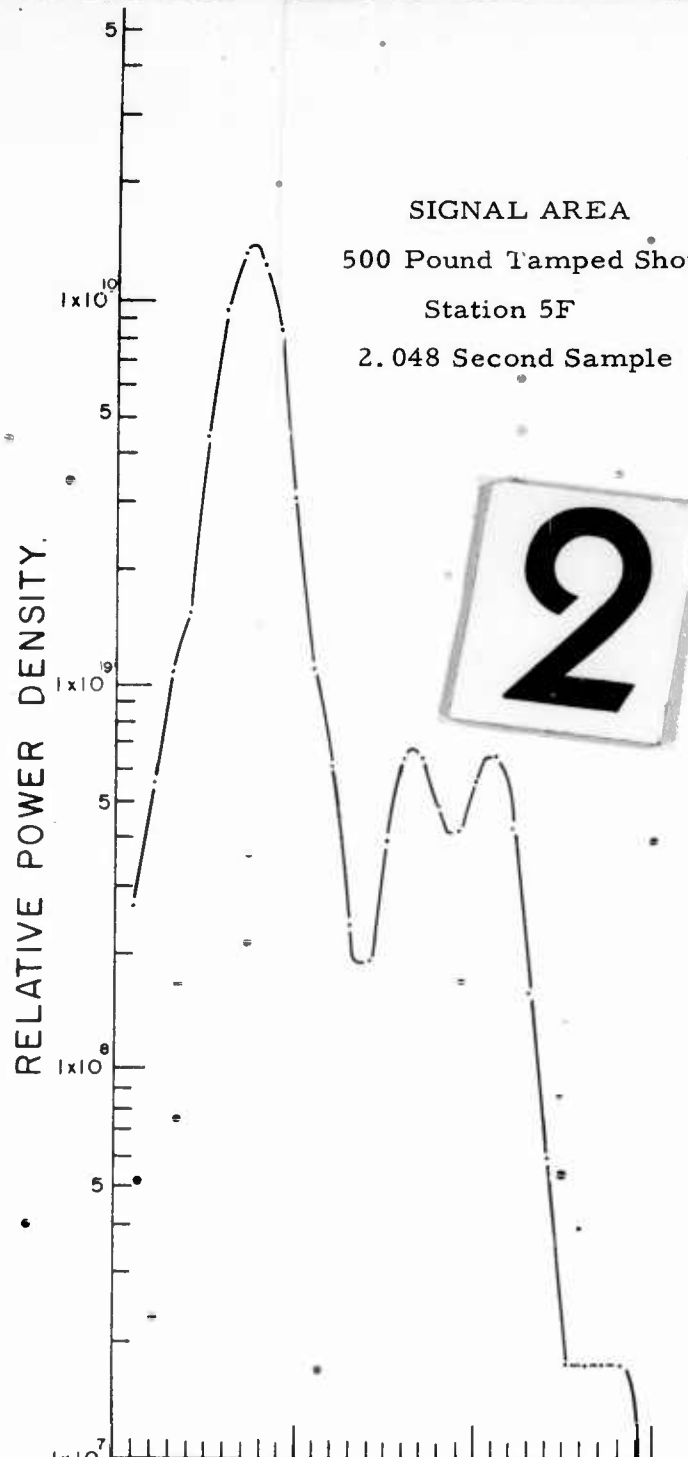

2

SIGNAL A
500 Pound Decc
Station
.256 Second

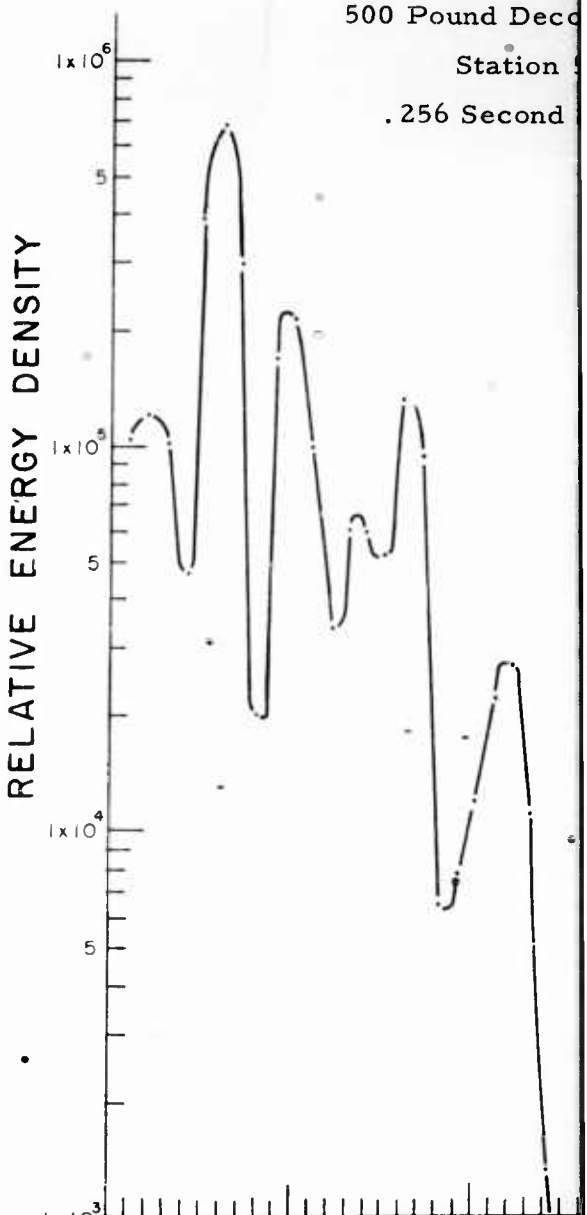

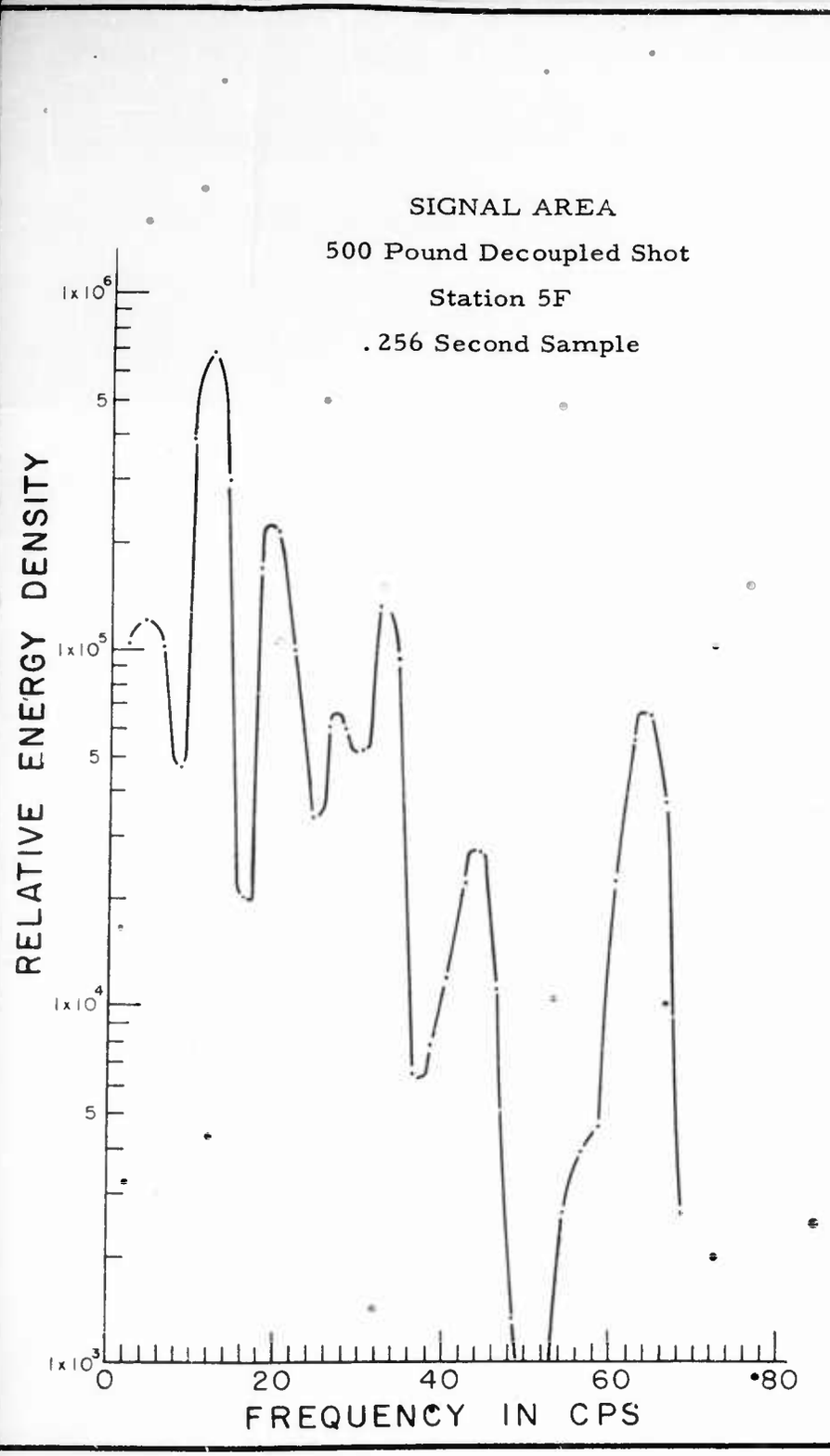

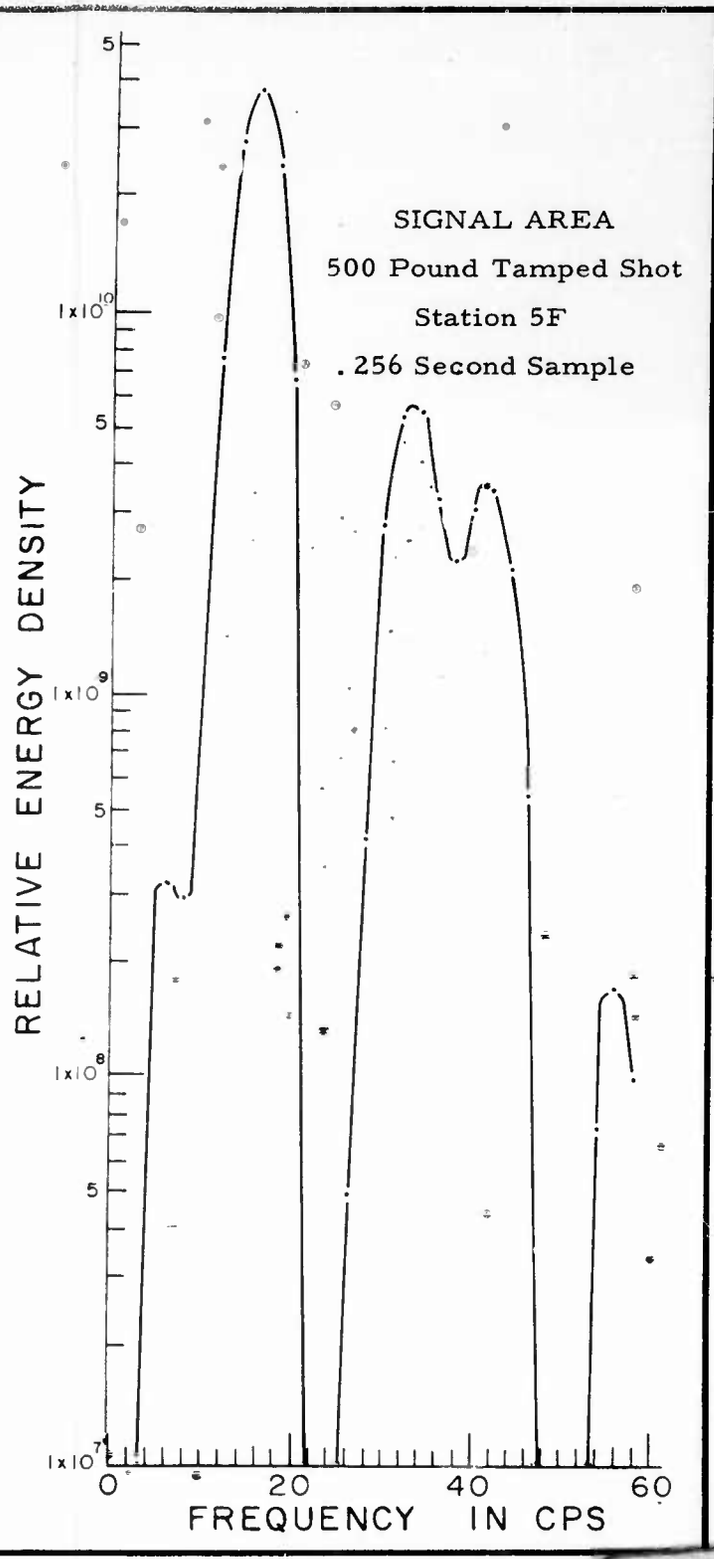

Fig. 10

Smoothed Energy Density Spectra of Signals and Power Density Spectra of the Noise Samples for the 500 pound Decoupled and Tamped Events

3

NOISE AREA

1000 Pound Decoupled Shot (#10)

S-41 at Station 5B

2.048 Second Sample

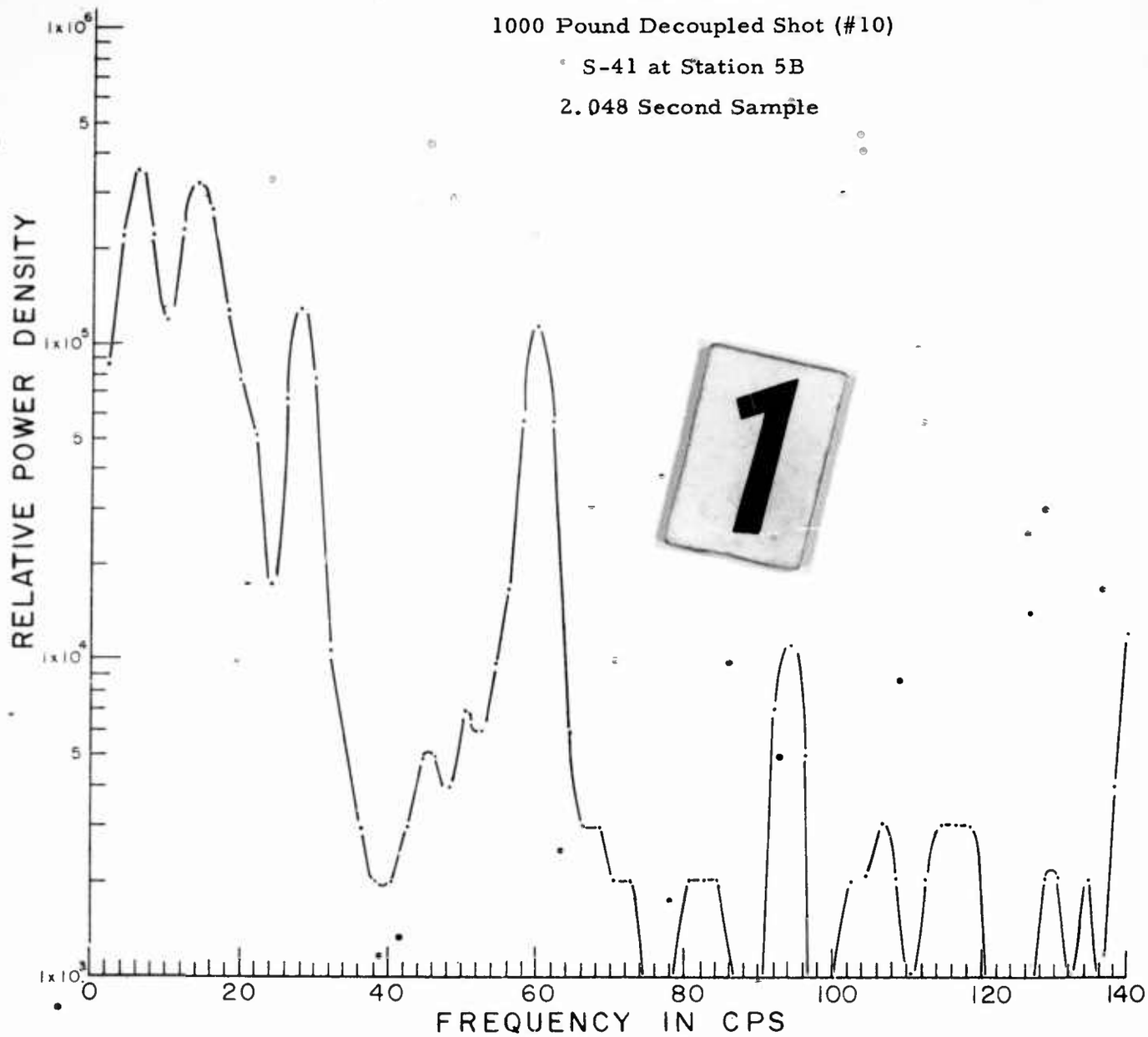

1

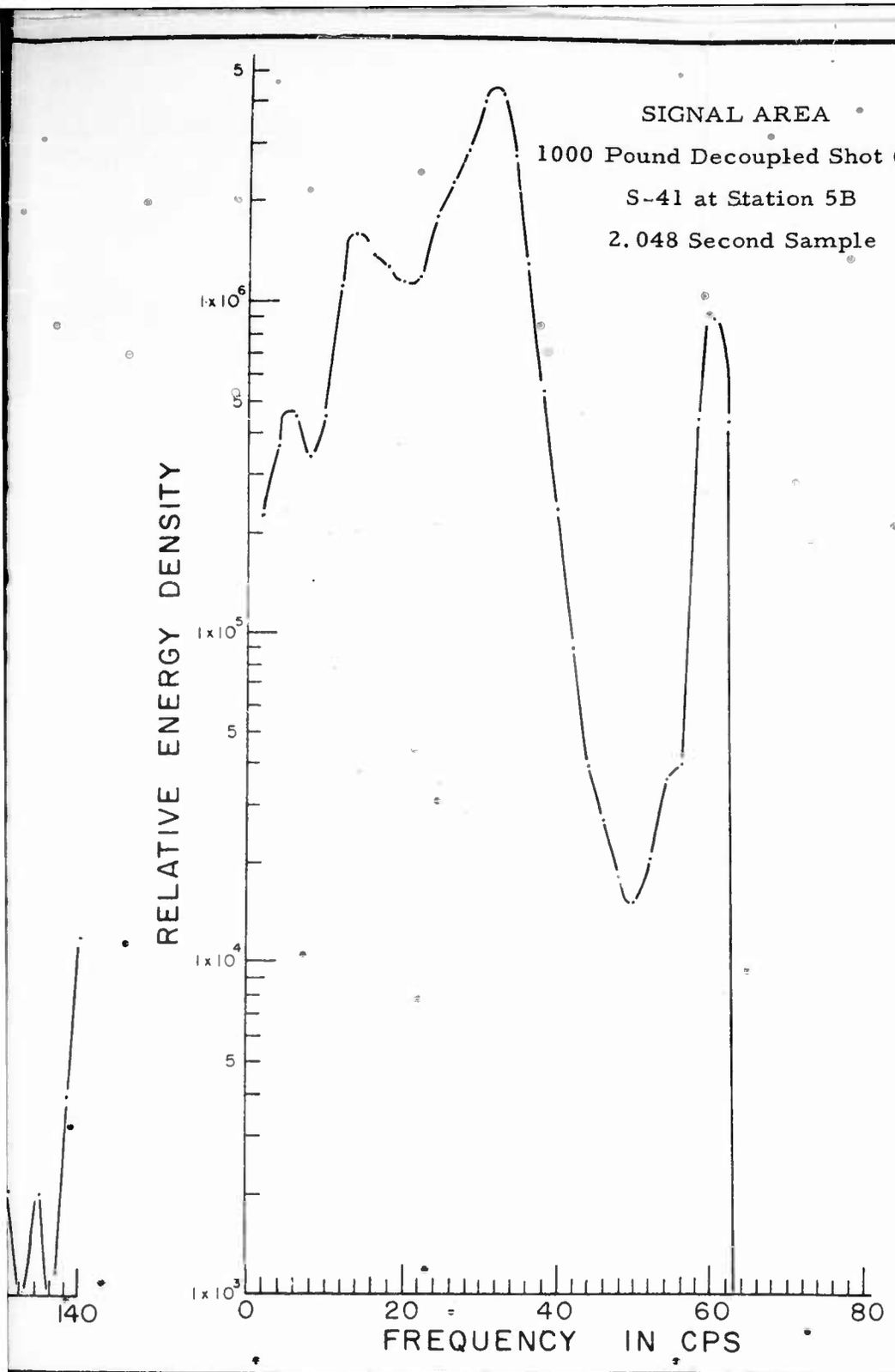
SIGNAL AREA
1000 Pound Decoupled Shot (#10)
S-41 at Station 5B
2.048 Second Sample
RELATIVE ENERGY DENSITY
1x10^6
1x10^5
1x10^4
1x10^3
0
20
40
60
80
140
FREQUENCY IN CPS

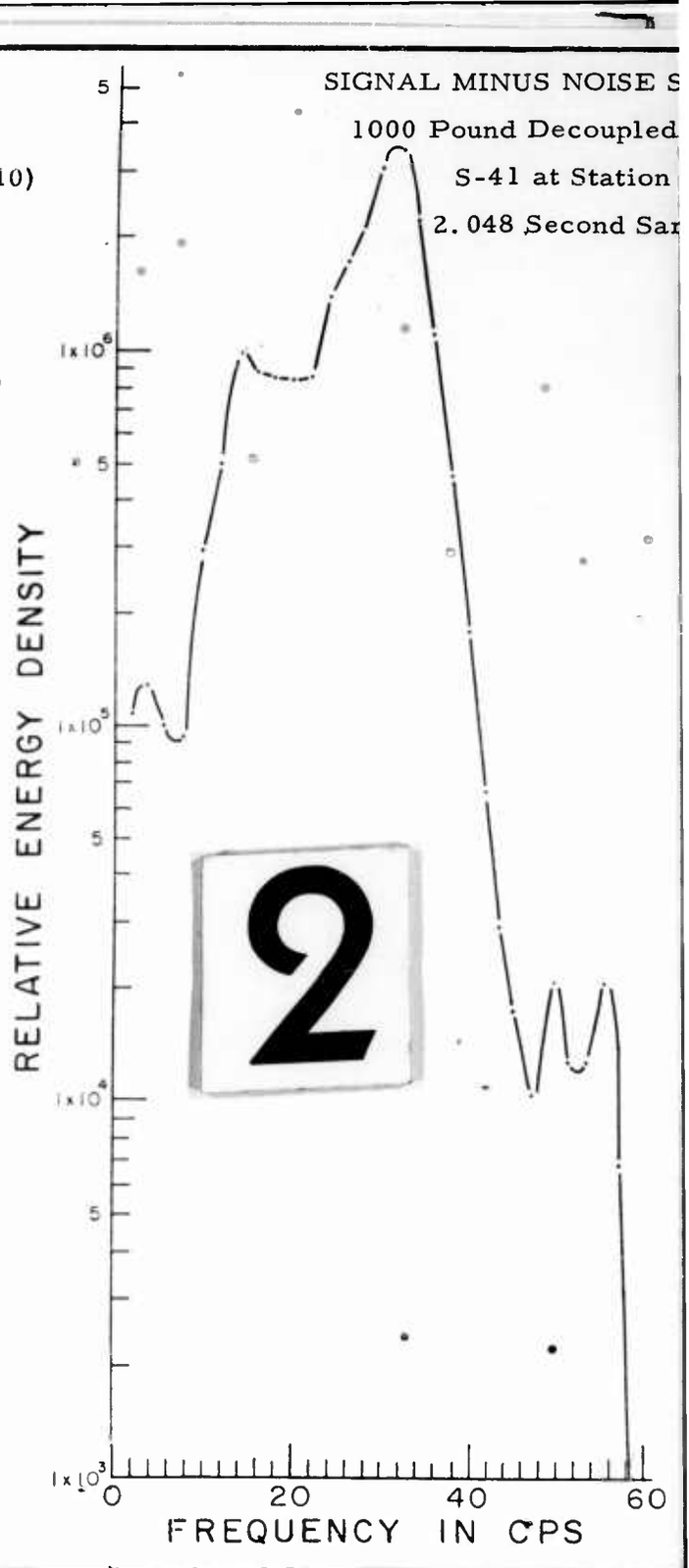
SIGNAL MINUS NOISE S
1000 Pound Decoupled
S-41 at Station
2.048 Second Sar
RELATIVE ENERGY DENSITY
1x10^6
1x10^5
1x10^4
1x10^3
0
20
40
60
FREQUENCY IN CPS

2

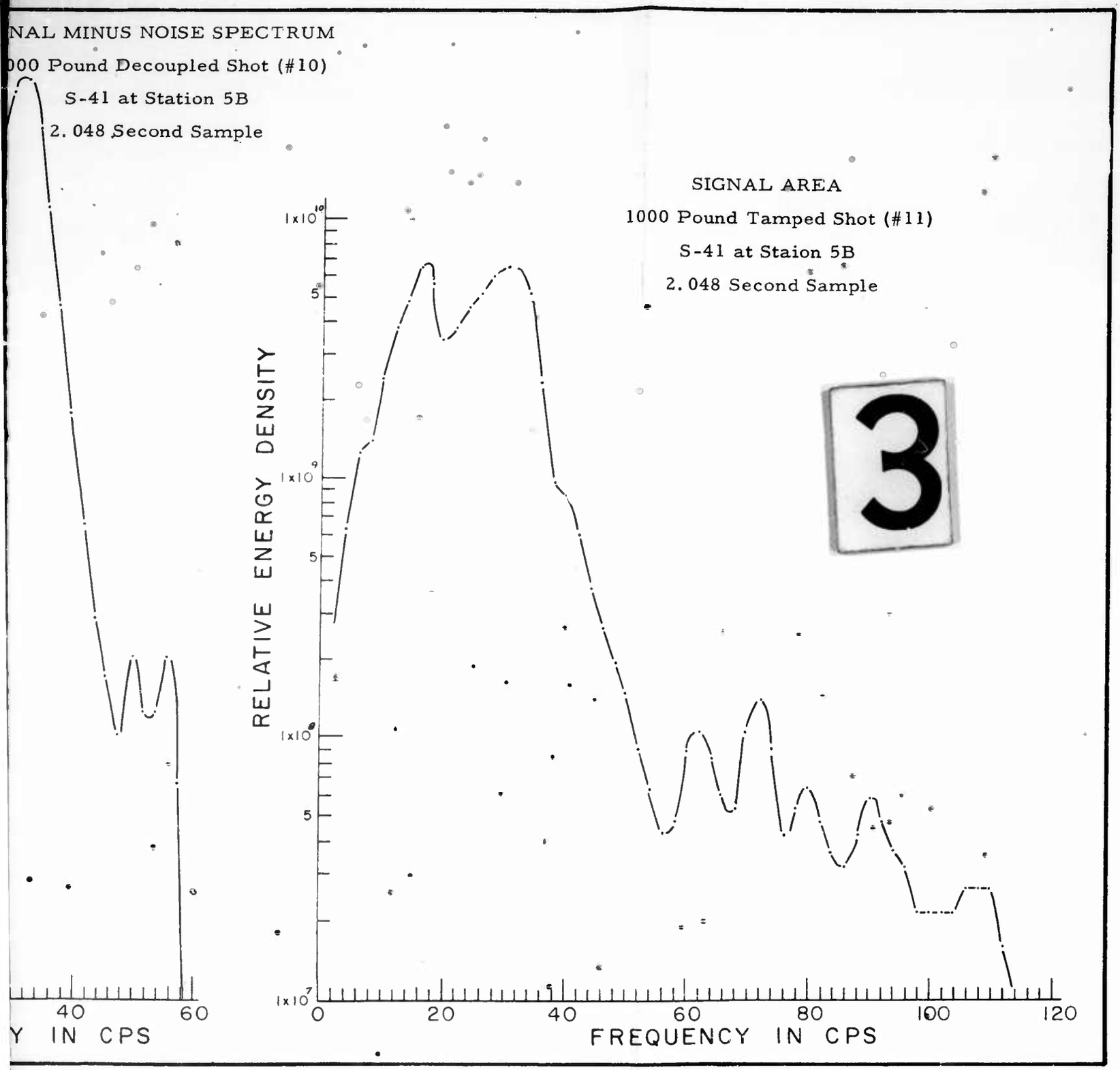

Fig. 11
Smoothed Energy Density Spectra of Signals and
Power Density Spectra of the Noise Samples
for the 1000 pound Decoupled
and Tamped Events

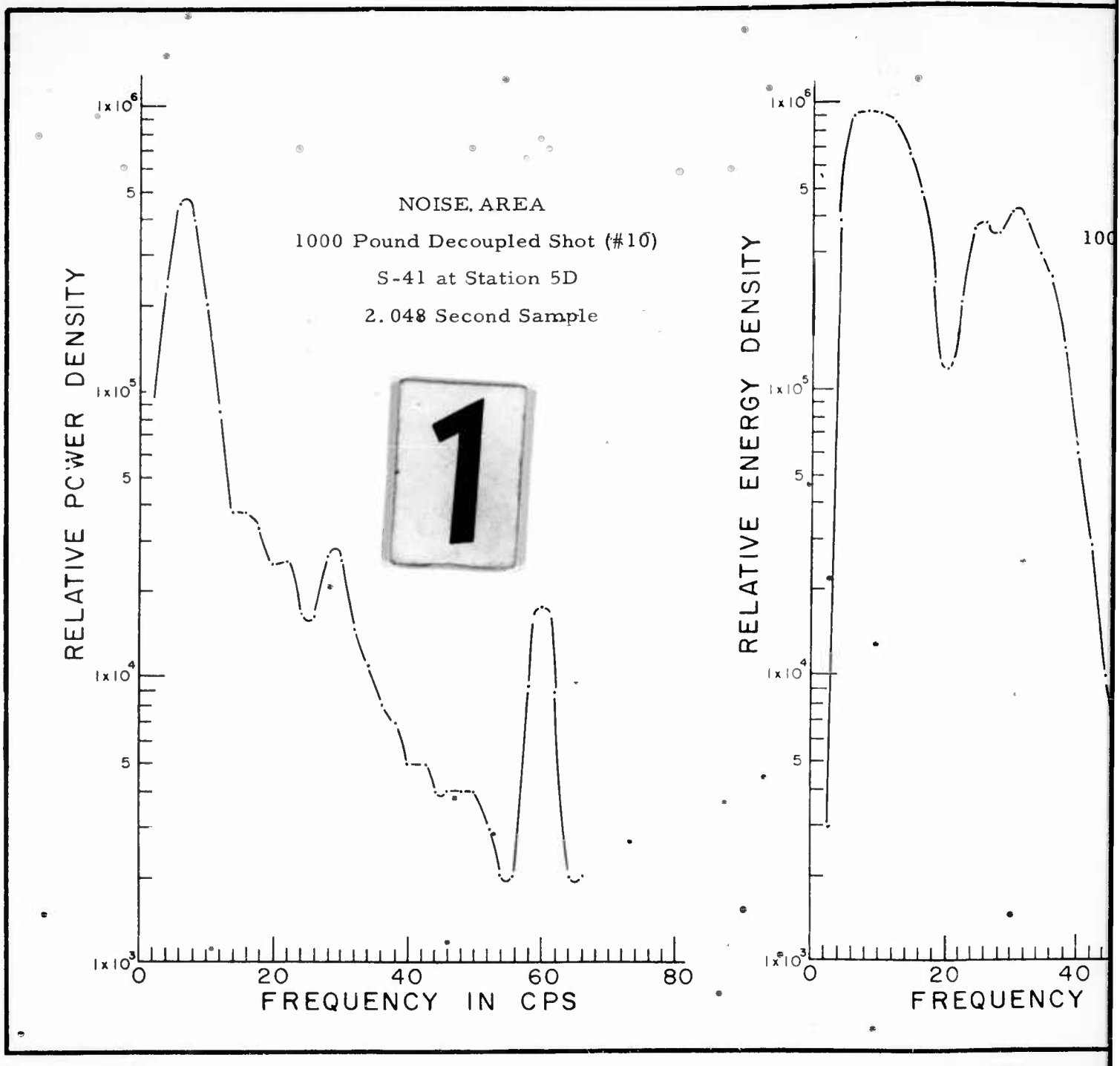
NOISE. AREA
1000 Pound Decoupled Shot (#10)
S-41 at Station 5D
2.048 Second Sample
1
RELATIVE POWER DENSITY
1x10^6
5
1x10^5
5
1x10^4
5
1x10^3
0
20
40
60
80
FREQUENCY IN CPS
RELATIVE ENERGY DENSITY
1x10^6
5
1x10^5
5
1x10^4
5
1x10^3
0
20
40
FREQUENCY

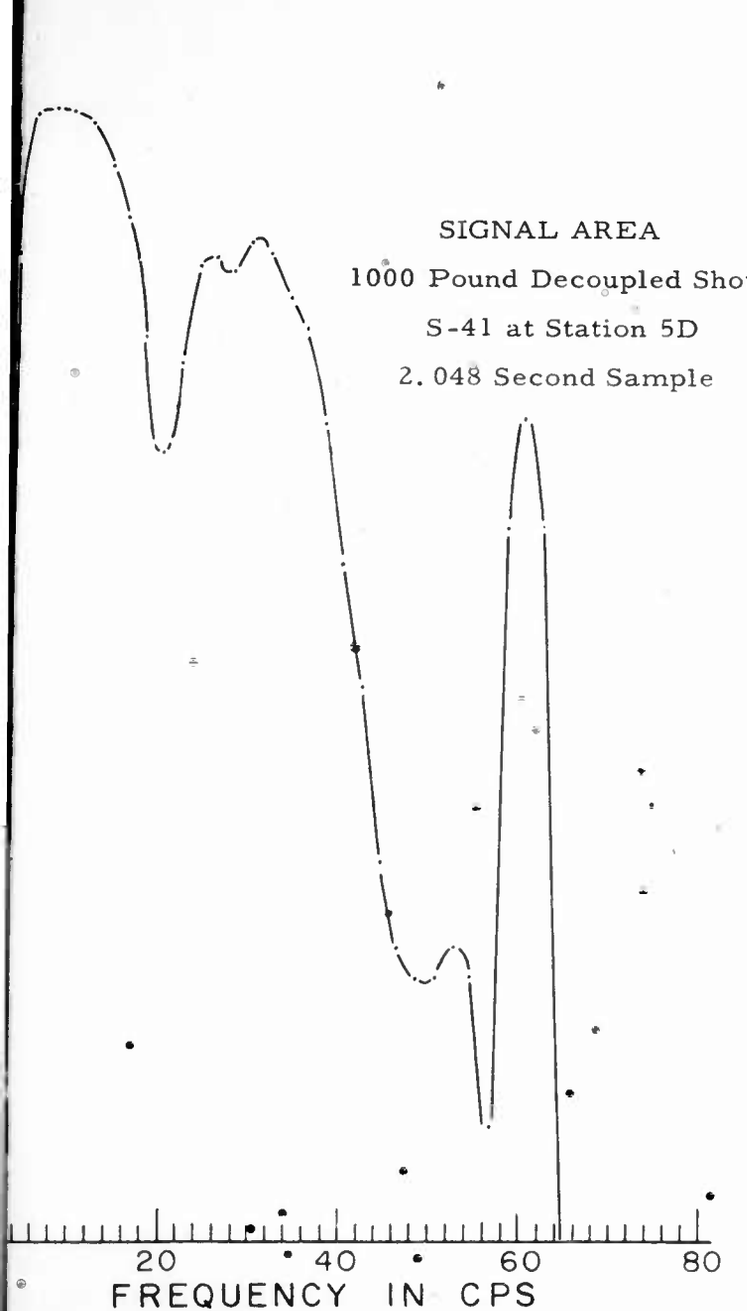

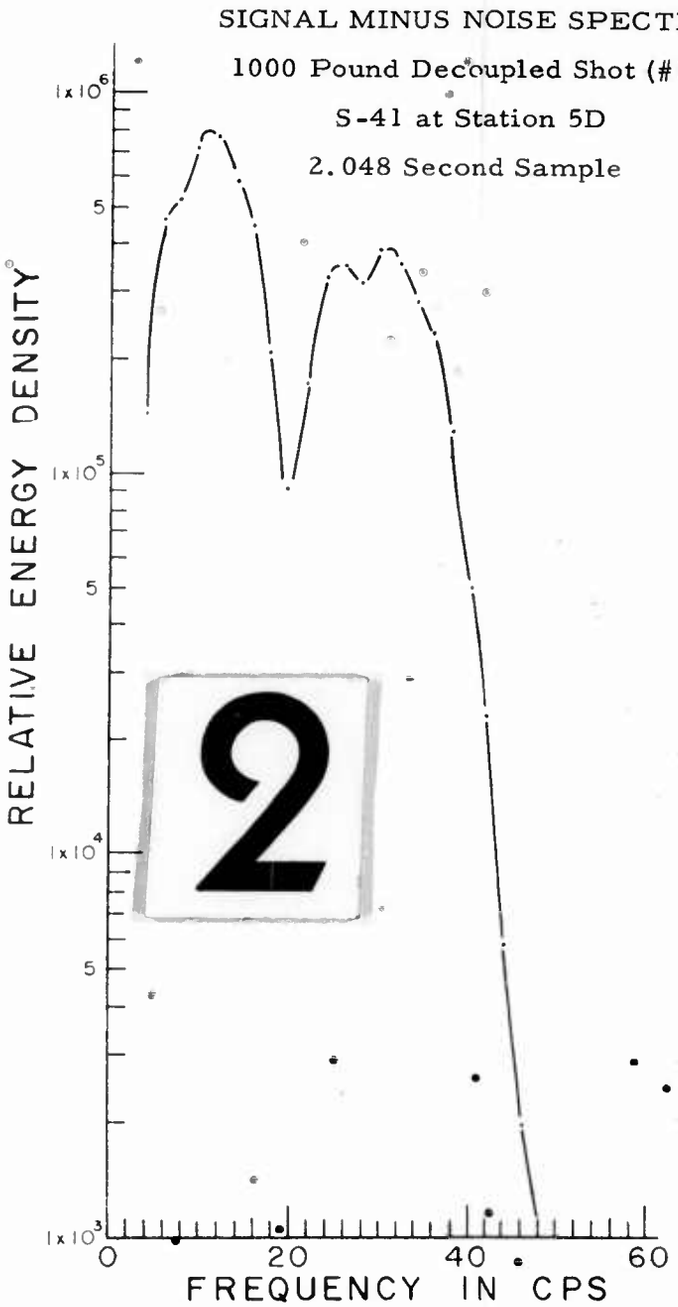

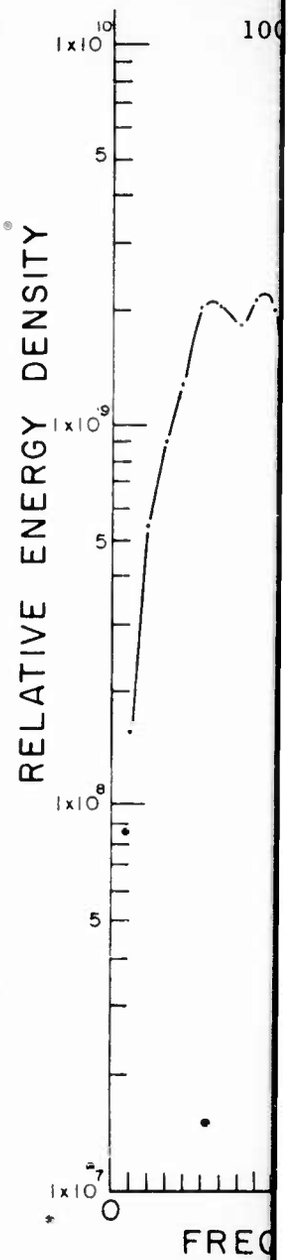

Fig. 12
Smoothed Energy Density Spec
Power Density Spectra of the
for the for the 1000 pound I
and Tamped Eve

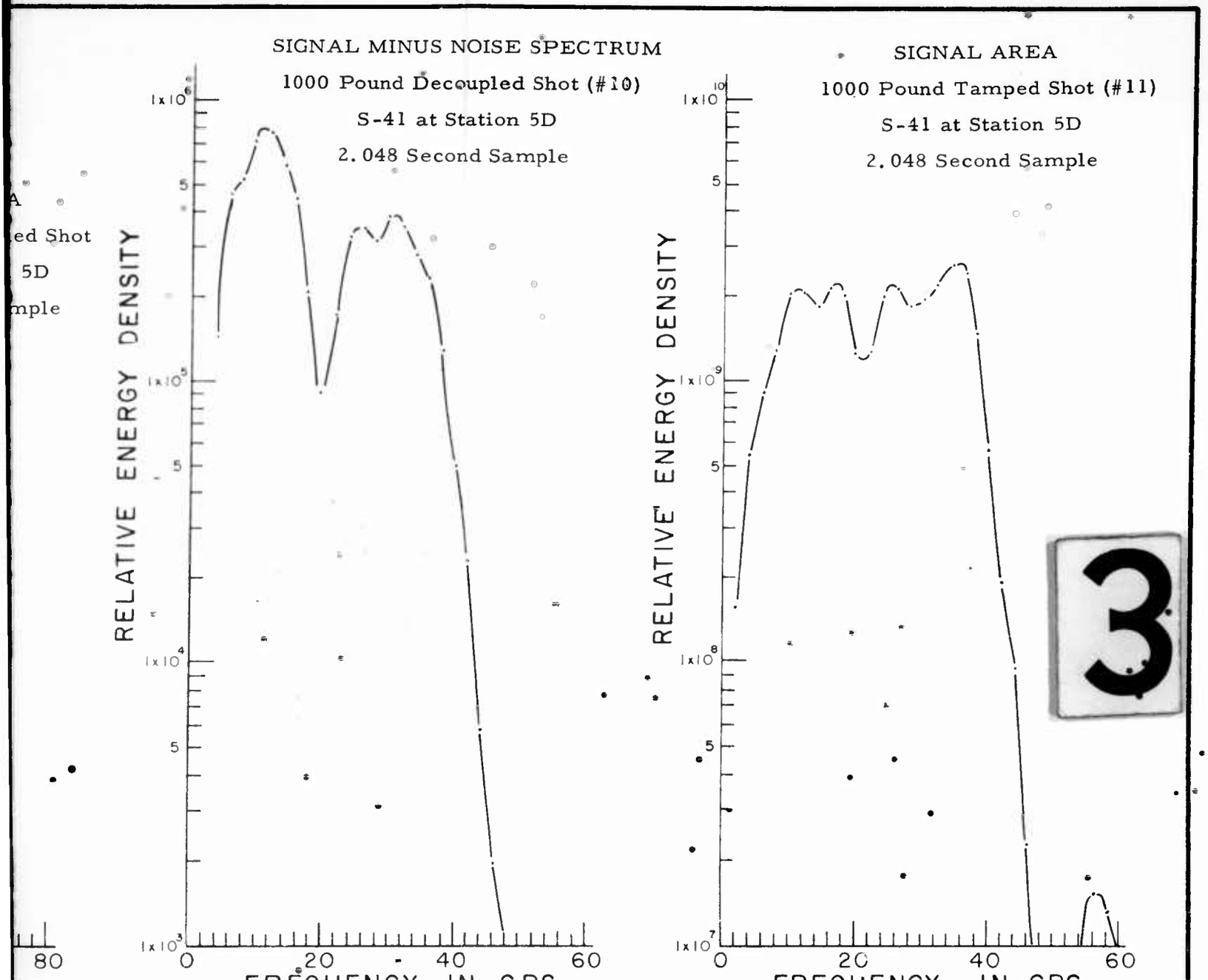

Fig. 12

Smoothed Energy Density Spectra of Signals and Power Density Spectra of the Noise Samples for the for the 1000 pound Decoupled and Tamped Events

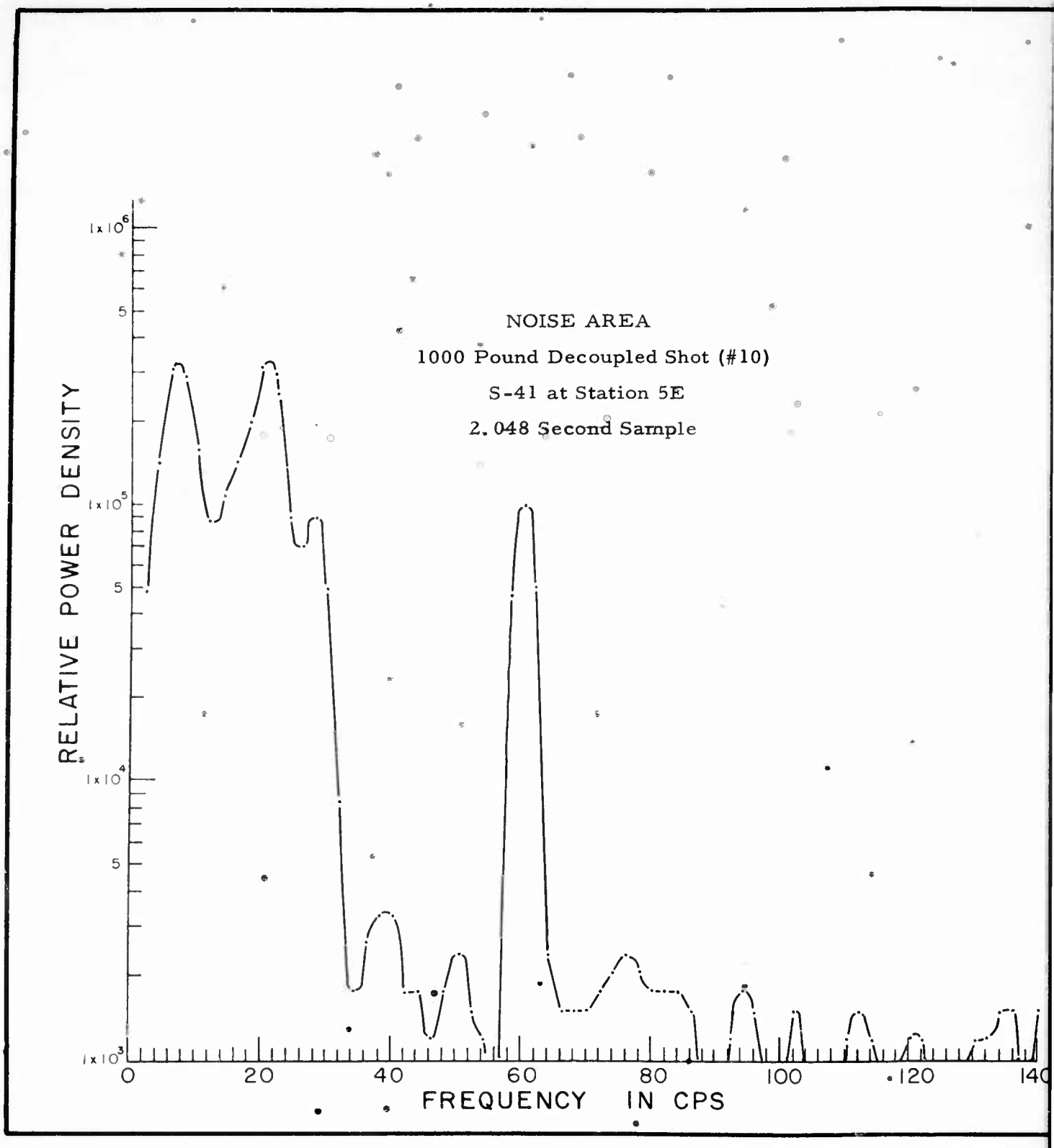
NOISE AREA
1000 Pound Decoupled Shot (#10)
S-41 at Station 5E
2.048 Second Sample
RELATIVE POWER DENSITY
1x10^6
5
1x10^5
5
1x10^4
5
1x10^3
0
20
40
60
80
100
120
140
FREQUENCY IN CPS

1

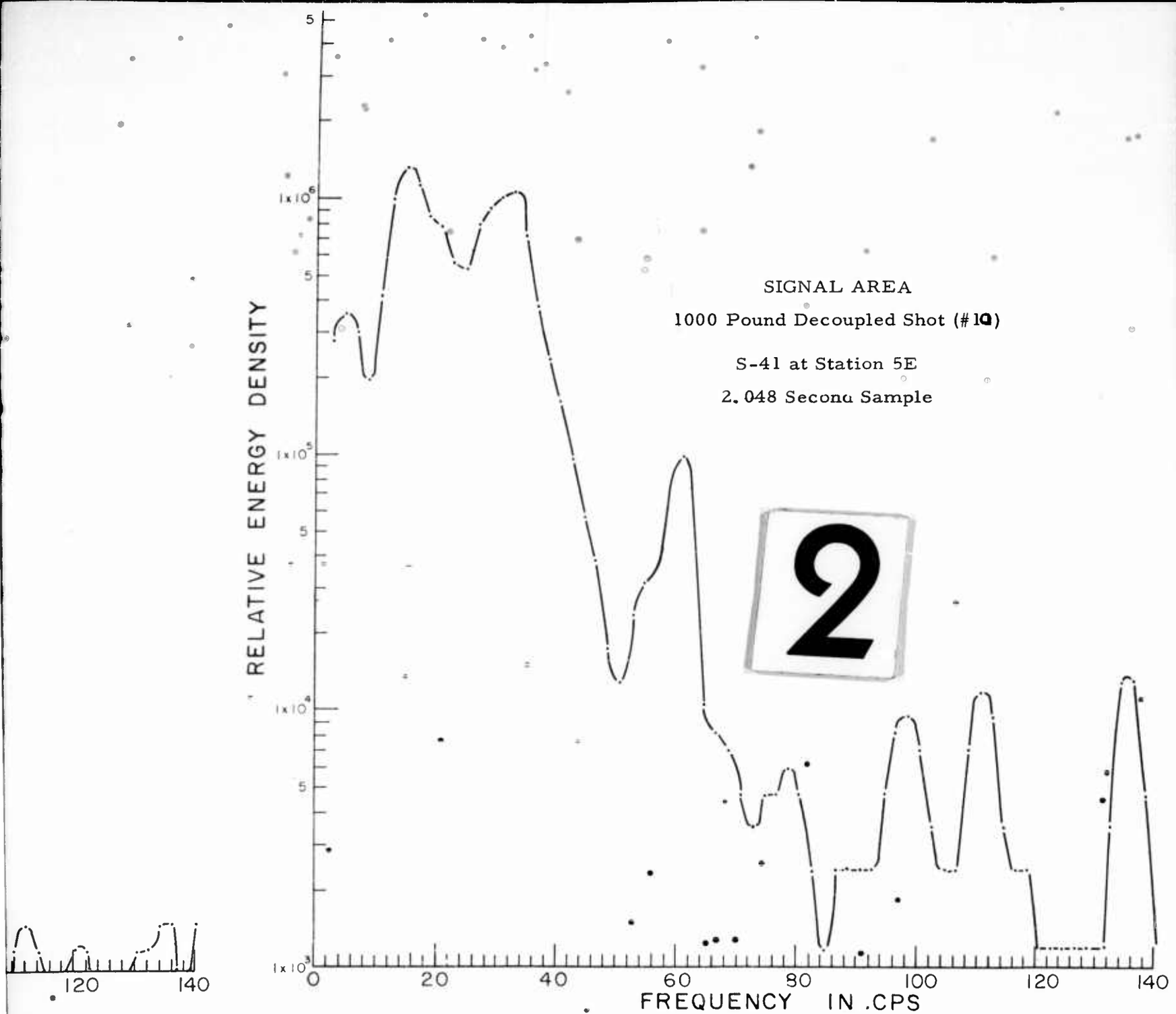
SIGNAL AREA
1000 Pound Decoupled Shot (#10)
S-41 at Station 5E
2.048 Second Sample
2
RELATIVE ENERGY DENSITY
5
1x10^6
5
1x10^5
5
1x10^4
5
1x10^3
0
20
40
60
80
100
120
140
FREQUENCY IN .CPS
120
140

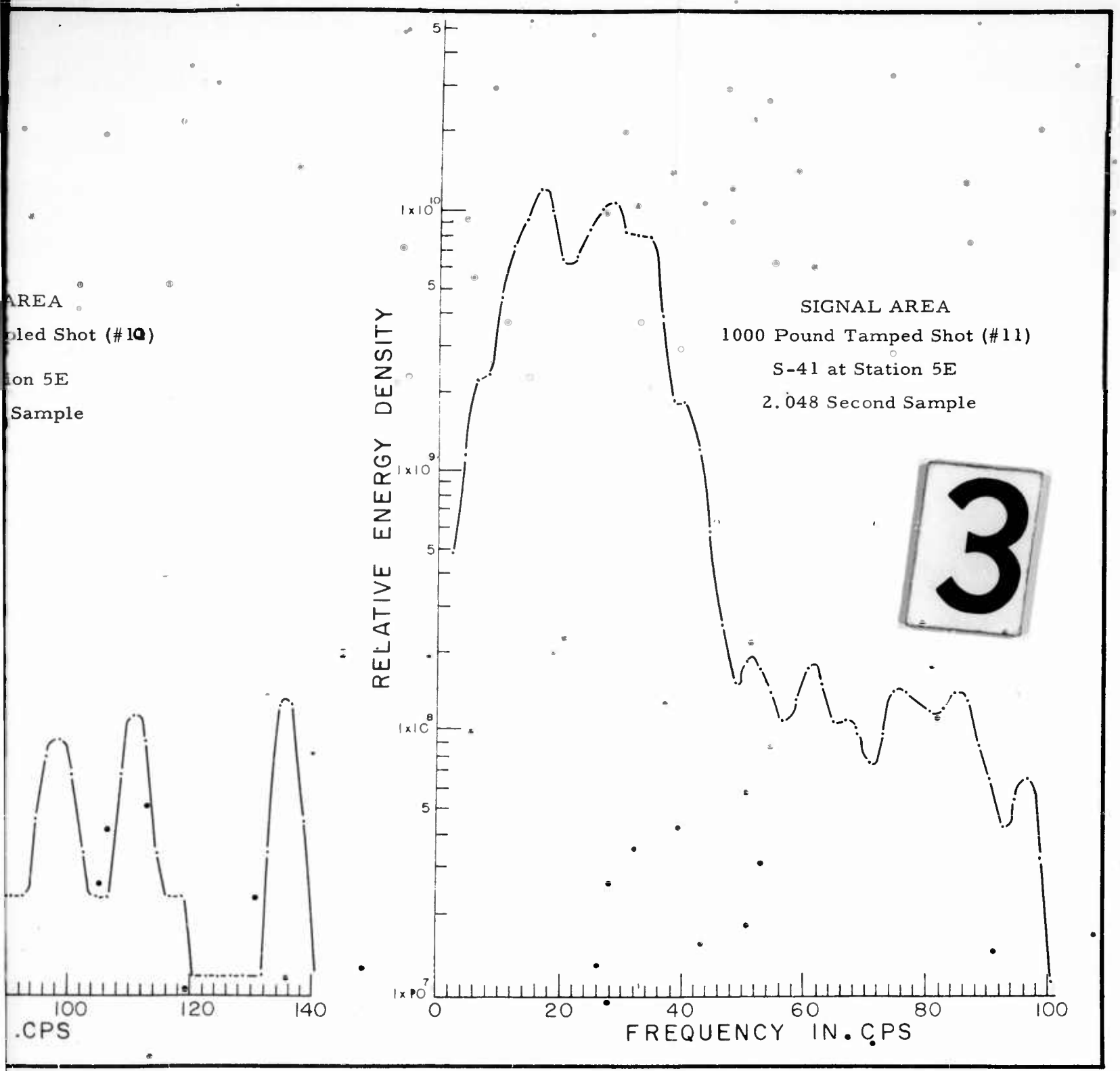

Fig. 13

Smoothed Energy Density Spectra of Signals and Power Density Spectra of the Noise Samples for the 1000 pound Decoupled and Tamped Events

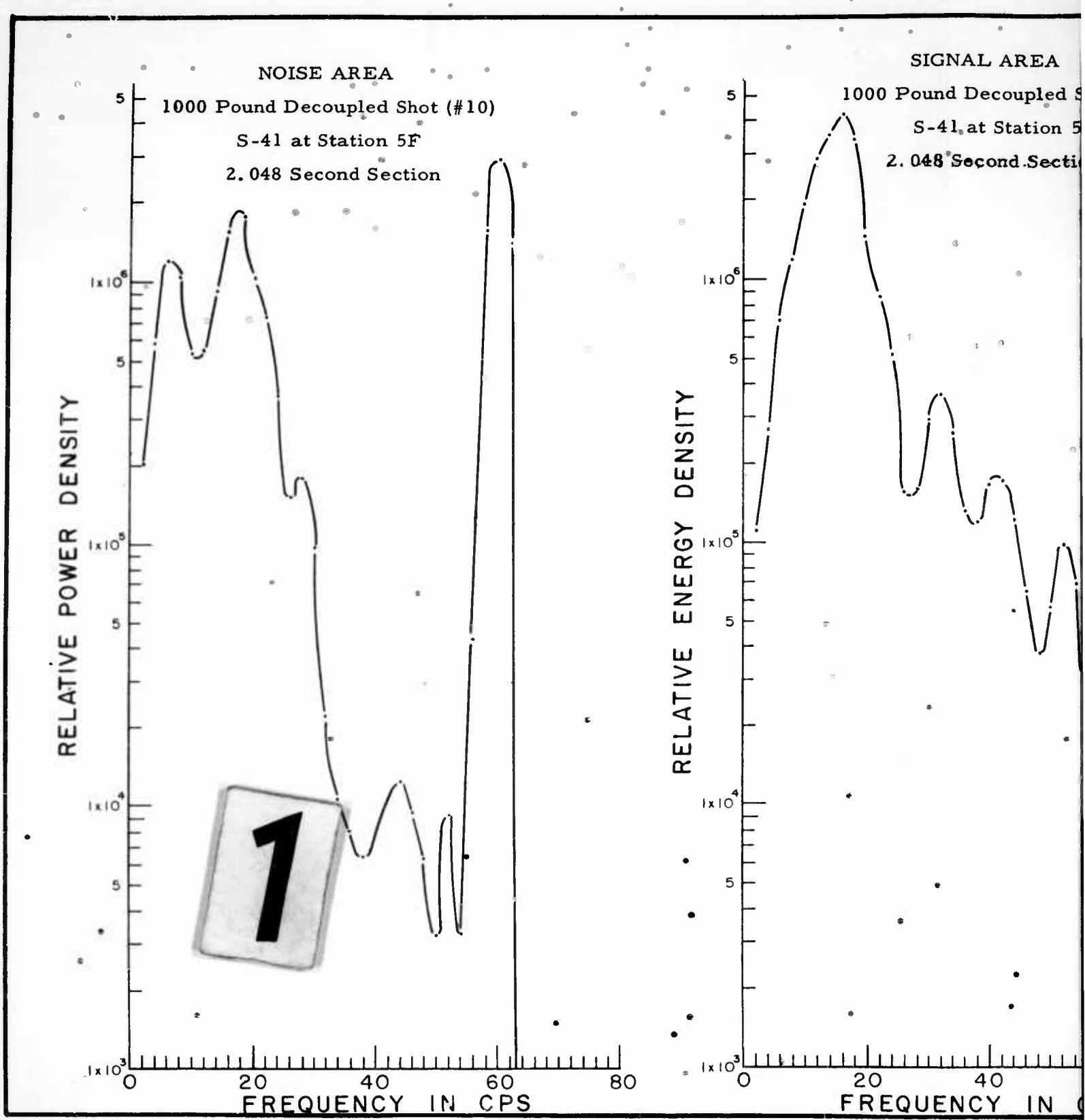
NOISE AREA
1000 Pound Decoupled Shot (#10)
S-41 at Station 5F
2.048 Second Section
RELATIVE POWER DENSITY
1x10^6
5
1x10^5
5
1x10^4
5
1x10^3
0
20
40
60
80
FREQUENCY IN CPS
1
SIGNAL AREA
1000 Pound Decoupled S
S-41 at Station 5
2.048 Second Secti
RELATIVE ENERGY DENSITY
1x10^6
5
1x10^5
5
1x10^4
5
1x10^3
0
20
40
FREQUENCY IN

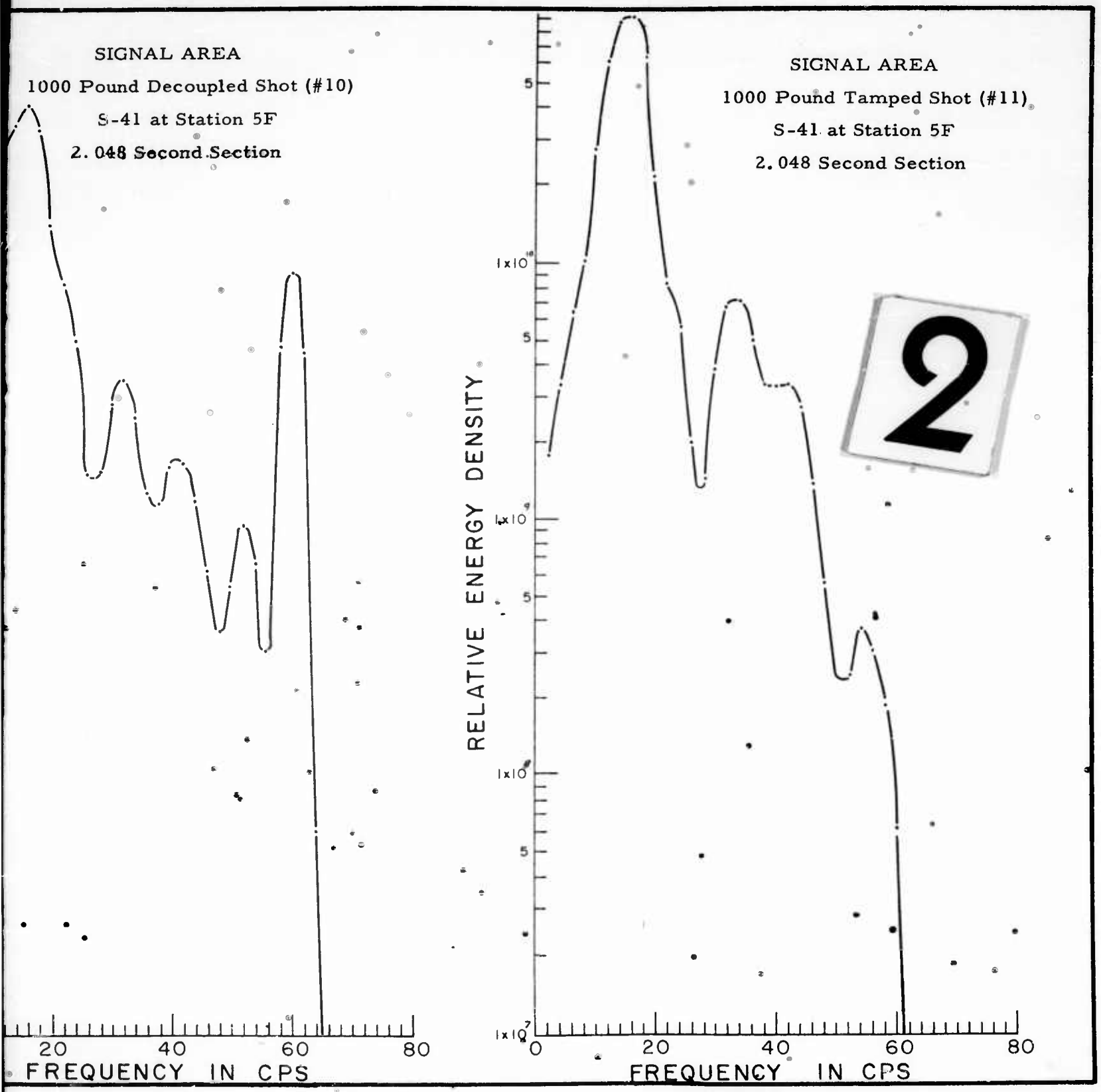

Fig. 14
Smoothed Energy Density Spectra of Signals and Power Density Spectra of the Noise Samples for the 1000 pound Decoupled and Tamped Events

5F so that these values might be compared to the amplitude density ratios as a function of frequency.

TABLE II

S-41 SEISMOMETER RESPONSE DATA FOR STATIONS 5A-5F

Station	Separation Distance Decoupled	Separation Distance Tamped	Decoupling Factor
5A	22,100 feet	21,690	116
5B	22,696 feet	22,285	75.6
5C	23,292 feet	22,880	77
5D	24,683 feet	24,270	105
5E	25,279 feet	24,865	94.5
5F	25,975 feet	25,561	95.6

The data presented in Table II, was computed from values which were plotted in Figures 15 and 16. The 500-pound decoupled and tamped unfiltered recordings shifted in time to correspond to a correction for a 17,500 foot/sec apparent velocity. The amplitude scale of the 500-pound decoupled recordings are 100 times less than the scale on the 500-pound tamped records of Figure 16. Summing the shifted decoupled traces produced the curve shown in Figure 17 and doubled the signal-to-noise ratio of the largest return recorded at Station 5B. The composite trace (Figure 17) has a great deal of noise preceding the first arrival, whereas the signal amplitudes recorded for all tamped shots are much greater than the background noise.

2. Two Second Averages of Amplitude Density Ratios as a Function of Frequency

The energy density spectra for the signal and noise samples presented in Section III, B present estimates of the average energy recorded during the time sampled as a function of frequency. The spectral estimates of the noise are assumed stationary for the few seconds between the analyzed noise and signal samples. The values obtained for the noise energy density estimates were then subtracted from the corresponding signal energy density spectra which was in reality a spectral response of signal plus noise. If the assumption of stationarity is upheld or the values of the noise spectra are relatively small the resulting spectra are estimates of the true noiseless signal return. No attempt was made to subtract a noise estimate from the tamped signal estimates as the signal-to-noise amplitude ratios were of the order of 50 or more, or when the signal-to-noise amplitude ratios were of the order of one or less.

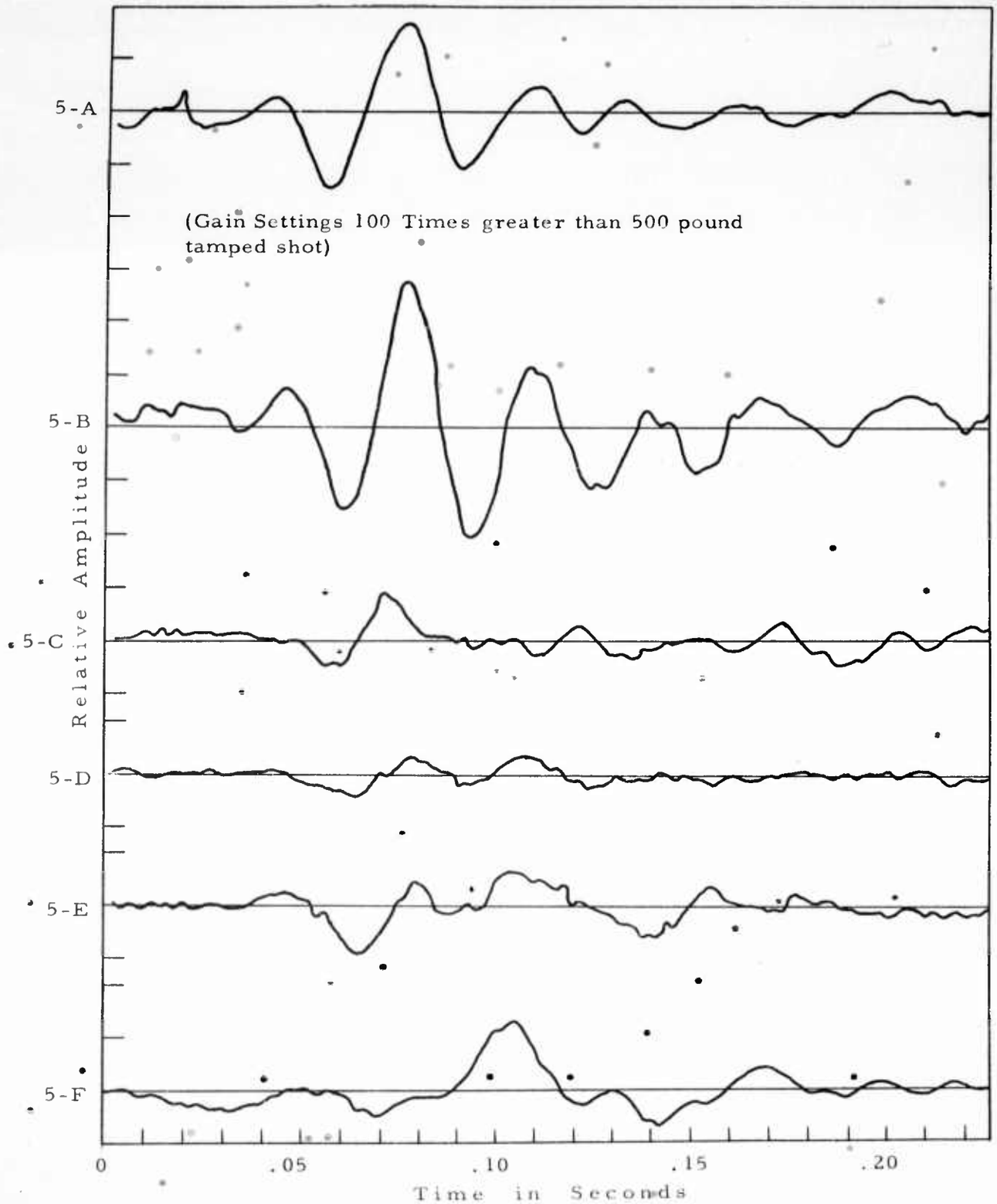

Fig. 15
S-41 Seismometer Response of First Arrivals at Stations 5A-F

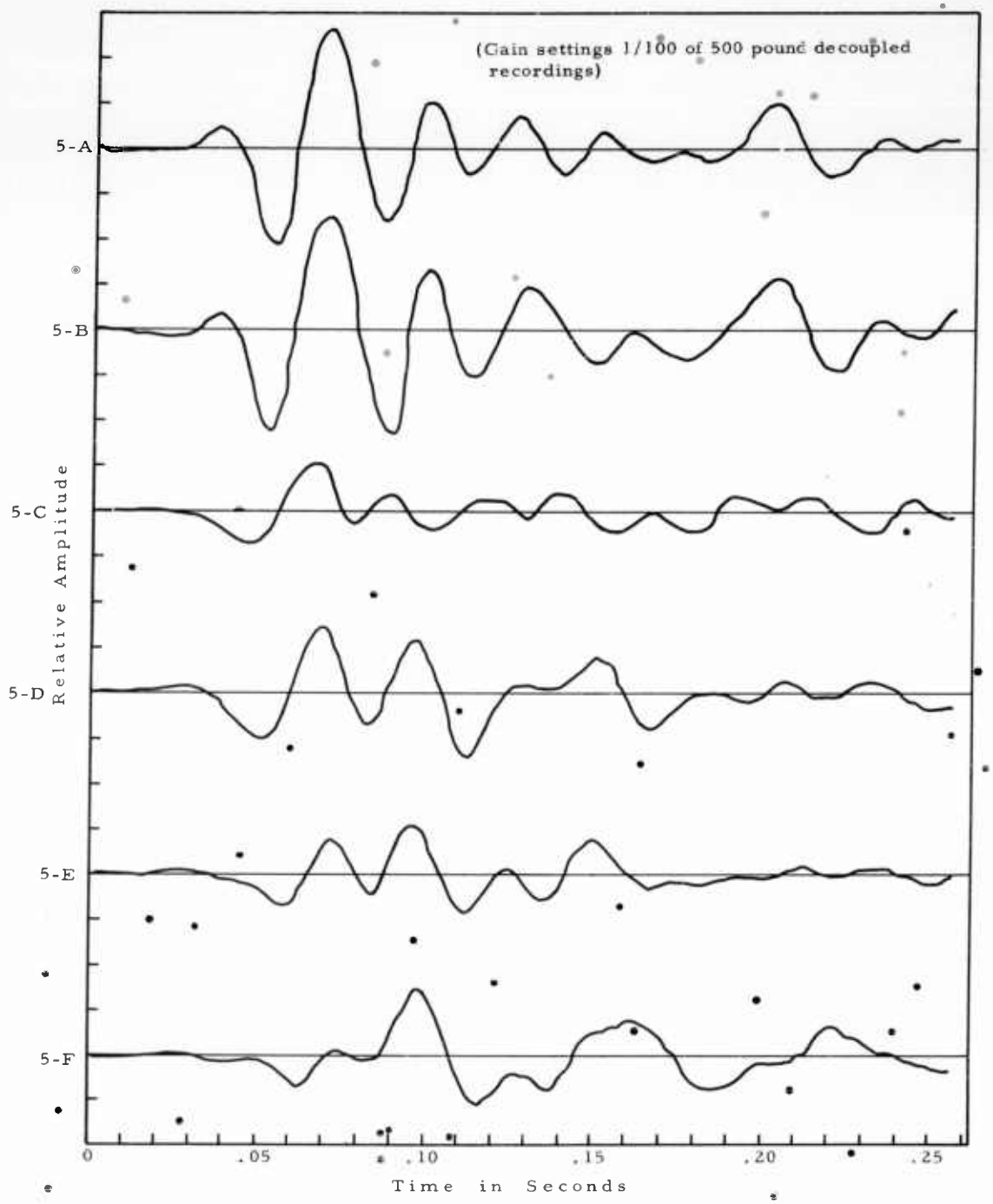

Fig. 16
S-41 Seismometer Response of First Arrivals at Stations 5A-F

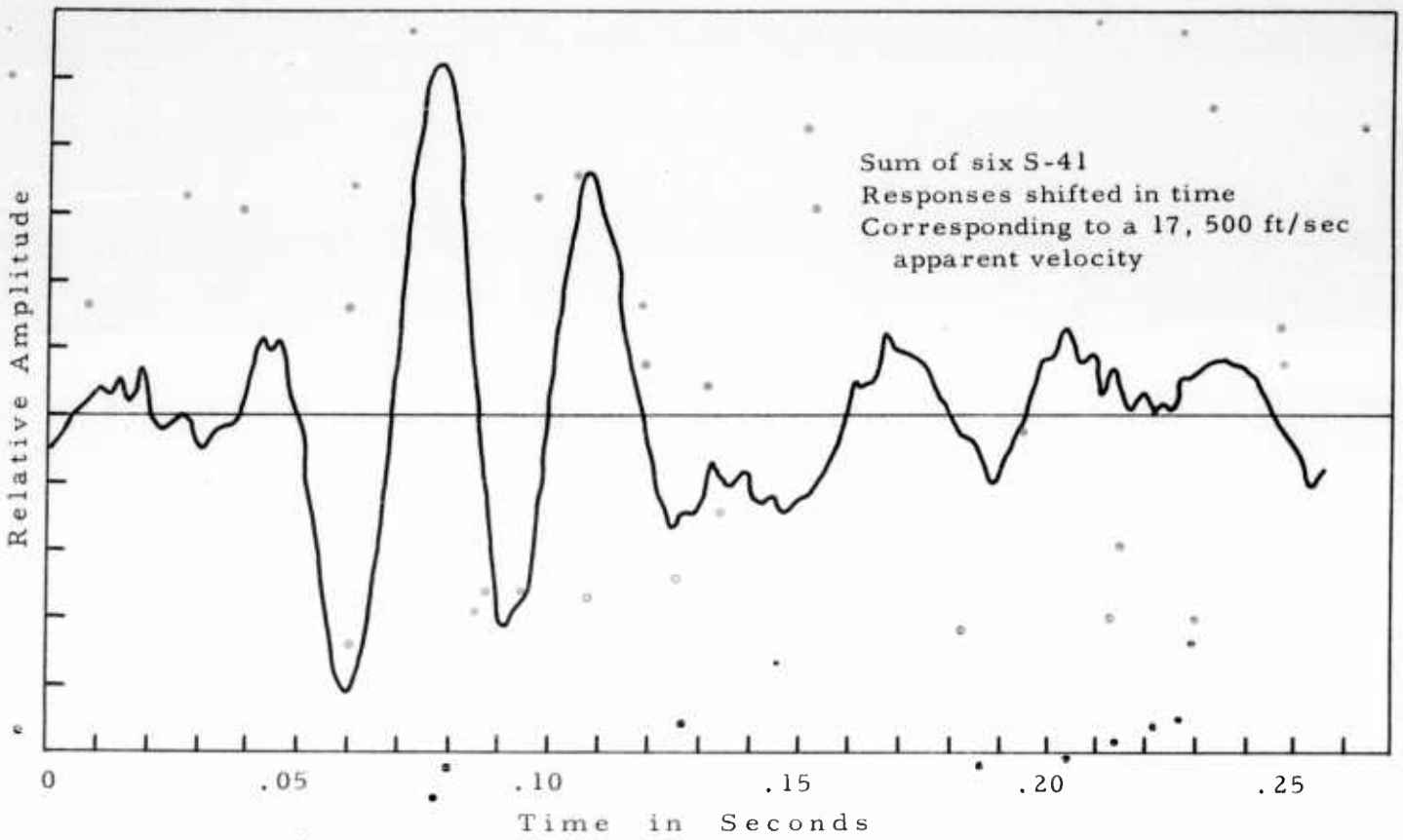

Fig. 17
Composite Record for First Arrivals
of 500-pound Decoupled Shot Test

The decoupling computations consisted of dividing the energy density estimates of the decoupled signal samples, with or without compensation for the noise, into the values of the energy density estimates of the tamped signal samples and taking the square root of this result to produce an amplitude density ratio as a function of frequency. Since the energy density spectra presented drop in magnitude quite sharply at frequencies above 40 to 50 cps and below 6 to 10 cps, the bands containing 90% and 99% of the energy of the tamped signal response are therefore indicated, and ratios were not computed outside this region. This was done in order to neglect regions where minor variations in the noise would cause erroneous ratios.

The amplitude density ratios can be represented algebraically,

$$A(f_i) = \sqrt{\frac{S_T(f_i) \cdot S_T(f_i)^*}{(S_{DC}(f_i) + N_{DC}(f_i))(S_{DC}(f_i) + N_{DC}(f_i))^* - N_{DC}(f_i) \cdot N_{DC}(f_i)^*}}$$

where $A(f_i)$ = amplitude density ratio centered at frequency f_i.

$S_T(f_i)$ = Signal Amplitude Density Spectral Estimate at (f_i) for the Tamped Shot Signal Sample.

$(S_{DC}(f_i) + N_{DC}(f_i))$ = Signal plus Noise Amplitude Density Spectral Estimates at (f_i) for Decoupled Shot Signal Sample.

$N'_{DC}(f_i)$ = Noise Amplitude Density Spectral Estimates for Noise Preceding Decoupled Event.

(* denotes complex conjugate)

The desired ratio corresponds to

$$a(f_i) = \sqrt{\frac{S_T(f_i) \cdot S_T(f_i)^*}{S_{DC}(f_i) \cdot S_{DC}(f_i)^*}}$$

which, depending on the correctness of the assumptions mentioned above concerning the stationarity of the noise or values of signal-to-noise ratios, will be approximated by $A(f_i)$.

The assumption that the cross terms $S_{DC}(f_i) N_{DC}(f_i)^*$ and $S_{DC}(f_i)^* N_{DC}(f_i)$ are negligible assumes that the signal and the noise are statistically independent, an assumption that should be valid.

In the case of the 500-pound decoupled shot recorded at Station 5B the first arriving energy represents a signal which is much higher in amplitude than the level of the ambient noise. Hence, in an analysis involving the energy density spectra of the first .256 seconds of the decoupled and coupled signals very little error will be involved if the expected noise spectra is not subtracted. The aforementioned analysis is shown in Figure 18. This curve indicates very low values between 20 and 28 cps with an apparent high value around 16 cps. Referring first to the spectra and then to the field records this data indicates that not only is the surface wave response relatively low on the decoupled records but also some of the lower frequency content of the body wave arrivals are greatly attenuated. This may be analogous to the observation on the records for the decoupled shot 12, (the 1000-pound shot in the 12-foot diameter hole), where several arrivals are evident which are not present on the other decoupled shot records recorded, 6, 8, and 10.

For the 500-pound test shots 8 and 9, as recorded at 5B, an analysis was also conducted for a 2.048-second segment of signal and noise.

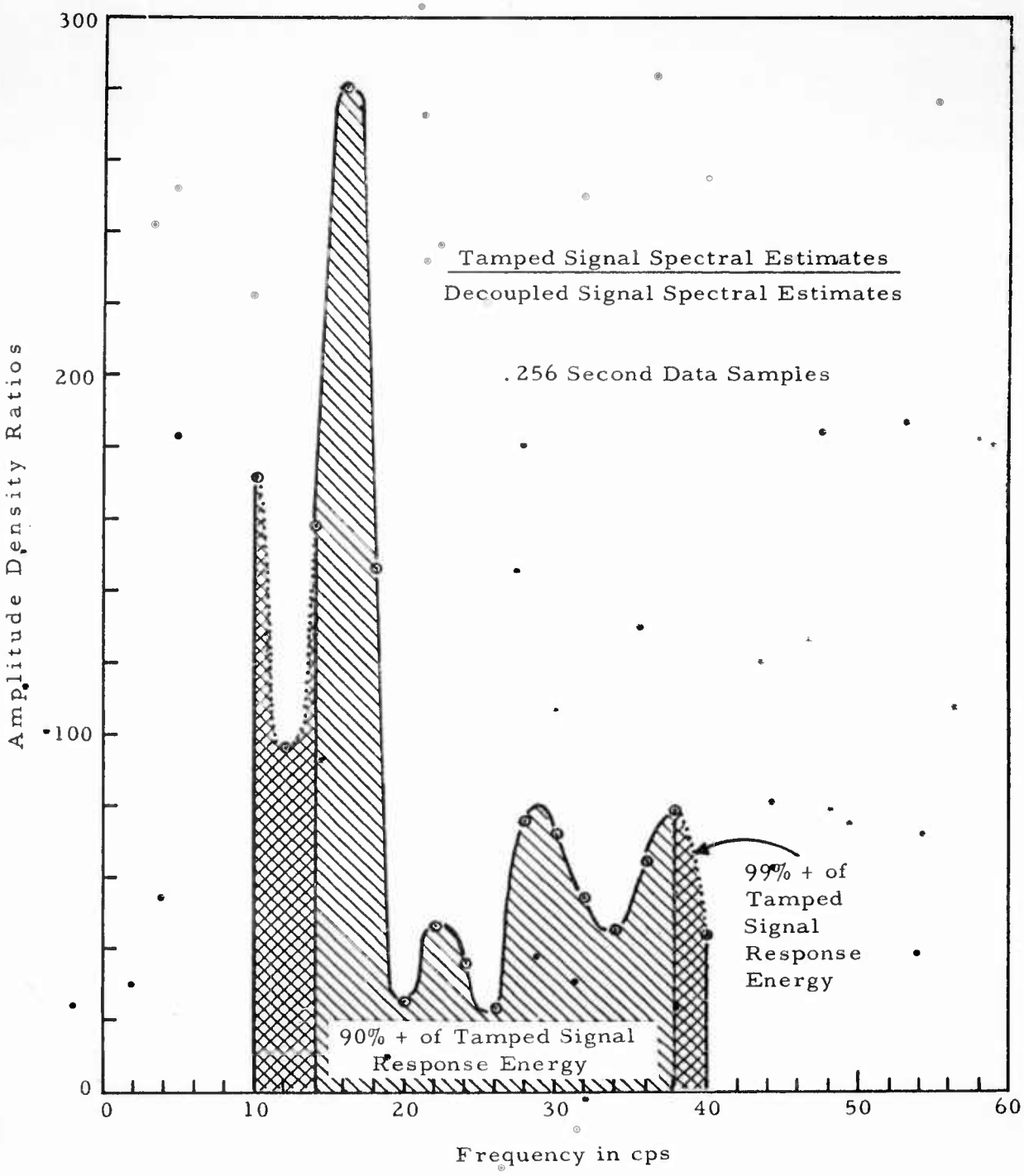

Fig. 18
Amplitude Density Ratios for 500 pound Shots at Station 5B

In this case noise compensation carried out as the assumption of stationarity seemed valid and the sample lengths were long enough to attain a true estimate of the expected noise spectra. The plot of this result is presented in Figure 19. The general level of decoupling is much greater than that indicated by the short segment analysis of Figure 18 and substantiates the observation that the predominant energy of the decoupled signals is concentrated in the first few arrivals, whereas the tamped signals are characterized by many arrivals of rather constant amplitude. As reiterated above, the low frequencies recorded appear to be better decoupled. Similar differences in the partitioning of energies for decoupled and tamped shots are implied from a comparison of the energy density estimates for the 2.048-second and .256-second signal samples presented in Section III, B for the S-41 seismometer responses at stations 5D, 5E, and 5F for the 500-pound test shots. This data indicates that the first arriving refractions contain the majority of the decoupled shot energy which is recorded and that the decoupling is frequency dependent.

The set of amplitude density ratios presented in Figure 20 represents the decoupling $A(f_i)$ as seen for the 1000-pound shot tests 10 and 11 at stations 5B, 5D, 5E, and 5F for 2.048-second data samples. Comparing the first curve (5B) to that one on Figure 19, it is seen that the decoupling as computed for the same travel path for the 1000 pound shots #10 and #11 are decreased by a factor of about 2. The curves are similar in shape but the lower frequencies for the larger decoupled shot are not as drastically attenuated. There appears to be very little correlation of the curves for the 1000-pound ratios at stations 5B, 5D, 5E and 5F. The general feature which is difficult to explain is that these curves increase in amplitude with distance from the source. Since the analysis is created to take out the effects of the earth's transmission characteristics, as well as those of the receiver and recording system, this result leads to an indefinite paradox which may or may not be explained by variations in excitation of various modes of propagation for different travel paths.

D. ERROR ANALYSES

In each case where noise compensation was attempted the signal-to-noise ratios were quite high and the noise also appeared to be stationary. Hence, the large variations from the predicted noise spectra are not expected and at best would cause a second order effect in the resultant decoupling function $A(f_i)$. In the case of the tamped signals the noise is down by a factor of about 50 in amplitude and hence a factor of about 2.5×10^{-3} in energy. Therefore, in the numerator of the expression for $A(f_i)$ the noise has not been considered.

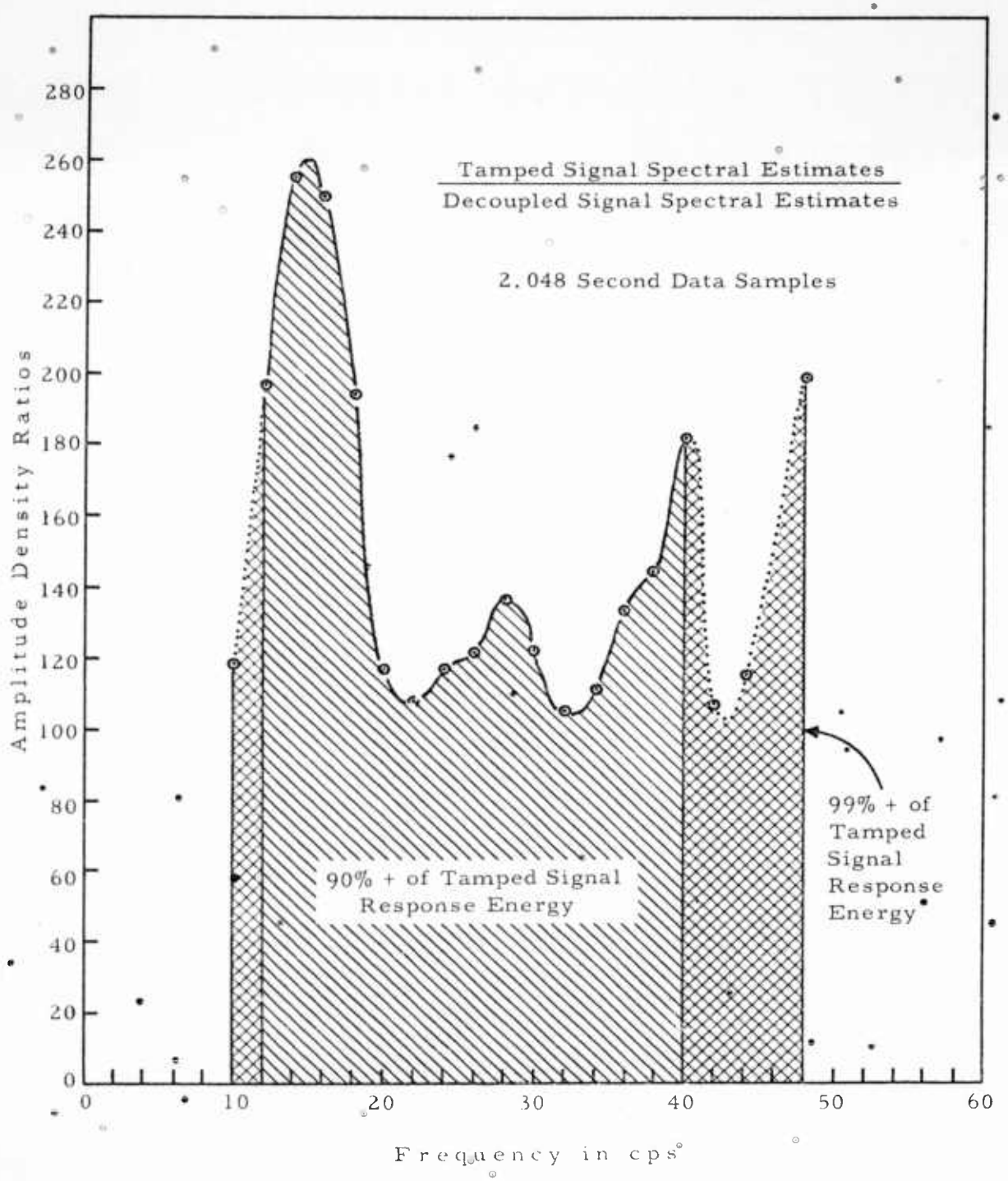

Fig. 19
Amplitude Density Ratios for 500 pound Shots at Station 5B

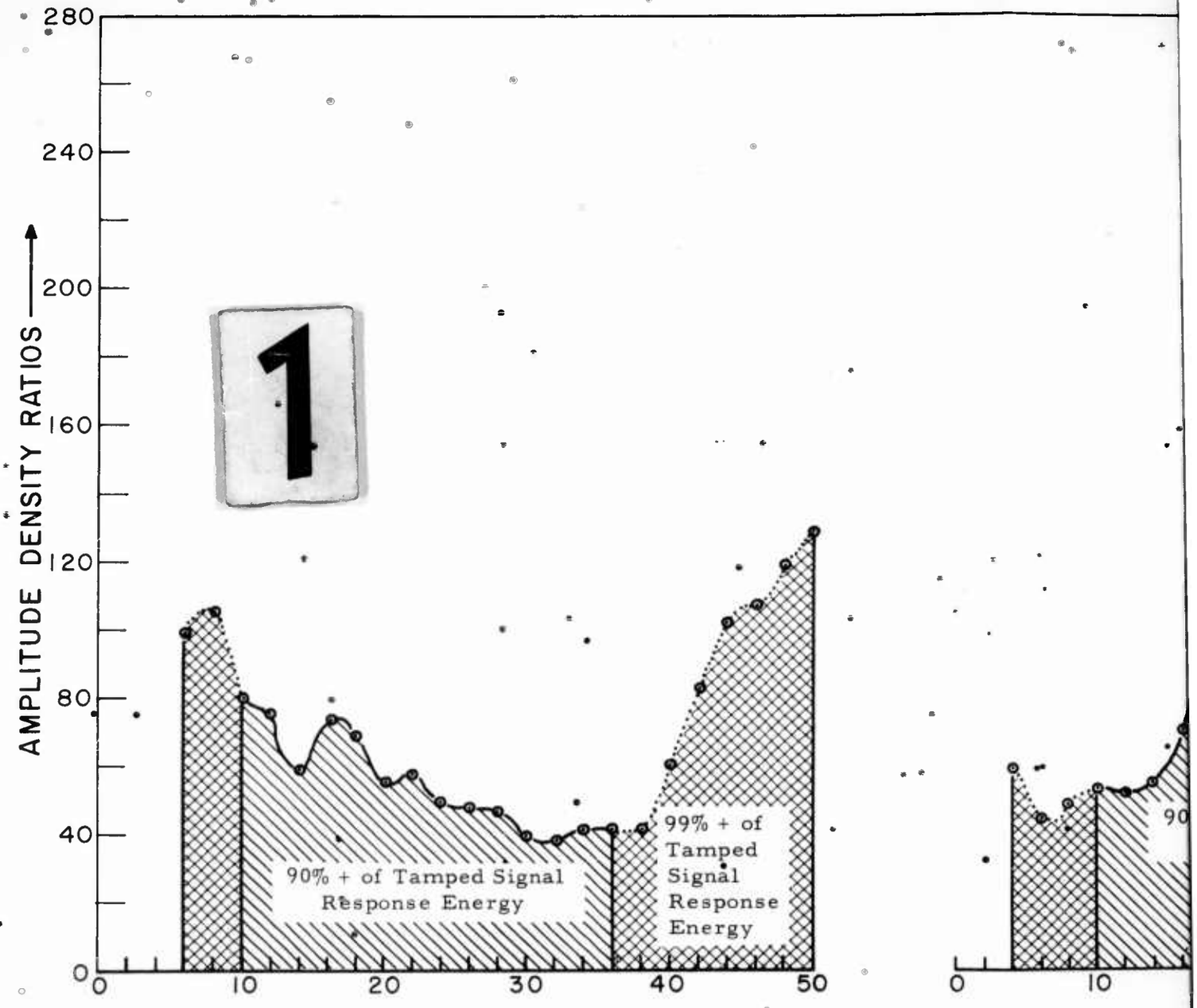
AMPLITUDE DENSITY RATIOS
280
240
200
160
120
80
40
0
0
10
20
30
40
50
1
90% + of Tamped Signal Response Energy
99% + of Tamped Signal Response Energy
90

Tamped Signal Spectral Estimates

Decoupled Signal minus Noise Spectral Estimates

2.048 Second Data Samples

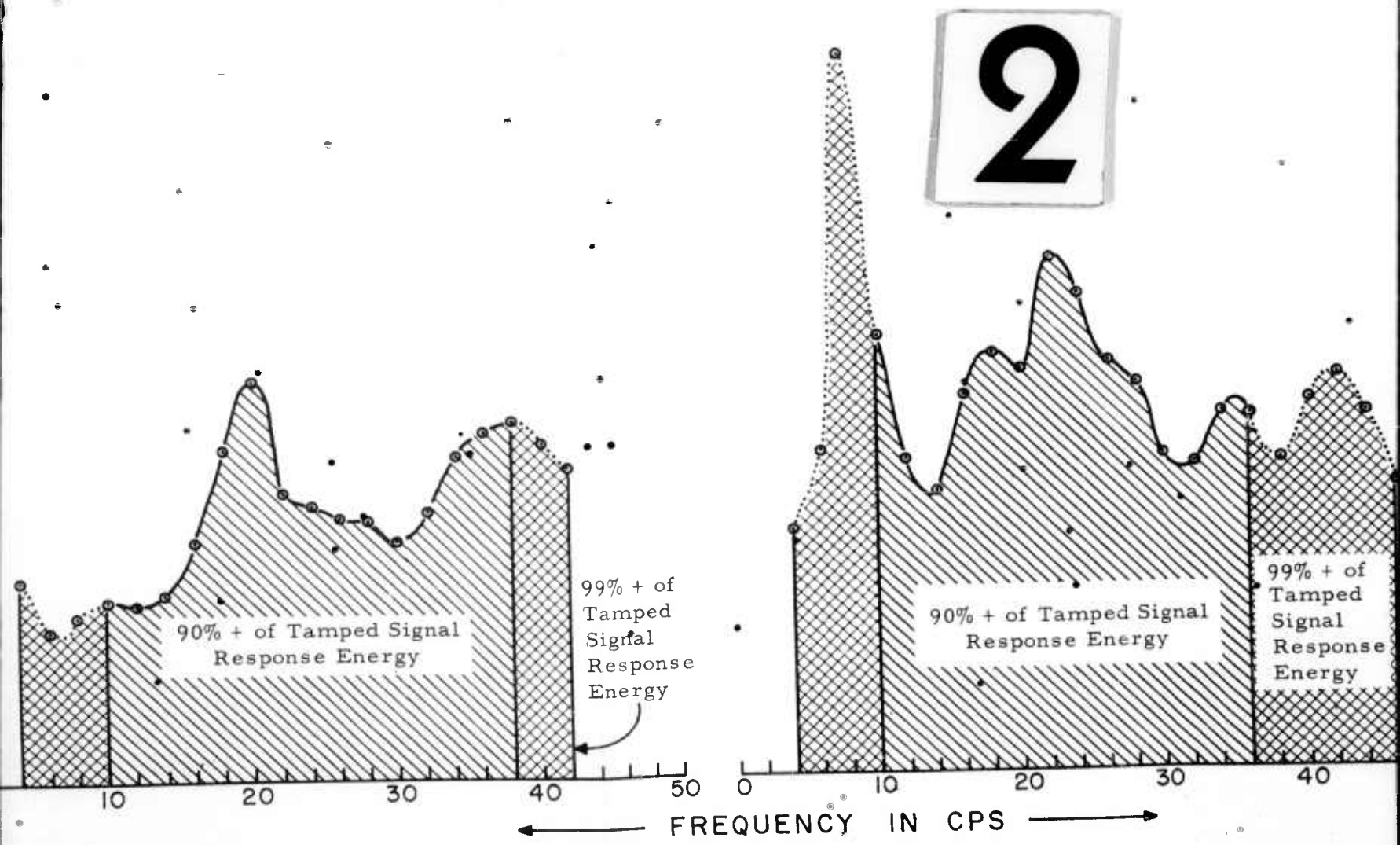

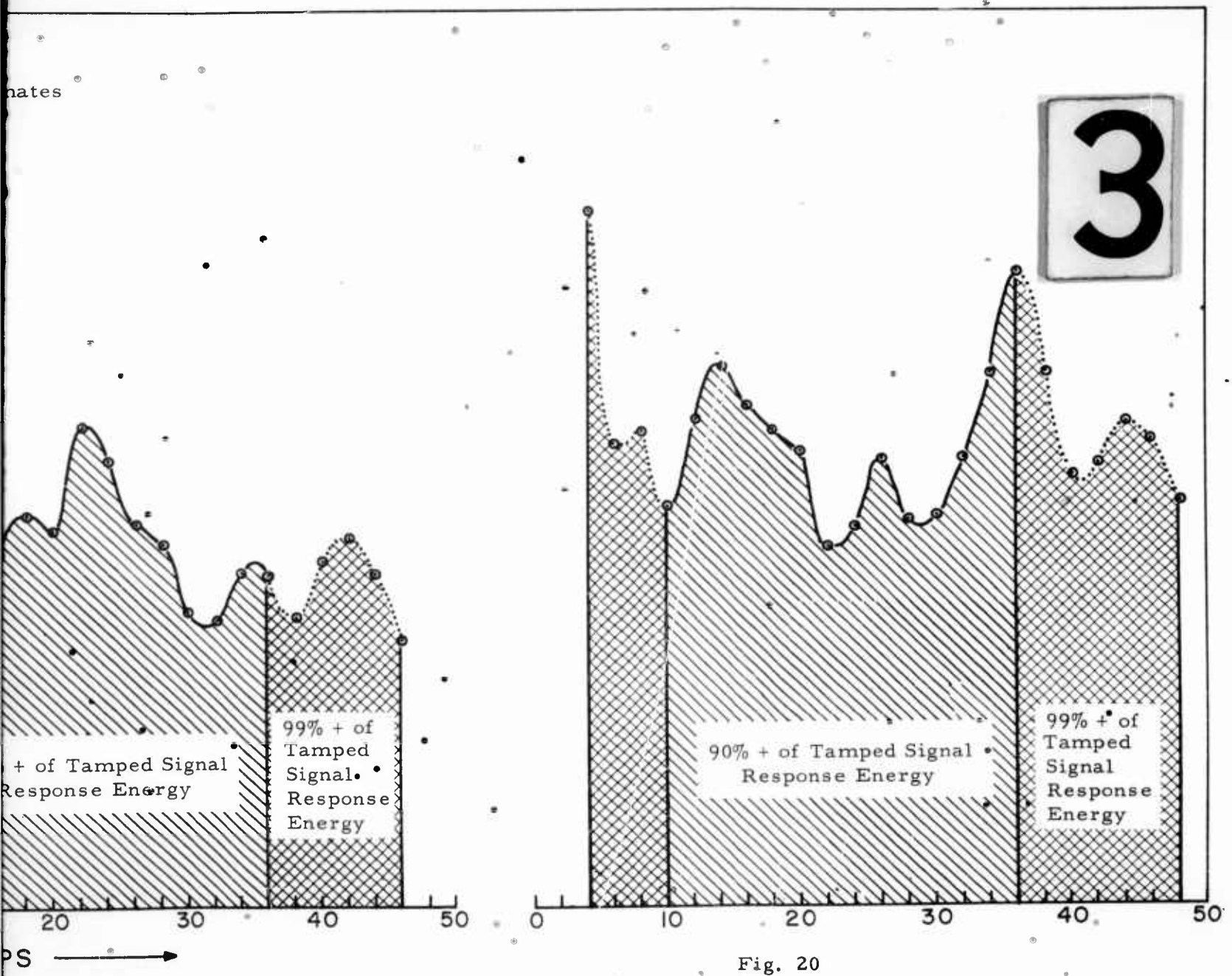

Fig. 20
Amplitude Density Ratios for the 1000 pound
Shots at Station 5B, 5D, 5E, and 5F

$$A(f_i) = \sqrt{\frac{S_T(f_i) \cdot S_T(f_i)^*}{(S_{DC}(f_i) + N_{DC}(f_i))(S_{DC}(f_i) + N_{DC}(f_i))^* - N^1_{DC}(f_i) \cdot N^1_{DC}(f_i)^*}}$$

Dropping the notation (f_i) and allowing it to be assumed the denominator then becomes

$$\sqrt{S_{DC} \cdot S^*_{DC} + N_{DC}\ N^*_{DC} - N^1_{DC}\ N^{1*}_{DC}}$$

and as stated previously the cross terms $S_{DC}\ N^*_{DC}$ and $S^*_{DC}\ N_{DC}$ can be neglected if there is statistical independence of signal and noise. The argument of the denominator can then be expressed as $S^*_{DC}\ S_{DC} + \epsilon$ where ϵ is an expected error function. If ϵ is small compared to $S_{DC}\ S^*_{DC}$ the function $A(f_i)$ which has been computed approximates the desired function $a(f_i)$.

$$A(f_i) \approx a_{f_i} = \sqrt{\frac{S_T\ S^*_T}{S_{DC} \cdot S^*_{DC}}}$$

ϵ will be small if the signal-to-noise ratio for the decoupled shot

$$\frac{S_{DC}}{N_{DC}} >> 1 \qquad \text{or if } N_{DC} \approx N_{DC}{}^1$$

Thus, since the analysis has been limited to cases where the first condition is met, variations (usually small) in the noise will only contribute to second and third order variations in the computation of $A(f_i)$.

E. COHERENCE CALCULATIONS

At a given station the travel paths will be similar for the coupled and decoupled signals and the recording system will be the same. Hence, by following the theory of Latter, et al[3], the decoupling as seen at the surface should be similar to a linear filtering of the tamped shot signals. As predicted by Latter's theory the tamped source signal function attenuated by a linear filter is the expected form for the decoupled shot signal. Computations were conducted for a recording of the 500-pound decoupled and tamped tests #8 and #9 since the smaller decoupled shot was less likely to have exceeded the elastic limits on the wall of the 30 foot cavity than the larger shots and hence should be a better practical test. This modeling is represented in Figure 21.

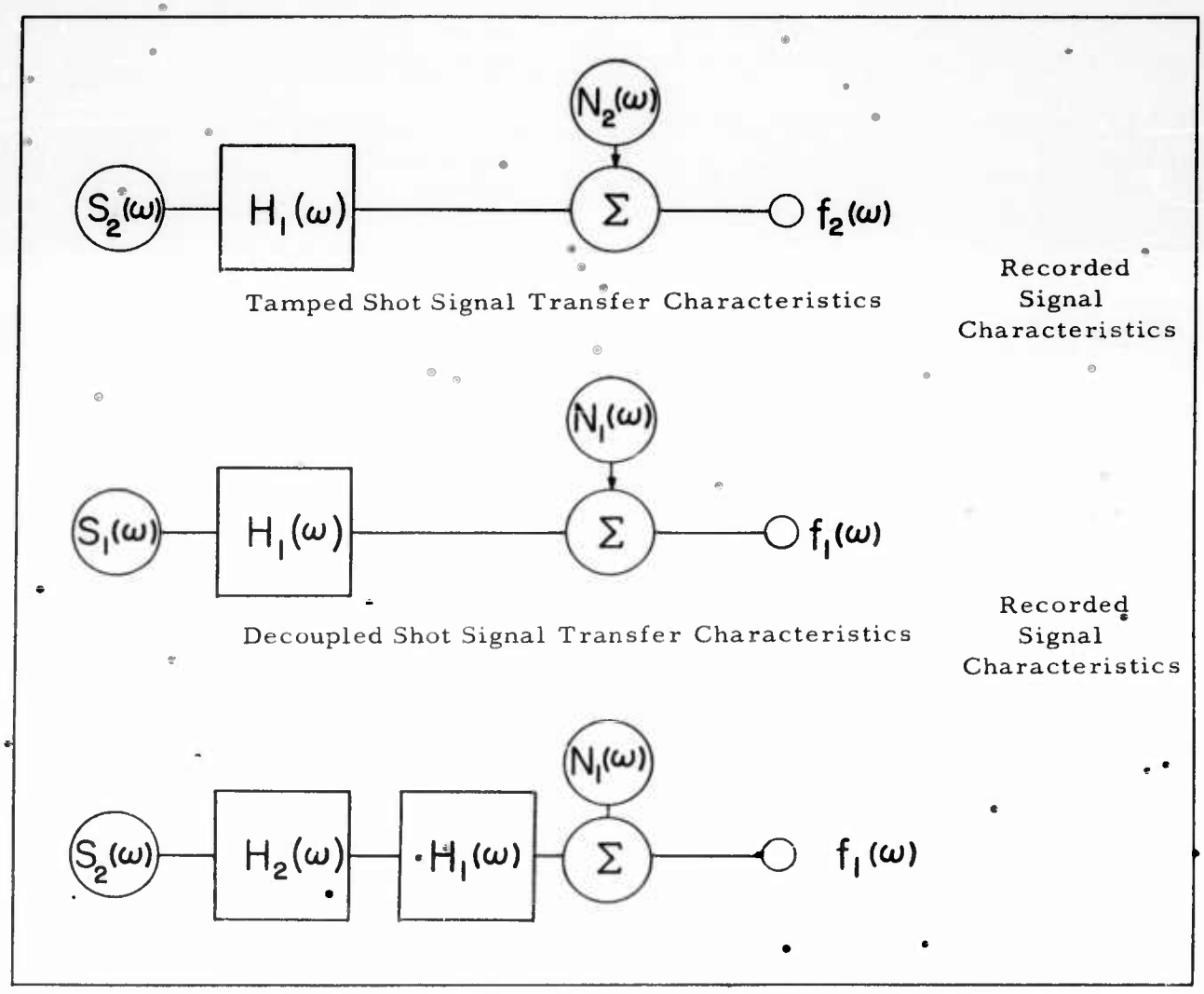

Fig. 21
Assumed Modeling of Decoupled Signal by Linear Filtering of Tamped Shot Source Characteristics

The following notations are used, in which the dependence on frequency is assumed:

S_1 = the frequency response of the decoupled shot as it leaves the source region

S_2 = the frequency response of the tamped shots as it leaves the source region

H_1 = the filtering due to the ground path

N_1 = the noise amplitude spectra recorded at the seismometer for the decoupled shot

N_2 = the noise amplitude spectra recorded at the seismometer for the tamped shot

H_2 = the assumed linear filter for which $S_1 = H_2\ S_2$, then the tamped shot response can be given as $S_2\ H_1 + N_2$ and the decoupled responses $S_1\ H_1 + N_1$ can be represented as $S_2\ H_2\ H_1 + N_1$.

The energy density spectra of the decoupled signal response can then be represented as:

$$\Phi_{11} = (S_2\ H_2\ H_1 + N_1)\ (S_2^*\ H_2^*\ H^* + N_1^*)$$

where * represents complex conjugate.

If the noise is statistically independent of the signal

$$S_2^*\ H_2^*\ H_1^*\ N_1 = N_1^*\ S_2\ H_2\ H_1 = 0$$

and the above relation becomes $\Phi_{11} = S_2\ H_2\ H_1\ S_2^*\ H_2^*\ H_1^* + N_1\ N_1^*$.

The energy density spectra of the tamped signal response can be represented similarly:

$$\Phi_{22} = (S_2\ H_1 + N_2)\ (S_2^*\ H_1^* + N_2^*).$$

Again, if the noise and signal are independent

$S_2\ H_1\ N_2^* = S_2^*\ H_1^*\ N_2 = 0$ and the relation becomes

$$\Phi_{22} = S_2\ H_1\ S_2^*\ H_1^* + N_2\ N_2^*.$$

The cross energy density spectrum of the coupled and decoupled signal response can be represented as:

$$\Phi_{12} = (S_2\ H_2\ H_1 + N_1)\ (S_2^*\ H_1^* + N_2^*).$$

Now if the two noise samples and noise and signals can be assumed as statistically independent

$N_1\ N_2^* = N_1\ S_2^*\ H_1^* = N_2^*\ S_2\ H_2\ H_1 = 0$ and the above relation becomes

$$\Phi_{12} = S_2\ H_2\ H_1\ S_2^*\ H_1^*.$$

Now if we define coherence as

$$K_{12} \triangleq \frac{\left|\Phi_{12}\right|^2}{\Phi_{11}\,\Phi_{22}}$$

$$\text{then } K_{12} = \frac{S_2\ S_2^*\ H_1^*\ H_1^*\ H_2\ S_2^*\ S_2\ H_1\ H_1\ H_2^*}{(S_2\ H_2\ H_1\ S_2^*\ H_2^*\ H_1^* + N_1\ N_1^*)\,(S_2\ H_1\ S_2^*\ H_1^* + N_2\ N_2^*)}$$

therefore, if

$$\frac{S_2\ S_2^*\ H_1\ H_1^*}{N_2\ N_2^*} \gg 1$$

$$\text{and } \frac{S_2\ S_2^*\ H_1\ H_1^*\ H_2\ H_2^*}{N_1\ N_1^*} \gg 1$$

then $K_{12} \approx 1$. K_{12} must be equal to or less than unity. Therefore, if the noise spectra are small in comparison to both the tamped and decoupled spectral estimates the nearness of K_{12} to a value of unity will be directly related to the validity of the assumption that $S_1 = S_2\ H_2$. The effect of decoupling can be thought of as a linear filtering of the tamped signal response.

As a test of this hypothesis the recordings of the signals from the 500-pound tests 8 and 9 as recorded by the S-41 seismometer at station 5B were analyzed for K_{12}.

This data is appropriate since the signal-to-noise ratio is quite large for both the decoupled and tamped shot recordings. The values computed were $K_{12} = \frac{\left|\Phi_{12}\right|^2}{\Phi_{11}\,\Phi_{22}}$ for samples of signal response data of 2.048-seconds duration.

The analysis of the two second data samples is shown in Figure 22. It is interesting to note that the highest value shown is that at 2 cps corresponding to a coherence of the 2-cps microseismic noise. The values shown between 22 cps and 40 cps indicate that the assumption

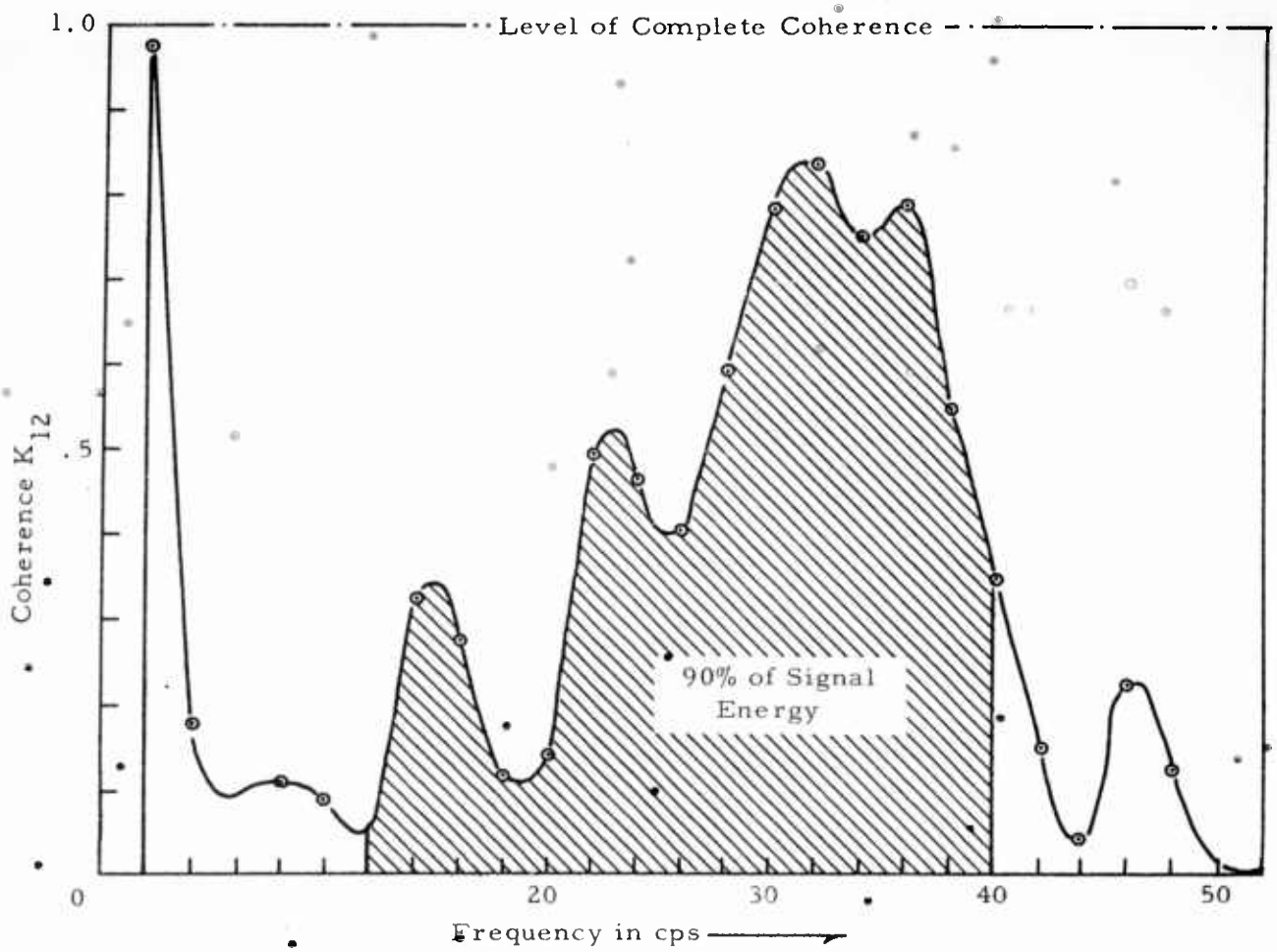

$$\text{Coherence } K_{12}(\omega) = \frac{\left(\Phi_{12}(\omega)\right)^2}{\Phi_{11}(\omega)\,\Phi_{22}(\omega)}$$

for 2.048 second signal samples from the response of the S-41 Seismometer at Station 5-B for the 500 pound Tamped and Decoupled Test Shots #8 & #9

Seismometer to source separations: Shot #8 - 22,696 feet
Shot #9 - 22,285 feet

Fig. 22
Coherence between Tamped and Decoupled Shot Responses

of the linear filter characteristics of decoupling are reasonably upheld within this pass band. Above 40 cps the signal return dropped off sharply and below 20 cps the energies prominent in the tamped recordings had greater attenuation in the decoupled response.

The transfer characteristics of the source environment filter $H_2(\omega)$ can now be determined.

Since $\Phi_{12} \approx S_2 \; H_2 \; H_1 \; S_2^* \; H_1^*$

and $\Phi_{22} \approx S_2 \; H_1 \; S_2^* \; H_1^*$ under the assumption that the noise response is smaller as compared to the signal, then

$\frac{\Phi_{12}}{\Phi_{22}} \approx H_2$ the transfer characteristic of the source environment. The amplitude response of $H_2(\omega)$ as predicted from the linear filtering hypothesis is shown in Figure 23. There is an alternative way to compute $H_2(\omega)$.

Theoretically, since

$$\Phi_{11} = S_2 \; H_2 \; H_1 \; S_2^* \; H_2^* \; H_1^* + N_1 \; N_1^*$$

and

$$\Phi_{22} = S_2 \; H_1 \; S_2^* \; H_1^* + N_2 \; N_2^*$$

if the contribution of the noise is subtracted or is relatively small

$$\frac{\Phi_{11}(\omega)}{\Phi_{22}(\omega)} \approx H_2(\omega)$$

$H_2(\omega)$ is the filter required to change the amplitude response of the tamped source $S_2(\omega)$ into the amplitude response of the decoupled source $S_1(\omega)$. If linearity were exact the H_2 amplitude characteristics found in this manner would be the same as that shown above in figure 23. The result of these computations with and without noise compensation are presented in Figures 24 and 25 respectively.

The differences between these three curves are indications of the degree of variations from the assumptions of a linear source environment filter and neglectablity of noise affects and cross product terms. The general character of all three curves is quite similar and indicates quantitatively the frequency dependence of the attenuation of the cavity environment for one particular test.

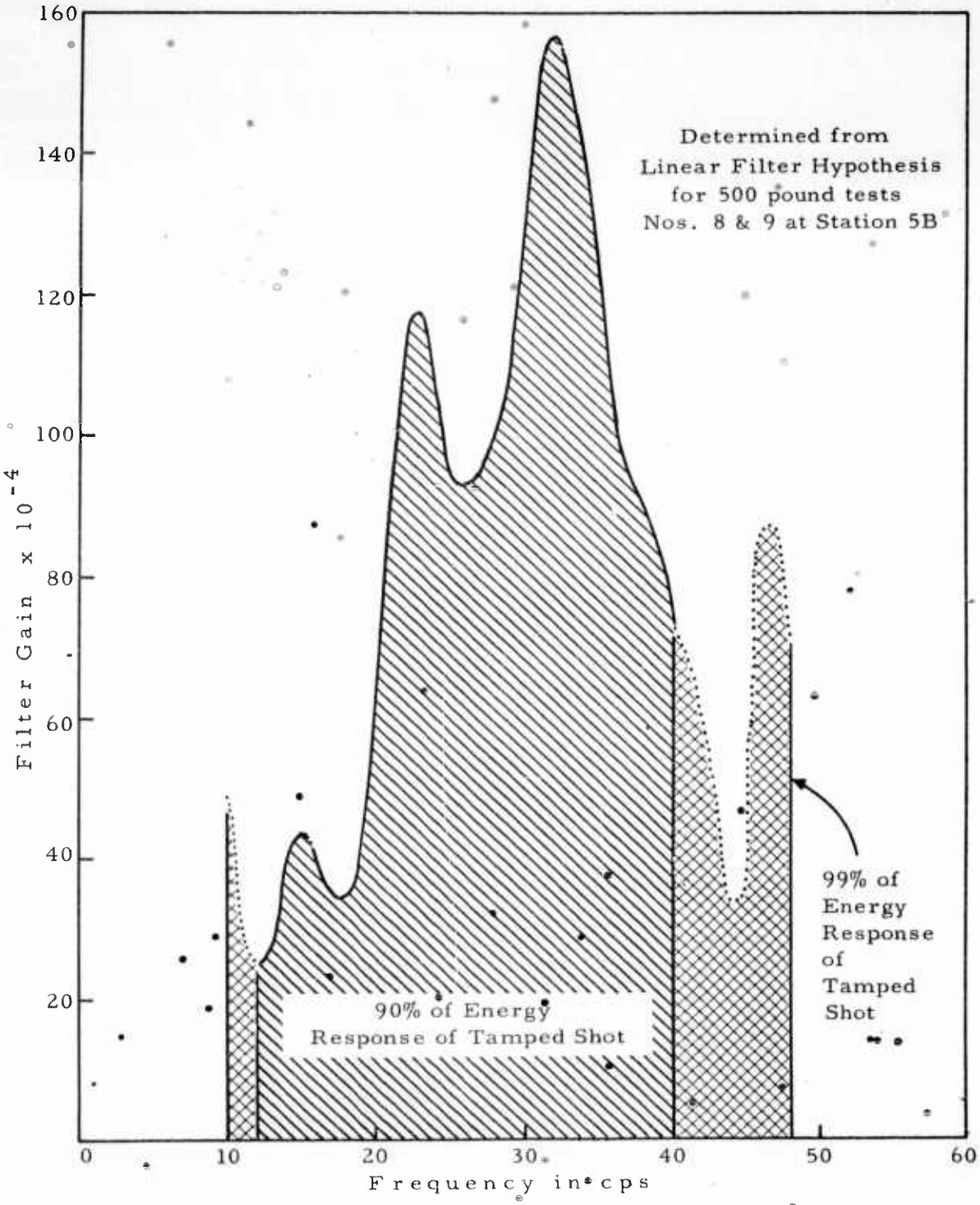

Fig. 23
Source Environment Filter Amplitude Characteristics

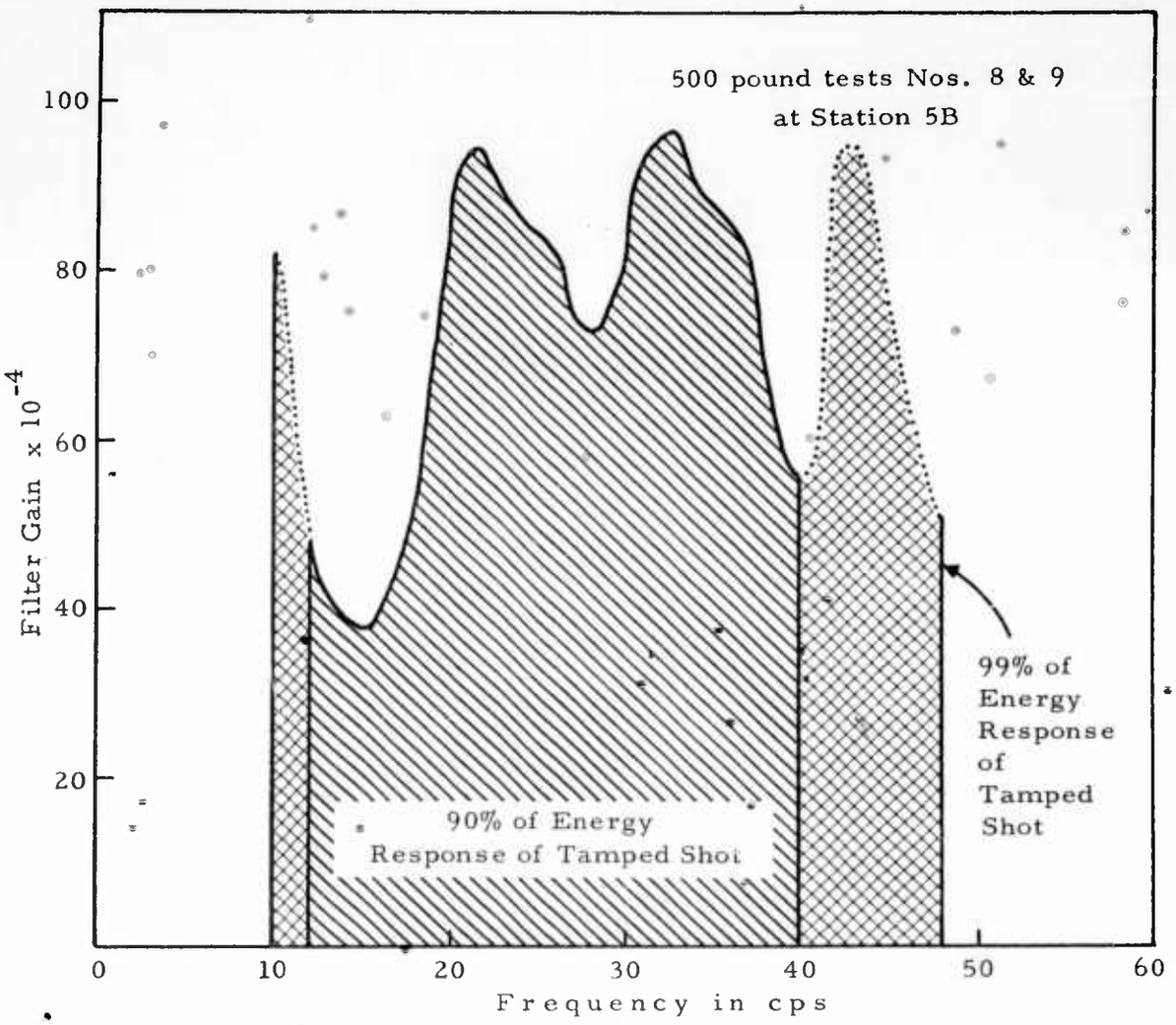

Fig. 24
Amplitude Response of Filter Necessary to Convert
Tamped Signal Response to Decoupled Signal
Response (Noise Compensated)

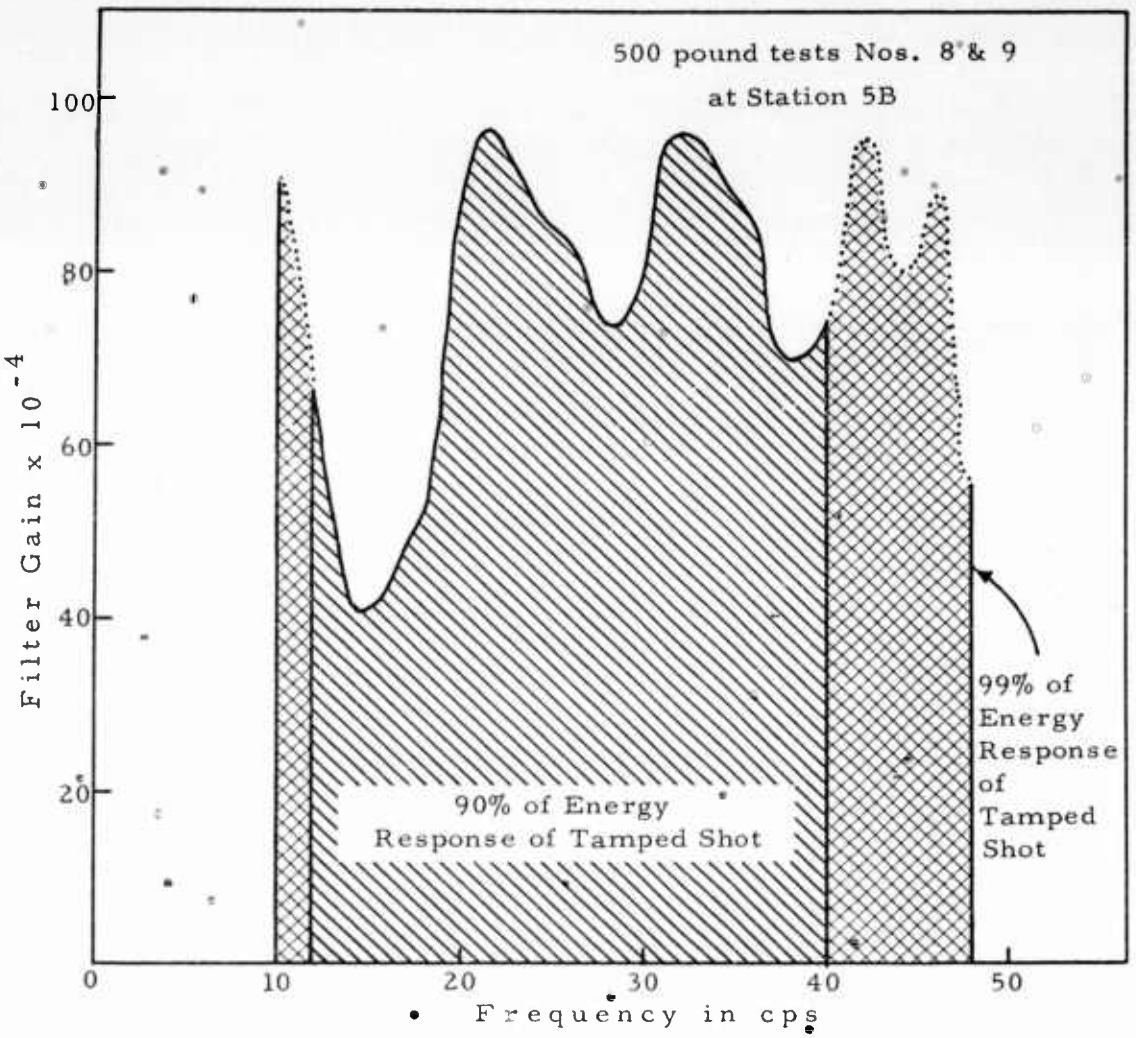

Fig. 25
Amplitude Response of Filter Necessary to Convert
Tamped Signal Response to Decoupled Signal
Response (Noise not Compensated)

SECTION IV

CONCLUSIONS

It can be concluded from this study that the partition of energy in a decoupled shot is different from that radiating from a tamped shot. This partitioning refers to the amounts of energy present in various types of elastic wave propagation and to the relative amounts of elastic wave motion in various modes. For the various decoupled shots of different sizes this partitioning change indicates that the degree and type of decoupling varied with the size of the charge and the cavity in which it was fired. Therefore, the values of the amplitude density ratios of tamped to decoupled shots are dependent on frequency, the modes contained in the section of the response which is analyzed, and on the size and disposition of the decoupled shot. In addition, for some of the body wave modes recorded from a tamped and decoupled shot pair at a single station, the decoupled signal can be approximated by linear filtering of the tamped shot source function. However, the decoupling as analyzed at different stations is seen to increase with distance from the source. This phenomenon is difficult to explain in that it seems to require different attenuation characteristics for tamped and decoupled shots.

In general, it is possible to greatly attenuate the seismic energy radiating from a given size shot by detonation in a cavity environment. As recorded at the surface, the degree of decoupling is only roughly predictable and extrapolation to the decoupling of underground nuclear explosions at much greater distances will be quite difficult.

SECTION V

REFERENCES

1. Adams, William M. and Dewitt C. Allen, "Seismic Decoupling for Explosions in Spherical Cavities," Project Cowboy Final Report, UCRL 6086 (Contract No. W-7405-eng-48), August 1960.

2. Lee, Y. W., Statistical Theory of Communication, John Wiley & Sons, 1960.

3. Latter, A. L., R. E. LeLevier, E. A. Martinelli, and W. G. McMillan, "A Method of Concealing Underground Nuclear Explosions," Journal of Geophysical Research, Vol. 66, No. 3, March 1961, pp. 943-946.

4. Murphy, Byron F., "Particle Motion Near Explosions in Halite," Journal of Geophysical Research, Vol. 66 No. 3, March 1961, pp. 947-958.

APPENDIX A

GROUND PARTICLE VELOCITIES

APPENDIX A

GROUND PARTICLE VELOCITIES

Absolute determination of the instantaneous and average ground particle velocities as recorded by the S-41 seismometers have been made. Some peak signal values are presented here with a formulation for obtaining average values directly from the energy density spectra presented in this report.

The absolute particle velocity for the peak amplitudes recorded for the 500 pound tamped and decoupled shots 8 and 9 by S-41 seismometers at station 5A through 5F are presented in Table A1

TABLE A1

PEAK PARTICLE VELOCITIES FOR SHOTS 8 AND 9

Station	Tamped	Decoupled
5-A	1.075×10^{-2} in/sec	9.3×10^{-5} in/sec
5-B	1.08×10^{-2} in/sec	1.425×10^{-4} in/sec
5-C	3.7×10^{-3} in/sec	4.8×10^{-5} in/sec
5-D	6.23×10^{-3} in/sec	5.96×10^{-5} in/sec
5-E	4.58×10^{-3} in/sec	4.86×10^{-5} in/sec
5-F	6.5×10^{-3} in/sec	6.85×10^{-5} in/sec

The effects of seismometer coupling, environment, and travel paths are quite evident from the above data.

It is possible to compute 4-cps band averages of particle velocities from the energy density plots if they are desired. The process is quite simply that of taking the square root of this product and multiplying the result by 6.35×10^{-8} inches/second. This constant is directly related to the S-41 response characteristics.

APPENDIX B

GENERAL ANALYSIS OF FIELD DATA

APPENDIX B

GENERAL ANALYSIS OF FIELD DATA

Some of the general features of the data which were analyzed are presented here as background information to the prime purpose of determining decoupling characteristics. The data included can be derived directly from the field records shown in Section II.

1. The 200-pound decoupled shot cannot be detected in Figure 4 but all larger shots were observable on the field monitor and playback records.

2. The records for the tamped shots revealed a long train of energy with amplitudes recorded at a rather constant level over several seconds as both body and surface wave energy.

3. The decoupled shots, on the other hand, appear to have recorded a short duration body wave or two (refraction arrivals) and little else. The later arrivals being of lower amplitude are obscured in the noise and hence are not seen.

4. The records made for the 1000-pound shot decoupled in the 12-foot diameter hole (shot 12 presented in Figure 6) indicate the occurrence of several refraction arrivals which were not apparent on any of the other decoupled shot recordings. This later arriving energy is present on the tamped shot recordings, however, and indicates that shot 12 was not decoupled to the same extent as the shots in the larger hole. Hence, following the theory of Latter, et. al.[3], it is presumed that this shot exceeded the elastic limit of the wall of the 12-foot sphere. It is interesting to note that the later arriving surface waves for the 12-foot sphere shot are still attenuated below visual detectability.

A closer look at this data reveals that the first arriving energy does not travel the same refraction path from shot to shot or along the same refraction interface from seismometer to seismometer. As indicated by the travel-time curves of Figure 4.2 of the Project Cowboy report of Adams and Allen,[1] there may be a number of intersecting refractions arriving at similar times for stations between 20,000 and 26,000 feet from the source. This is unfortunate from the standpoint of separation of events but it may help to explain variations in the arrival times and in the calculated apparent velocities. Table B1 shows values of apparent velocities determined from these records.

TABLE B1

VALUES OF APPARENT VELOCITIES AS TIMED FOR STATION 5-A

Shot #		First Apparent Velocity	Picked Time at Station 5A	Later Arrival Velocity	Picked Time at 5A
200# Tamped	7	19,000 ft/sec	2.220 seconds		
500# DC	8	17,500	2.240		
500# Tamped	9	17,500	2.200	9000 ft/sec	2.935 seconds
1000# DC	10	16,000 & 19,000	2.198 & 2.240		
1000# Tamped	11	19,000 & 17,500	2.200 & 2.238	9000	2.950
1000# DC	12	17,500	2.200	9000	2.895

These arrival times are not always the first arriving energy but are the times corresponding to a peak or trough which can be correlated from trace to trace.

Table B2 presents the time increment from the shot to the first arriving energy which is obviously not part of the noise.

TABLE B2

GROUP VELOCITIES (AS TIMED FOR STATION 5-A)

Shot #	Δt	Distance	Distance/Δt
6	?	22,100 feet	----------
7	2.208	21,600 feet	9,783 ft/sec
8	2.204	22,100 feet	10,027 ft/sec
9	2.184	21,690 feet	9,931 ft/sec
10	2.197	22,100 feet	10,059 ft/sec
11	2.175	21,752 feet	10,001 ft/sec
12	2.192	21,858 feet	9,972 ft/sec

Thus, it is concluded that various wave paths have been traveled by the first arriving significant energy for the various shots for a given seismometer location. The group velocity is indicative of a deep traveling wave which has transversed much slower material upon leaving the refraction interface. The times are commensurate with the travel curves shown in Figure 4.2 of Adams and Allen,[1] although the apparent velocities of 17,500 ft/second of Table B2 do not appear in their Table No. 4.3. This may

indicate some changes in the stratigraphy but the data is too sparse and the possibility of overlapping refraction arrivals too great to prove or disprove any geologic interpretation. The arrivals as picked indicate an apparent velocity of 17,500 feet per second.

Filtering and Time Shift Computations. - With some knowledge of the signal and noise analysis presented in this report an attempt was made to recover the signal from the 200-pound decoupled shot by digital frequency filtering and applying move-out corrections for apparent velocities described above. The data from shot 6 was filtered with a 16 to 54 cps bandpass filter and a 32 to 56 cps bandpass filter. The broader filter was designed in order to reject 2-, 4-, 8-, and 60-cycle energy which showed up in some of the spectral analysis of the noise preceding the detonation time. The narrower filter was computed in an effort to also cancel any noise response below 30 cps since a greater signal-to-noise ratio was expected above this frequency. As can be seen in Figures B1 through B6, neither filter obtained an obvious signal. The problem being that the noise remaining in the selected pass bands is still much greater than the signal. The expected arrival times of the refraction for which the normal move out correction is made are indicated in each graph by .1 seconds on the time scale. Although some coherence may be seen, the presence of an observable signal remains questionable. It is felt that further frequency filtering is not justified.

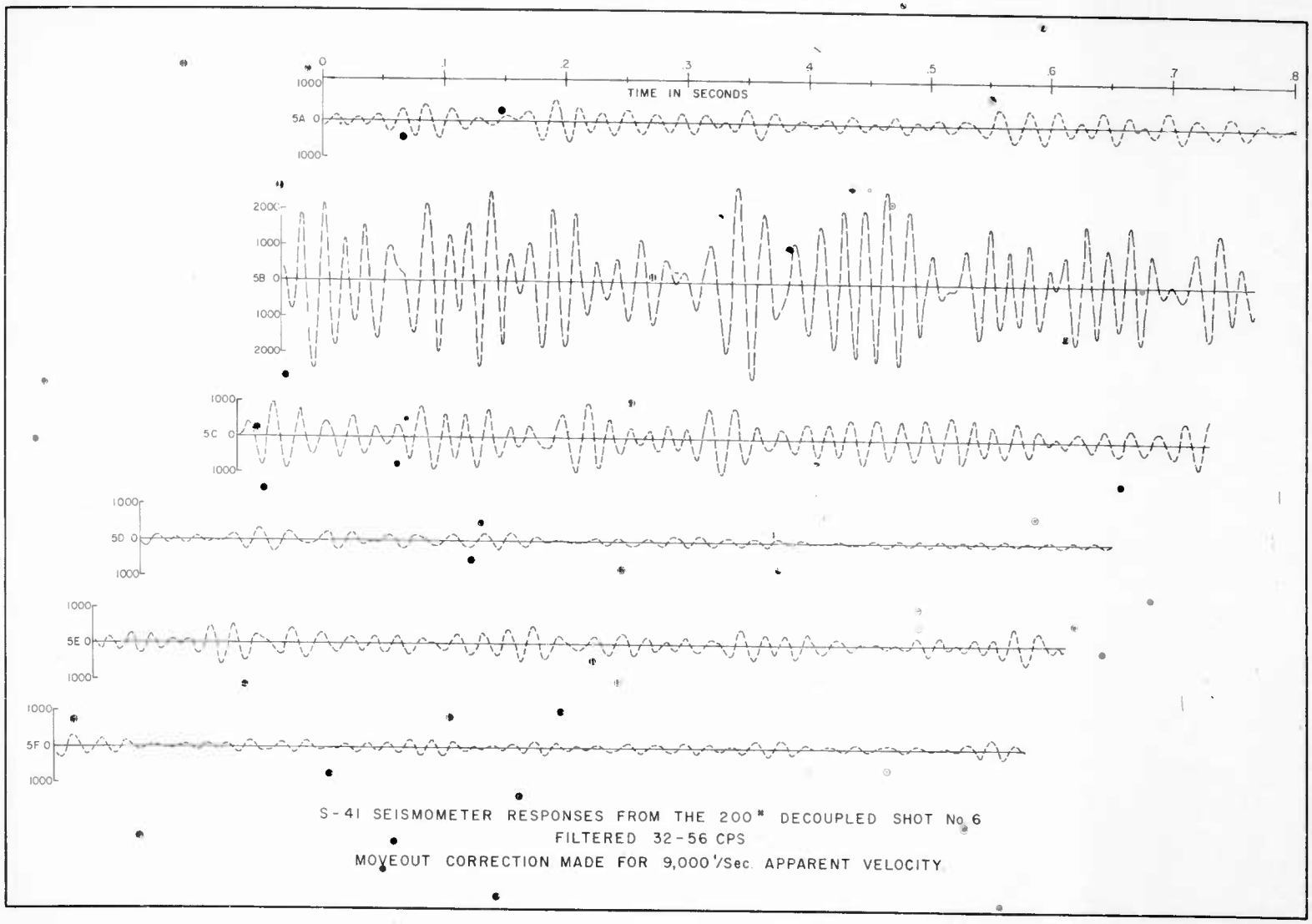

S-41 SEISMOMETER RESPONSES FROM THE 200* DECOUPLED SHOT No. 6
FILTERED 32-56 CPS
MOVEOUT CORRECTION MADE FOR 9,000'/Sec. APPARENT VELOCITY

Fig. B1

Filtered 32-56 cps Move-Out Correlation for 9000, 1/sec Apparent Velocity

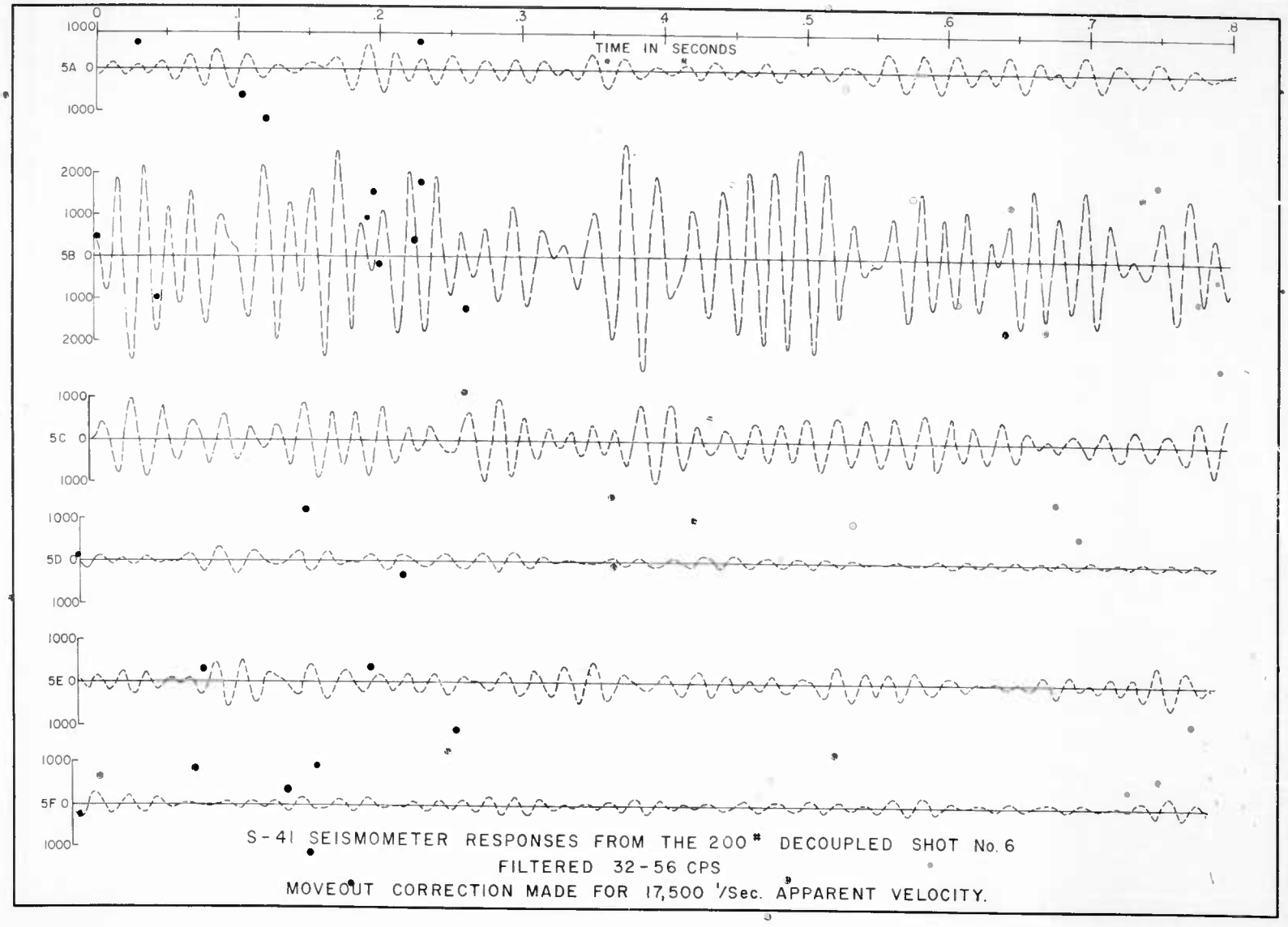

Fig. B2
Filtered 32-56 cps Move-Out Correlation for 17,500
• 1/sec Apparent Velocity

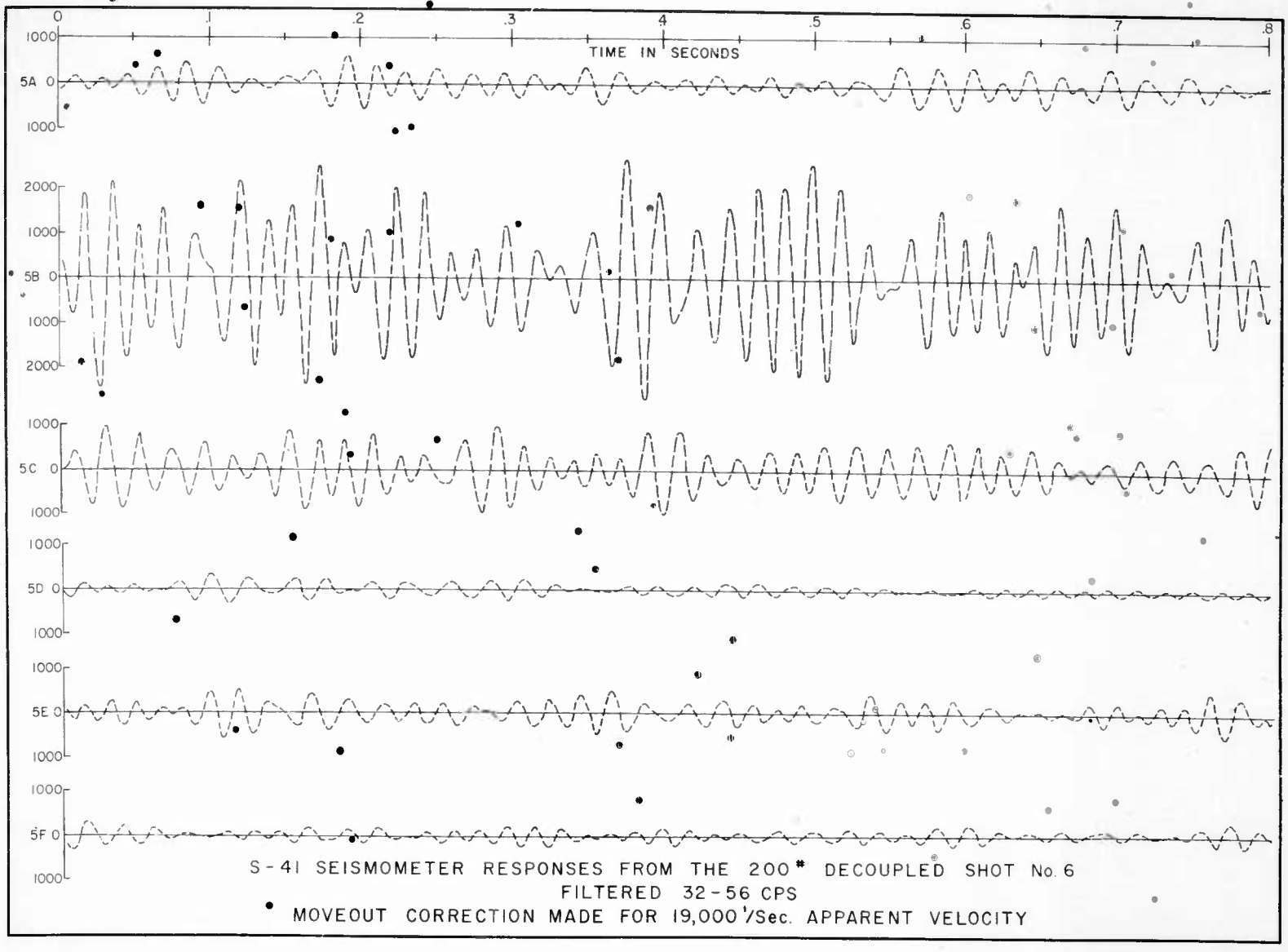

Fig. B3
Filtered 32-56 cps Move-Out Correlation for 19,000
1/sec Apparent Velocity

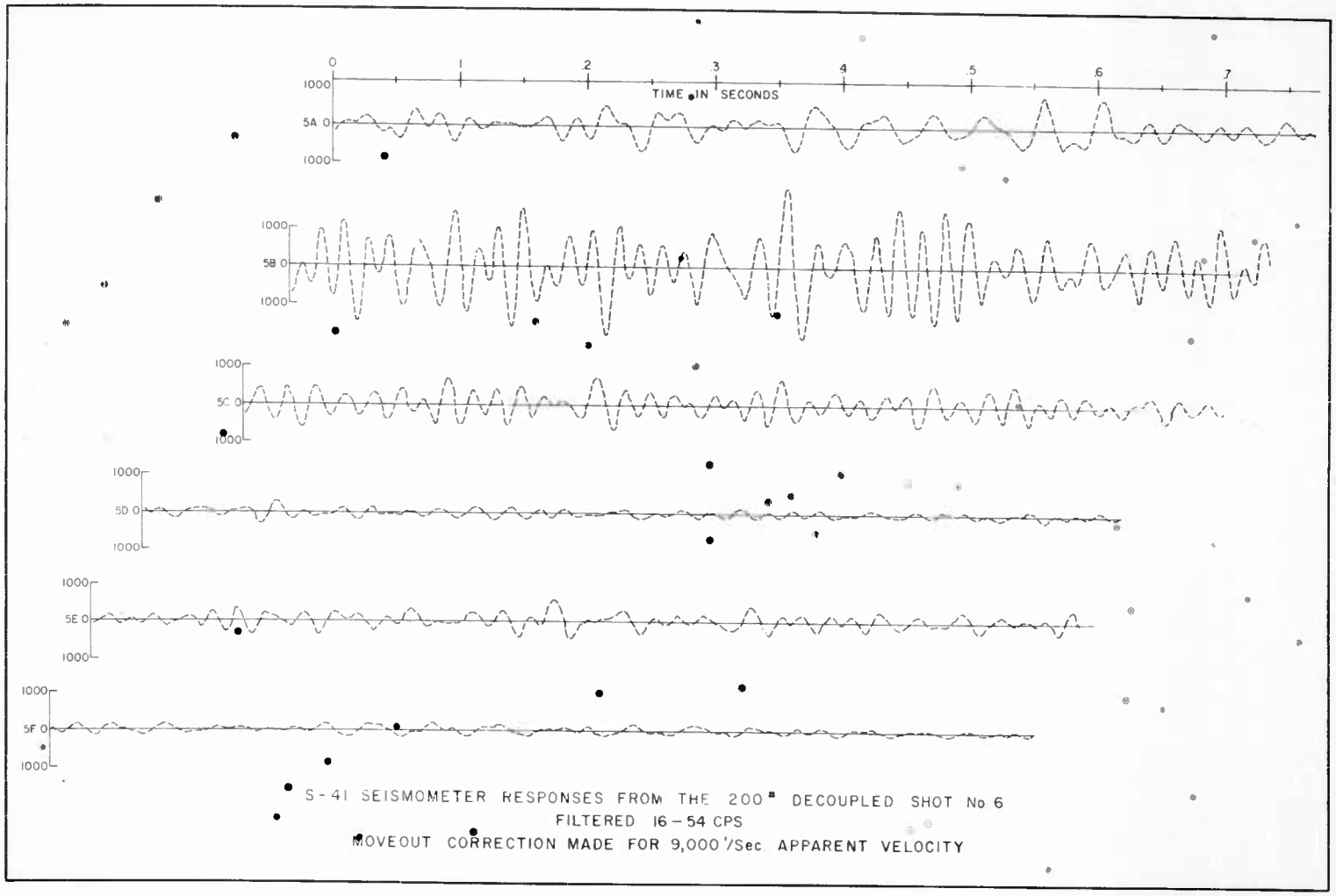

Fig. B4
Filtered 16-54 Move-Out Correlation for 9000
1/sec Apparent Velocity

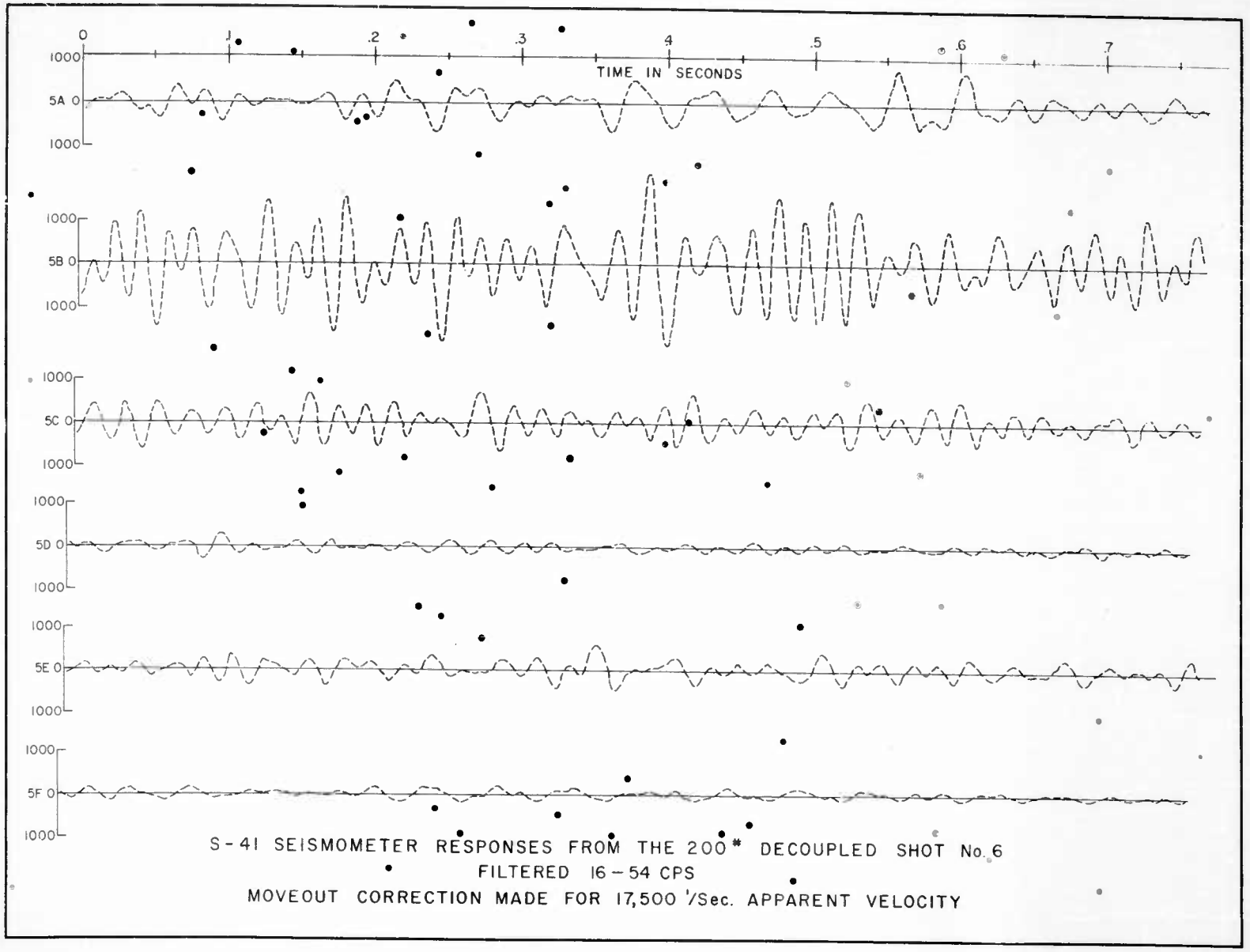

Fig. B5
Filtered 16-54 cps Move-Out Correlation for 17,500 1/sec Apparent Velocity

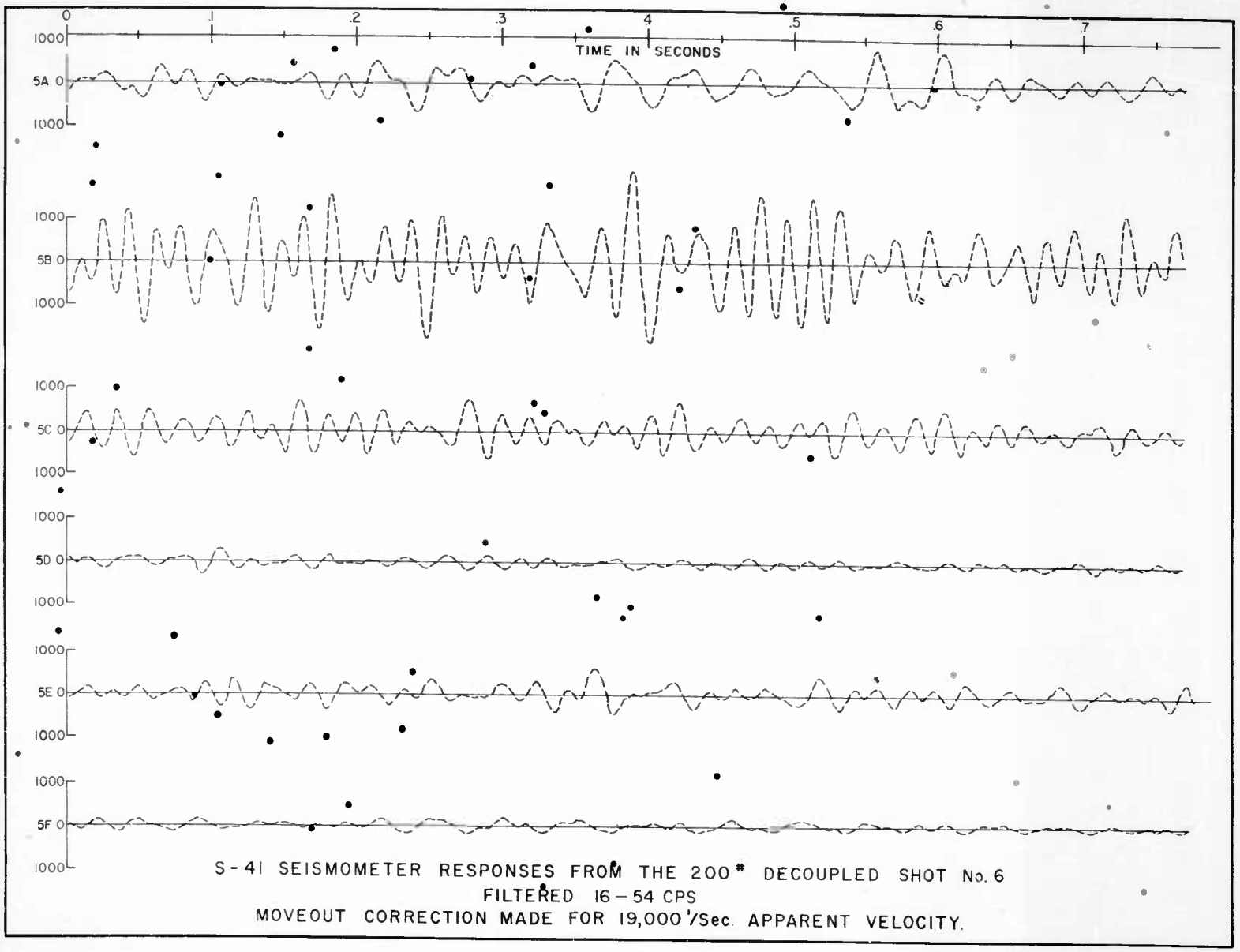

Fig. B6
Filtered 16-54 cps Move-Out Correlation for 19,000 1/sec Apparent Velocity

APPENDIX C

GENERAL NOISE ANALYSIS

APPENDIX C

GENERAL NOISE ANALYSIS

In the main text of this report it has been shown that the accuracy of the analysis depends on the characteristics of the noise. It is in this regard that this appendix contains the general characteristics of the noise. Some general statements concerning the noise are worthy of note.

1. The power density spectral estimates differ greatly from one station to the next and only the long time (2 second) averages can be expected to be quasi-stationary for individual seismometer responses over periods of several seconds. The quasi-stationarity is illustrated in Figures C1 and C2 which show the power density spectra obtained by analyzing two successive 2.048-second samples of noise from the same seismometer preceding the 500-pound decoupled shot.

2. The background noise level as well as individual predominant power density estimates vary markedly for samples separated by one hour (the time between the decoupled and tamped shots). This is illustrated in Figures C3 and C4 which show the average power density levels differing by a factor of 5 or greater.

3. The signal and noise spectral estimates may cover the same frequency ranges for any recording. Since the noise is not predictable from shot to shot or station to station such attempts of signal enhancement by frequency bandpass filtering, as presented in Appendix B for the 200-pound decoupled shot, are of questionable value.

4. Certain frequencies did appear predominant and consistent on some of the recordings. The two-cycle per second microseismic noise, although greatly attenuated by the response characteristics of the S-41 seismometers was present on many of the recordings. An eight-cps noise appeared consistent at several stations and is probably relatable to the proximity of a pumping station to these seismometers.

The analysis of the stationarity of noise preceding each decoupled shot such as presented in Section III provides a guide to the general signal-to-noise ratios expected and establishes where errors in the noise estimates will cause only secondary errors in the computation of amplitude density ratios.

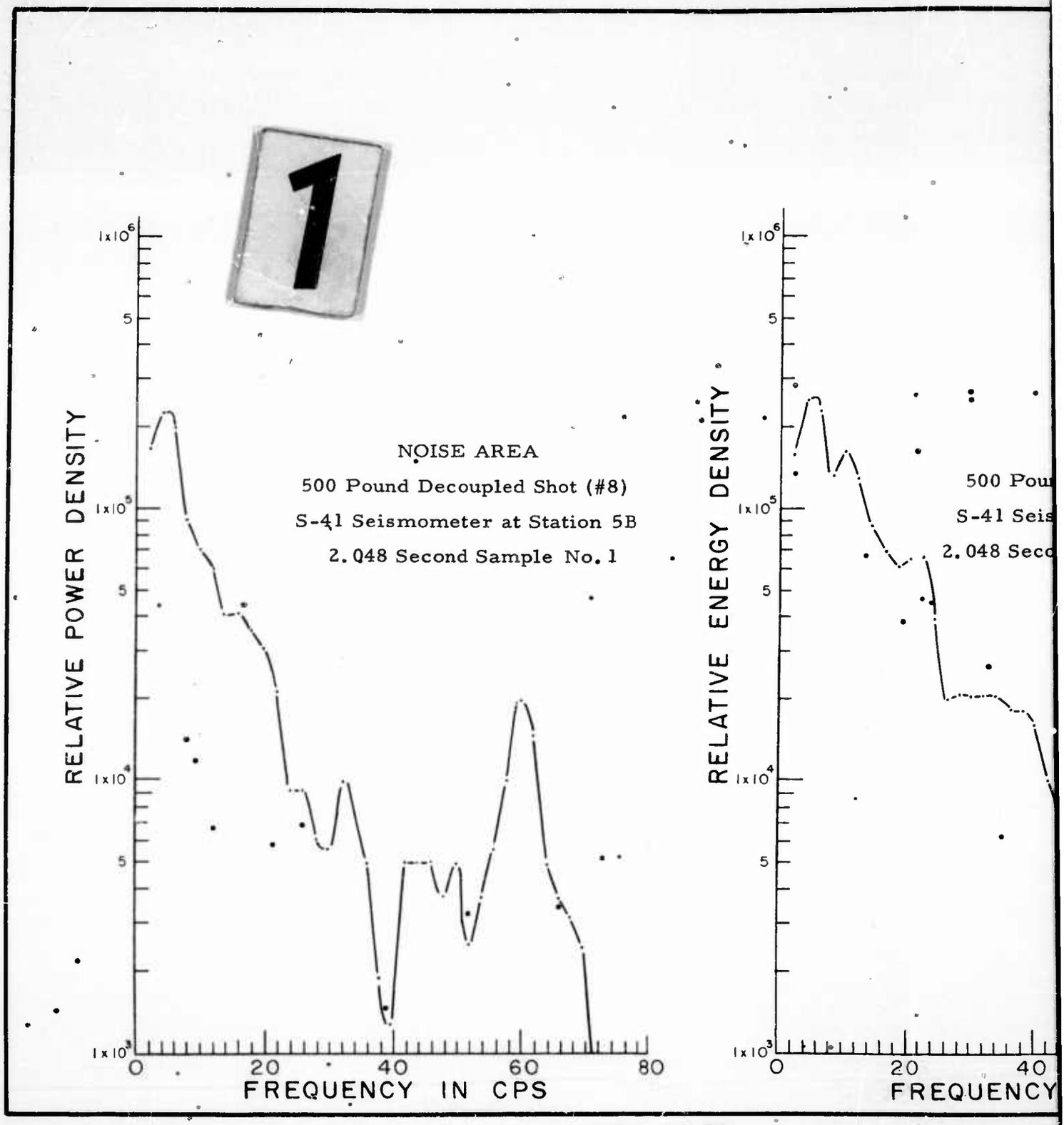

Fig. C1, C2

Power Density Spectra from Two Successive 2.048 second Samples of Noise from the Sa

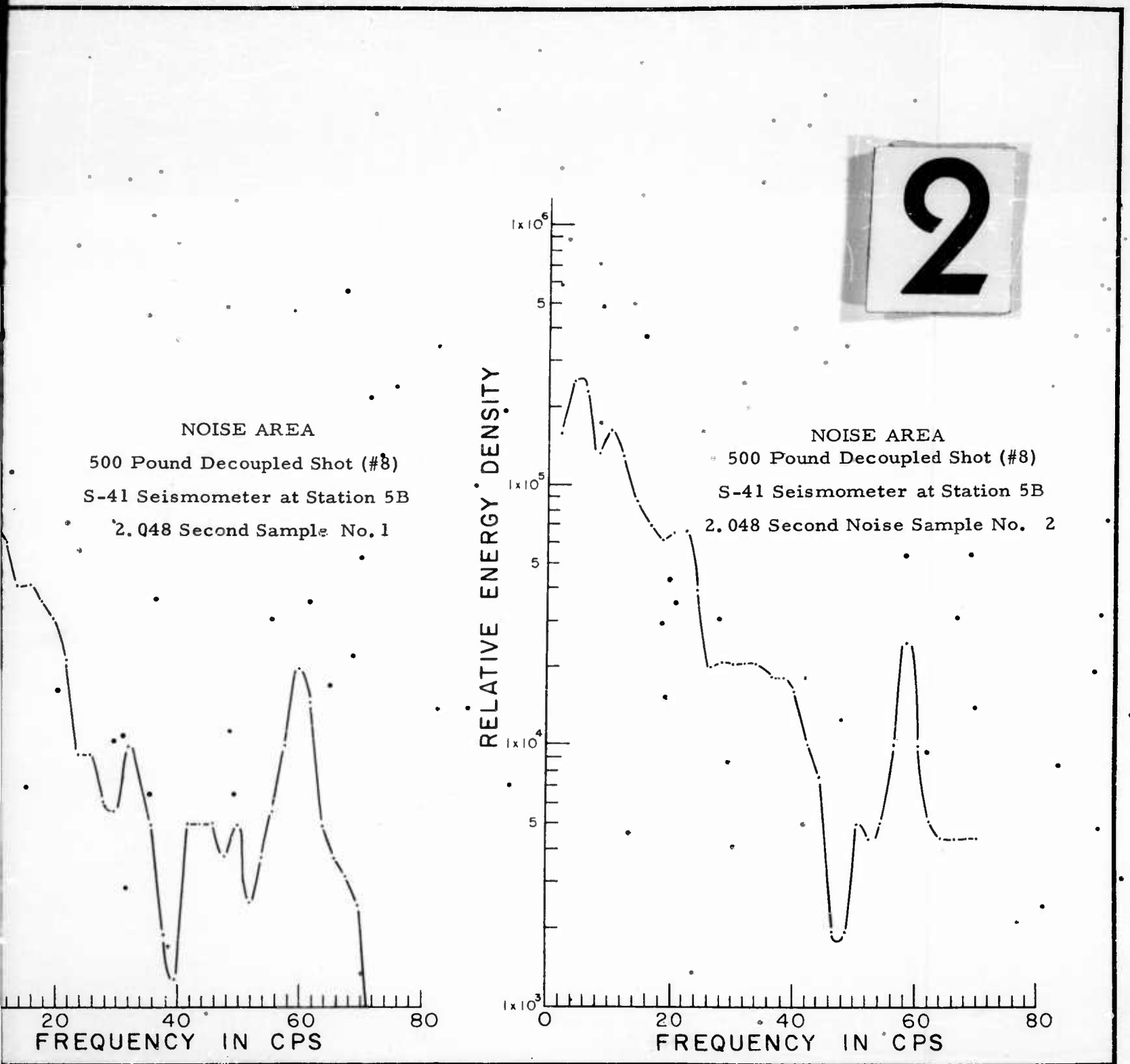

Fig. C1, C2

nsity Spectra from Two Successive 2.048 second Samples of Noise from the Same Seisemometer

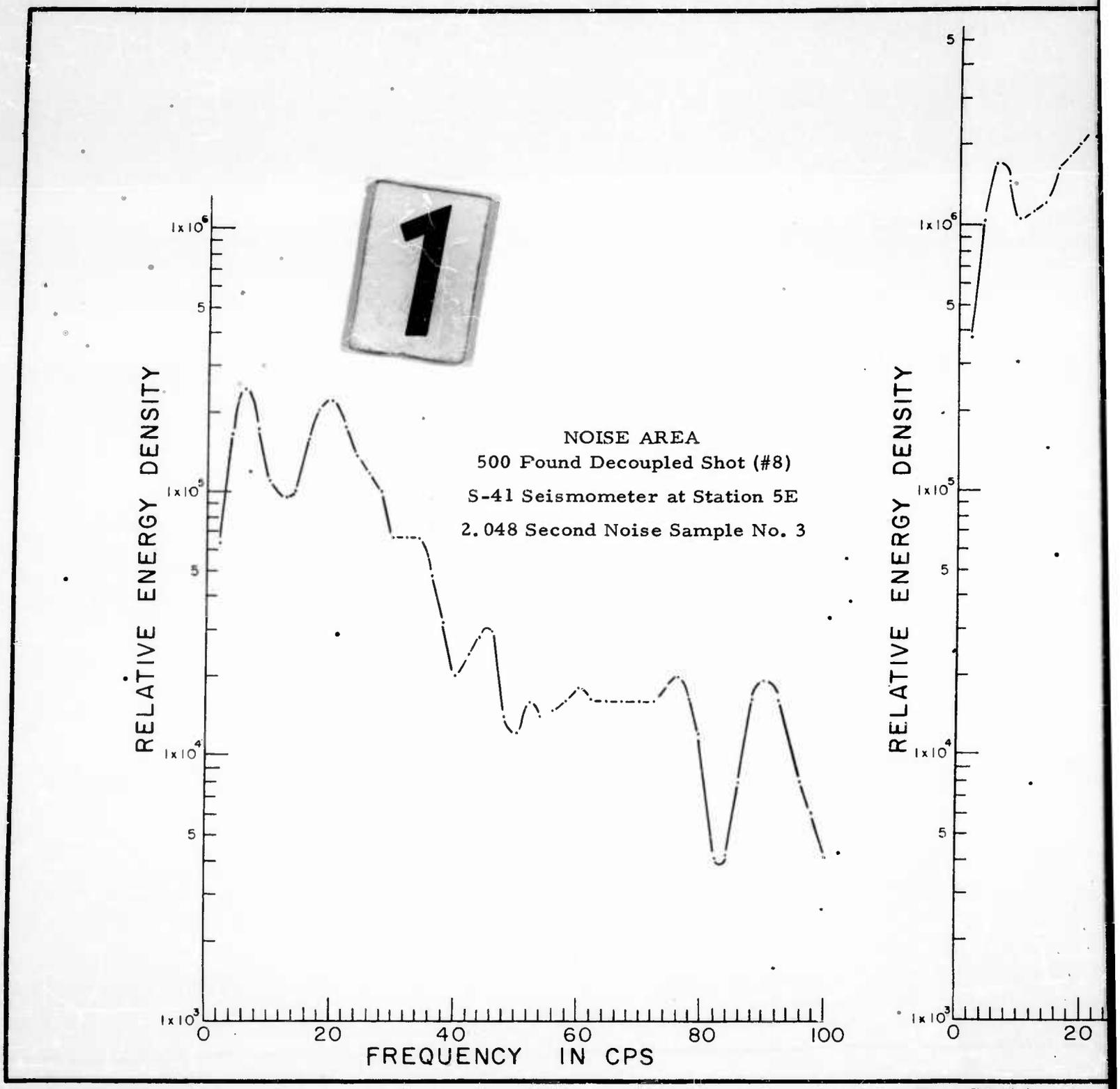

Fig. C3, C4
Power Density Spectra from Two 2.048 Second Samples of Noise f
One Hour Apart

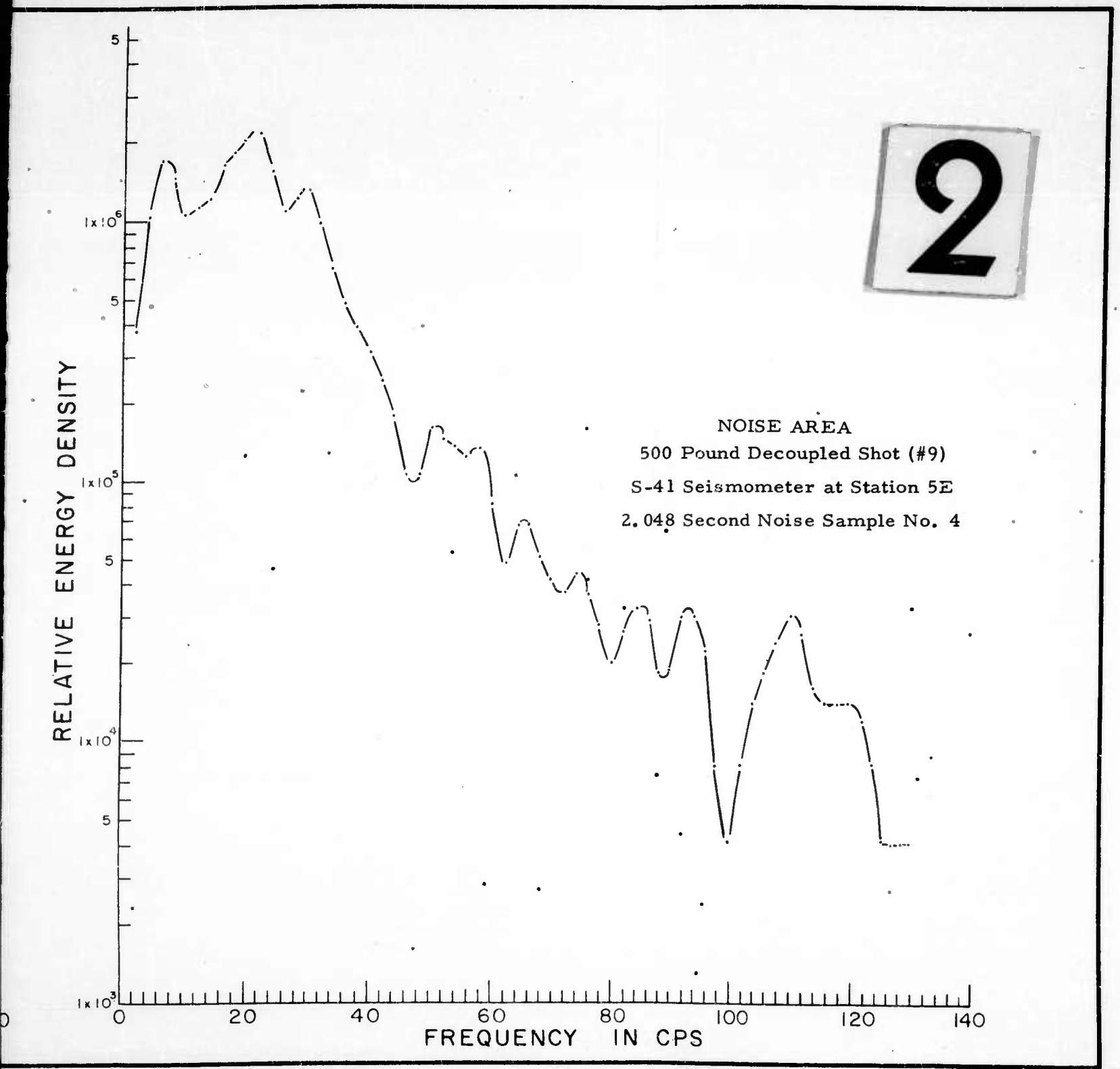

Fig. C3, C4
Second Samples of Noise from the Same Seismometer at Times One Hour Apart

UNCLASSIFIED

UNCLASSIFIED